L'Institut Agro Rennes-Angers
☐ **Site d'Angers** ☒ **Site de Rennes**

Année universitaire : 2021-2022 Spécialité : Ingénieur agronome Spécialisation (et option éventuelle) : Sciences halieutiques et aquacoles (Ressources des écosystèmes aquatiques)	**Mémoire de fin d'études** ☒ d'ingénieur de l'INP-ENSAT (Ecole Nationale Supérieure Agronomique de Toulouse) ☐ de master de l'Institut Agro Rennes-Angers (Institut national d'enseignement supérieur pour l'agriculture, l'alimentation et l'environnement) ☐ de l'Institut Agro Montpellier (étudiant arrivé en M2) ☐ d'un autre établissement (étudiant arrivé en M2)

Is there phylosymbiosis between octocorals and their associated bacterial microbiota in the mesophotic zone of the Mediterranean and Red Seas?

Par : Camille PRIOUX

Soutenu à Rennes le 14/09/2022

Devant le jury composé de :

Président : Pablo Brosset

Maître de stage : Christine Ferrier-Pagès

Enseignant référent : Pablo Brosset

Autres membres du jury (Nom, Qualité) :

Bastien Sadoul (Enseignant-chercheur Institut Agro Rennes-Angers)

Bérangère Bailet (Post-Doc chargée de recherche Projet LAMINET - UMR DECOD INRAE)

Les analyses et les conclusions de ce travail d'étudiant n'engagent que la responsabilité de son auteur et non celle de l'Institut Agro Rennes-Angers

Fiche de confidentialité et de diffusion du mémoire

Confidentialité

☒ Non ☐ Oui si oui : ☐ 1 an ☐ 5 ans ☐ 10 ans

Pendant toute la durée de confidentialité, aucune diffusion du mémoire n'est possible (1).

Date et signature du **maître de stage** (2) :
(ou de l'étudiant-entrepreneur)

27/07/2022

A la fin de la période de confidentialité, sa diffusion est soumise aux règles ci-dessous (droits d'auteur et autorisation de diffusion par l'enseignant à renseigner).

Droits d'auteur

L'auteur(3) **Nom Prénom** PRIOUX Camille

autorise la diffusion de son travail (immédiatement ou à la fin de la période de confidentialité)

☒ Oui ☐ Non

Si oui, il autorise

☐ la diffusion papier du mémoire uniquement(4)

☐ la diffusion papier du mémoire et la diffusion électronique du résumé

☒ la diffusion papier et électronique du mémoire (joindre dans ce cas la fiche de conformité du mémoire numérique et le contrat de diffusion)

(Facultatif) ☐ accepte de placer son mémoire sous licence Creative commons CC-By-Nc-Nd (voir Guide du mémoire Chap 1.4 page 6)

Date et signature de l'**auteur** : 20/07/2022

Autorisation de diffusion par le responsable de spécialisation ou son représentant

L'enseignant juge le mémoire de qualité suffisante pour être diffusé (immédiatement ou à la fin de la période de confidentialité)

☒ Oui ☐ Non

Si non, seul le titre du mémoire apparaîtra dans les bases de données.

Si oui, il autorise

☐ la diffusion papier du mémoire uniquement(4)

☐ la diffusion papier du mémoire et la diffusion électronique du résumé

☒ la diffusion papier et électronique du mémoire

Date et signature de l'**enseignant** : 14/08/2022 P BROSSET

(1) L'administration, les enseignants et les différents services de documentation de l'Institut Agro Rennes-Angers s'engagent à respecter cette confidentialité.
(2) Signature et cachet de l'organisme
(3).Auteur = étudiant qui réalise son mémoire de fin d'études
(4) La référence bibliographique (= Nom de l'auteur, titre du mémoire, année de soutenance, diplôme, spécialité et spécialisation/Option)) sera signalée dans les bases de données documentaires sans le résumé

Remerciements

Je voudrais tout d'abord remercier le Centre Scientifique de Monaco pour avoir accepté de m'accueillir et de m'encadrer d'abord pour mon stage de fin d'étude puis pour ce beau voyage qu'est la thèse. Je remercie également l'équipe d'Ecophysiologie marine qui m'a accueilli chaleureusement et dans laquelle je me suis vite sentie intégrée, à la fois sur le plan humain et professionnel. Je suis toute particulièrement reconnaissante envers mes maîtres de stage, Jeroen Van De Water, Romie Tignat-Perrier et Christine Ferrier-Pages, qui ont su, chacun à leur manière, accompagner mon travail de manière bienveillante et toujours pertinente. Leurs conseils avisés et nos discussions (qu'elles soient scientifiques ou non !) m'ont permis de m'épanouir dans ce domaine nouveau pour moi. Je les remercie également de leur confiance, durant le stage et également pour la thèse qu'ils m'ont proposée.

Je voudrais également remercier l'unité de recherche sur la biologie des coraux précieux CSM- Chanel ainsi que le directeur scientifique du CSM Denis Allemand, sans qui ce projet n'aurait pas pu voir le jour et qui permet d'étudier ces écosystèmes essentiels de notre belle planète.

Merci à tout le personnel administratif et technique qui ont toujours tout fait pour que mon stage se déroule sans encombre (dédicace à Patrick pour les débogages informatiques).

Merci à Clémence, Kiara, Lucie, Guillaume, Alice, Maria, Lucas, Xavier, Benoît, Gaël et tous les autres « jeunes » du CSM pour nos discussions, afterworks, bons délires et baignades sur la digue qui ont rendus mon stage encore plus agréable.

Je voudrais également remercier toute la troupe de Villefranche, Paco, Elsa, Lou, Ewen, Olivier, Sam, Solène, Laetitia, Camille et tous les autres, vous avez été de magnifiques rencontres sans qui cet atterrissage sur la Côte d'Azur n'aurait pas eu la même saveur (je pense bien entendu à la citronnade et aux rhums arrangés). A nos nouvelles randos, expéditions à la pêche au poulpe et nos œuvres d'arts (RIP la forêt de flambloyants) !

Table of contents

List of illustrations and tables

Illustrations

Tables

Glossary

***16S rRNA* gene**: Gene encoding the RNA of the small ribosomal subunit of prokaryotic cells commonly used for a reference for microbes' identification.

Amplicon library: Preparation of samples to NGS sequencing by amplifying and adding specific primers and index to the region of interest of a specific gene.

Bioinformatics: The collection, classification, storage, and analysis of biochemical and biological information using computers especially as applied to molecular genetics and genomics.

Bootstrap replication: Method consisting in creating "new" statistical samples using random sampling with replacement in the dataset.

Co-evolution: The influence of closely associated species on each other in their evolution.

Cophenetic distance: The height of a dendrogram where the two branches that include the two objects whose distance are compared merge into a single branch.

Core microbiome: Microbiome characteristic of a host, present in all individuals.

Depth generalists: Coral species living along a depth gradient from shallow to deep.

Depth specialists: Coral species living only in deep or shallow zones.

DNA polymerase: Enzyme that creates DNA molecules from another DNA molecule (template) by assembling nucleotides, essential for the replication of DNA.

Ecosystem engineer: Species having a large impact on an ecosystem, especially on other species richness and landscape-level heterogeneity of an area.

Electrophoresis: A laboratory technique used to separate DNA, RNA or protein molecules based on their size and electrical charge.

fastq format: File format containing both the read sequences and the sequencing quality for each base

Forward read (R1): Read that has been sequenced from 5' to 3'.

Gorgonin: Complex protein that constitutes the skeleton of the Holaxonia suborder

Holobiont: Assemblage of a host and the many other species living in or around it.

Annealing temperature: The temperature required to ensure proper bonding of the primer to the DNA.

Mesophotic zone: Marine zone ranging from 30 to 150 m depth where light levels are low.

Metabarcoding: Method of DNA amplification and sequencing allowing for the simultaneous identification (barcoding) of many taxa within the same sample

Microbiome: The community of microorganisms (such as fungi, bacteria and viruses) of an individual.

Necto-benthic organism: Organism swimming freely on or near the bottom of the sea.

NGS sequencing: A high-throughput method used to determine a portion of the nucleotide sequence of an individual's genome. This technique utilizes DNA sequencing technologies that are capable of processing multiple DNA sequences in parallel.

Nucleotide: A nucleotide is the basic building block of nucleic acids (RNA and DNA). A nucleotide consists of a sugar molecule (either ribose in RNA or deoxyribose in DNA) attached to a phosphate group and a nitrogen-containing base. The bases used in DNA are adenine (A), cytosine (C), guanine (G) and thymine (T).

Octocorals: Subclass of the Anthozoa forming tree-like organisms with no hard skeleton and live on top of the calcareous structure.

Operational Taxonomic Unit (OTU): A group of bacterial sequences closely similar to one another. Considered here as an approximation of a bacterial species found in the sample

PCR reaction: A laboratory technique for rapidly producing (amplifying) millions to billions of copies of a specific segment of DNA by using short synthetic DNA fragments called primers and then multiple rounds of DNA synthesis to amplify that segment.

Phylogeny: The history of the evolution of a species or group, especially in reference to lines of descent and relationships among broad groups of organisms.

Phylosymbiosis: A link between host phylogeny and microbiome diversity.

Primer: A short sequence of RNA or DNA, complementary to the beginning of a fragment of interest in the sequence, used as a starting point for the synthesis of the complementary strand of the latter by a DNA polymerase.

Read (here): Short fragments of DNA that are amplified (copied) and then sequenced using NGS.

Rebreather: An aqualung in which the diver's exhaled breath is partially purified of carbon dioxide, mixed with more oxygen, and then breathed again by the diver.

Refugium: A reservoir of conserved biodiversity that can re-populate the degraded areas.

Reverse read (R2): Read that has been sequenced from 3' to 5'.

RNAlater: An aqueous storage solution used to preserve RNA integrity in tissue samples.

Sanger sequencing: Process of selective incorporation of chain-terminating dideoxynucleotides by DNA polymerase during *in vitro* DNA replication

Saturation diving: Deep-sea diving in which the diver's bloodstream is saturated with helium or other suitable gas at the pressure of the surrounding water, so that the decompression time afterward is independent of the duration of the dive.

Scleractinian: Subclass of the Anthozoa also called stony corals or hard corals that build themselves a hard skeleton.

Substitution: A type of mutation in which one nucleotide is replaced by a different nucleotide.

Taxonomy: The science of naming, describing and classifying organisms into hierarchical groups using morphological, behavioural, genetic and biochemical observations.

V3 chemistry: Optimized chemistry for MiSeq sequencing to increase read length, and improve sequencing quality scores, compared to earlier MiSeq reagent kit versions.

α-diversity: It summarizes the structure of an ecological community with respect to its richness (number of taxonomic groups) and evenness (distribution of abundances of the groups).

β-diversity: The measure of the change in diversity of species from one environment to another.

List of abbreviations

OTU: Operational Taxonomic Unit

bp: Base pair

DNA: DeoxyriboNucleic Acid

NGS: Next Generation Sequencing

nMDS: Non-metric MultiDimensional Scaling

PCoA: Principal Coordinates Analysis

PCR: Polymerase Chain Reaction

PERMANOVA: Permutational Multivariate Analysis Of Variance

RNA: RiboNucleic Acid

ROV: Remotely Operated Vehicle

List of supplementary documents

Table 1: Metadata for the samples (location, species and depth)

Table 2: Final merging ratios after bioinformatic treatment to the dataset

Table 3: Table with the AIC and BIC criterion for a range of nucleotides' substitution models

Table 4: Tukey's HSD test results after ANOVA on Chao1 index

Table 5: Pairwise PERMANOVA results on bacterial composition

Figure 1: Homoscedasticity checking graphs for the "raw data" ANOVA model

Figure 2: Homoscedasticity checking graphs for the log transformed ANOVA model

Figure 3: Juxtaposition of Red Sea species phylogeny (1) and microbiome dendrogram (2)

Figure 4: Poster presented during the International Coral Reef Symposium (ICRS, 3rd to 8th July 2022) in Bremen (Germany).

Script 1: Bioinformatic pipeline for the Illumina sequences

Script 2: R script for bacterial communities' analysis

Script 3: Pipeline for the phylosymbiosis analysis

I. Introduction

Coral reefs and coralligenous ecosystems are some of the most biodiverse ecosystems in the world (Roberts et al. 2002; Barlow et al. 2018; Casas-Güell et al. 2015). Tropical reefs are home to an astonishing variety of organisms, and there are likely still millions of undiscovered species living in and around these ecosystems (Fisher et al. 2015). Species associated with coralligenous areas in the Mediterranean in turn account for an estimated 15-20 % of the biodiversity (Casas-Güell et al. 2015; Coll et al. 2010). These biodiversity hotspots are also of high economic value, as they provide habitat for populations of fishes and their juveniles, thus contributing to commercial and subsistence fisheries. They also present business opportunities along with jobs through tourism and recreation (Worm et al. 2006).

Corals (phylum Cnidaria and class Anthozoa) form the 3-dimensional structure of these ecosystems. Scleractinian corals (subclass Hexacorallia), also called hard corals, provide the framework of coral ecosystems by building large calcium carbonate (CaCO3) skeletons. Octocorals (subclass Octocorallia) mainly include soft corals and gorgonians, which do not have a calcareous skeleton but form flexible tree-like colonies. Because of this structural complexity, corals create macro- and micro-habitats that act as a shelter for many benthic and nektonic organisms (Piazzi et al. 2021). Corals also play a major role in the benthic-pelagic coupling (*i.e.* processes that connect the 2 zones through the exchange of energy, mass, or nutrients), by capturing large quantities of plankton and thereby regulating the primary and secondary productions of coastal food chains (Rossi, Rizzo 2021).

Although corals have been extensively studied, most of the research has focused on Scleractinians. Octocorals have been much less studied in terms of their physiology, distribution, reproduction and association with microbial symbionts (Schubert, Brown, Rossi 2017; van de Water, Allemand, Ferrier-Pagès 2018). As all multicellular organisms, corals are holobionts, in that they form complex interactions with a range of microorganisms, such as protists, fungi, bacteria, archaea, and viruses (Knowlton, Rohwer 2003). These microbial symbionts play an important role in the health of their host. The best-known coral-microbe interaction is the symbiosis between corals and endosymbiotic algae from the family Symbiodininiaceae. This relationship is, however, exclusive to corals living in waters where light levels are sufficient for photosynthesis, allowing the algae to produce carbon-rich compounds (Muscatine, R. McCloskey, E. Marian 1981) that they share with the coral host to meet its nutritional needs. Other microbial symbionts, such as bacteria, are involved in other services such as nutrient provision through e.g. nitrogen fixation (Lema, Willis, Bourne 2012), carbon acquisition (Matthews et al. 2020) and sulphur-cycling (Raina et al. 2009), as well as protection against harmful microbes via antibiotic production (Kvennefors et al. 2012; Ritchie 2006; Nissimov, Rosenberg, Munn 2009) or the exclusion of pathogens by occupying available microbial niches (Rypien, Ward, Azam 2010).

The coral microbiota is composed of microbes that are consistently associated with a host species called “core microbiome” (Ainsworth et al. 2015), as well as transient microbes whose presence depends on local conditions (Hernandez-Agreda et al. 2016; van de Water et al. 2018;

2017a). These conserved 'core microbiomes' suggest the existence of a phylosymbiotic signal, *i.e.* a link between host evolutionary history and microbiome diversity (Lim, Bordenstein 2020). However, the composition and function of the microbial community may change under changing environmental conditions, which could lead to the emergence of pathogens and resultant disease (Bourne et al. 2009), but may also lead the coral to uptake beneficial microbes that may help it to survive stressful events (Peixoto et al. 2017). Assessing how symbiotic microbial communities are changing in response to climate change and seawater pollution is critical to the conservation of these important ecosystems. Considering this, it is essential to explore whether evolutionary relationships exist between corals and their microbes, or whether corals select their microbial communities based on the functions they possess and what the coral needs.

So far, few studies have been conducted on the microbiota of octocorals, and mostly on populations in shallow waters (van de Water, Allemand, Ferrier-Pagès 2018). Populations living in the mesophotic zone (30 – 150m depth), where light levels are low, remain largely unexplored, especially below 60 m depth. These sites are difficult to access and can only be reached by specialized divers or Remotely Operated Vehicles (ROV) (Wilkinson 2008). Its distance from the surface makes the mesophotic zone a more protected area from extreme events (storms with waves and swell) and human pressures (e.g maritime traffic, noise pollution, developments, fishing, pollution, boat anchoring). Furthermore, its depth provides more stable conditions: below 60 meters, the temperature in the Mediterranean Sea is the same all year round, whereas near the surface it can vary by more than 12 °C between summer and winter (Shaltout, Omstedt 2014). As global warming is likely to intensify, shallow water corals may experience more frequent bleaching episodes and/or disease outbreaks, leading to a loss of biodiversity. The colder deep waters, which have greater inertia as the water warms at the surface, would give ecosystems more time to adapt. Thus, because of their particularly remote and stable conditions, mesophotic ecosystems may represent a potential refugium for coral species, *i.e.* a reservoir of conserved biodiversity that can re-populate the degraded areas (Kahng et al. 2010). Because host-microbiome relationships of corals in these areas are not or only slightly disturbed by physical and anthropogenic factors, mesophotic ecosystems are an ideal environment to study evolutionary links between corals and their microbiota, *i.e.* a phylosymbiotic signal.

During the Gombessa V (2019) & VI (2021) expeditions and the ENCOR campaign (2019), 192 samples of 14 Octocorallia species from the Alcyonacea order were collected from the mesophotic zones (between 60 and 150 m depth) of the temperate Mediterranean Sea and tropical Red Sea. This dataset encompasses both depth specialists (living only in deep or shallow zones) and depth generalists (living along a depth gradient from shallow to deep). Using amplicon sequencing of the *16S rRNA* gene (metabarcoding), this study aims (1) to investigate the composition of the bacterial communities associated with these corals and (2) explore whether an evolutionary link between the corals and their microbiota exists.

II. Material and methods

1. Biological material

Figure 1 provides an overview of the morphology of most Octocorallia species of interest for this study in their natural habitat.

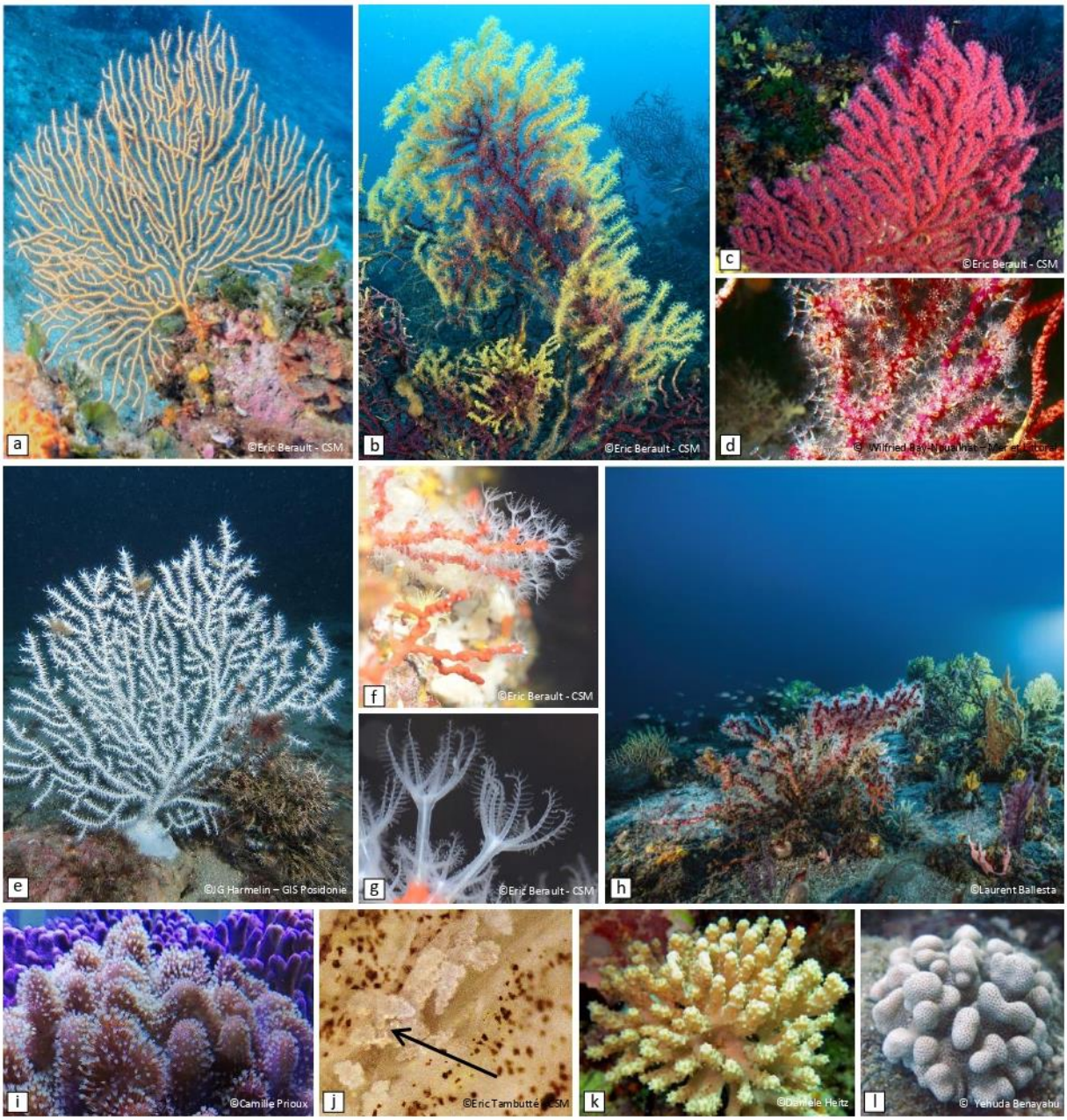

Figure 1: Octcorals species of interest a. Eunicella cavolini, b. Paramuricea clavata bicolor, c. Paramuricea clavata, d. Alcyonium coralloides, e. Eunicella verrucosa, f. Corallium rubrum g. Eightfold body symmetry in Corallium rubrum, h. Mesophotic gorgonian forest ecosystem, i. Sarcophyton glaucum, j. Sclerites (indicated by the arrow) inside the tissue of Sarcophython glaucum k. Paralemnalia thyrsoides, l. Klyxum utinomii

Corals are solitary or colonial animals (called polyps), which belong to the phylum Cnidaria and the class Anthozoa. Anthozoans can be further divided into 2 sub-classes:

- The Hexacorallia (Haeckel, 1896), presents a 6-fold symmetry and includes, among other orders, the Scleractinians or hard corals. Scleractinians are responsible for the reef framework as they produce large calcium carbonate ($CaCO_3$) skeletons.
- The Octocorallia (Haeckel, 1866) exhibit eight-fold symmetry (Figure 1.g). It is composed of 3 orders Alcyonacea, Helioporacea and Pennatulacea. Alcyonacea include the "soft corals" and "gorgonians". They form tree-like organisms with no hard skeleton and live on top of the calcareous structure. All Alcyonacea have tiny $CaCO_3$ structures embedded in the tissue called sclerites that support the structure (Figure 1.j). In addition, gorgonians have a central axis composed of proteins (gorgonin) or aragonite (only in the Coralliidae family) that allows them to maintain an upright position. Because of the 3-dimensional structures they create, they play an important role as ecosystem engineers. The coral bushy forests create specific environmental conditions in terms of light, currents, sedimentation, *etc*., which provide habitats for hundreds of necto-benthic organisms (Ponti et al. 2014), as shown in Figure 1.h.

Gorgonians are found in the Alcyonacea order in several suborders as described in figure 2, showing the summarized taxonomy of the species of interest for the following study. This diagram has been simplified for understanding purposes, providing the taxonomy classification only of the species studied here. The length of the branches does not correspond to a phylogenetic distance.

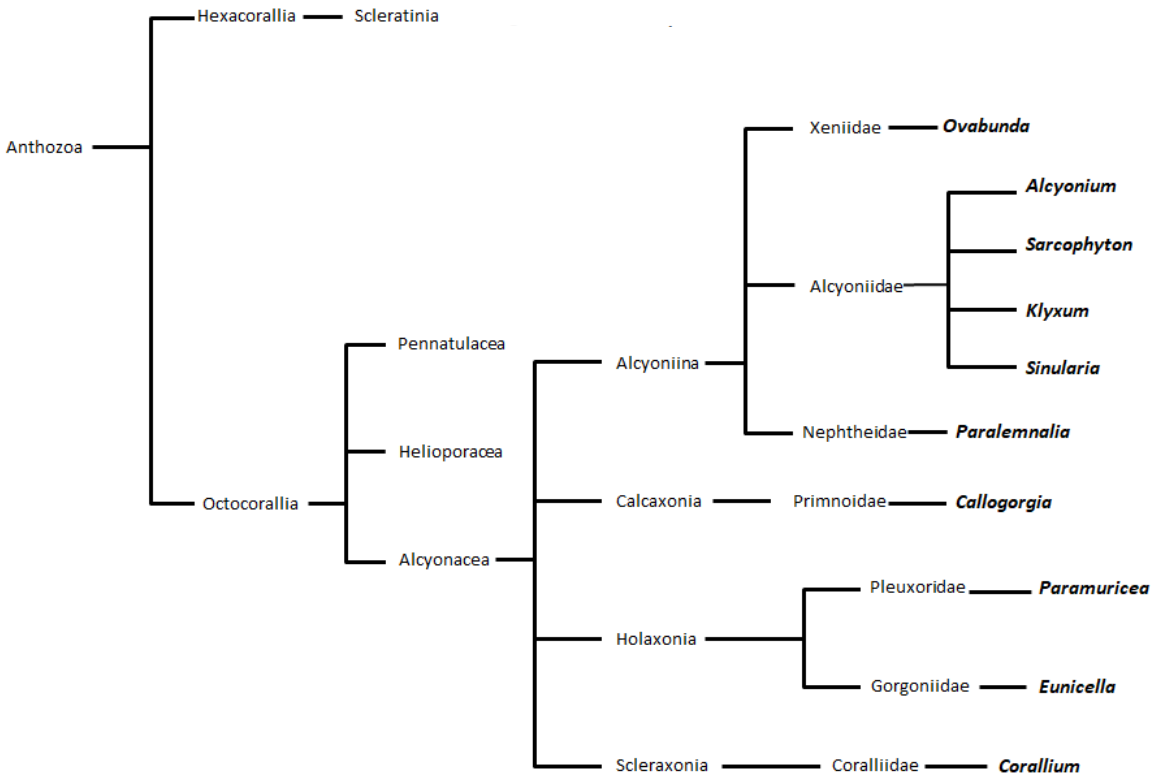

Figure 2: Summary of the taxonomy of coral species of interest (Source: Taxonomy annotation of WORMS)

Octocorals are holobionts forming relationships with a range of microorganisms such as bacteria, fungi, protists, archaea and viruses that provide them with different services (Figure 3). They can also host endosymbiotic algae from the Symbiodininiaceae family, which photosynthesize and provide the host with most of its energy and respiratory needs (Davy, Allemand, Weis 2012). However, many Octocorallia do not possess algal symbionts, especially for the Mediterranean species (van de Water, Allemand, Ferrier-Pagès 2018). Bacterial communities associated with octocorals have received more attention than fungi or viruses and this study will only focus on bacterial microbiota. Previous studies have shown that bacterial richness and diversity are lower in octocorals than in Scleractinian corals (Bayer et al. 2013), making them potentially suitable models for studying the co-evolution of host and microbial communities. Analyses of Holaxonia species revealed that their bacterial communities are highly dominated by Proteobacteria and in particular by the Oceanospirillales genus *Endozoicomonas*, that can make up to over 96 % of an octocoral's bacterial assemblage (Bayer et al. 2013; van de Water et al. 2017b).

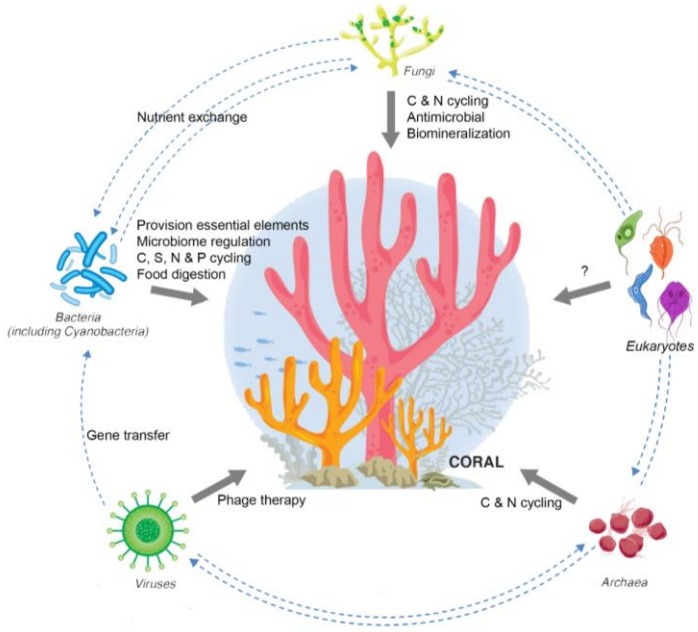

Figure 3: Schematic representation of the coral holobiont (Source: Peixoto et al. 2017)

Spirochaetes have previously received little attention in the field of coral microbial ecology, due to their low abundance in tropical hard corals (Ainsworth et al. 2015), cold-water corals (Kellogg, Lisle, Galkiewicz 2009), sea pens (Porporato et al. 2013), and deep-sea soft corals (Gray et al. 2011; Penn et al. 2006). However, since the discovery that the bacterial communities of the red coral *Corallium rubrum* are consistently composed of up to 70 % Spirochaetales (genus *Spirochaeta*, and *Leptospira* (van de Water et al. 2018; 2016)), their importance is now also increasingly recognized in other coral species. Other bacterial taxa are to be found in our samples depending on the coral species, sampling location and other biotic and abiotic parameters, which will be discussed later in this report.

2. Sampling process

The samples in this dataset come from several scientific campaigns conducted at different locations, the 2 Gombessa expeditions in the temperate Mediterranean Sea and the ENCOR expedition in the Red Sea, a tropical environment. A summary table of the different surveys and their characteristics is provided later in this section (Table 1).

a. Gombessa expeditions V and VI

Samples were collected by deep divers of the Gombessa team using a combination of saturation diving and electronically controlled rebreather diving with the permission of the Direction Interrégionale de la Méditerranée (DIRM). The divers remained pressurized for 28 days inside a 10m^2 "Bathyal station" in an atmosphere of helium and oxygen (24 days of exploration + 4 days of desaturation at the end). The pressure in the station was adjusted to the depth of the sites to be explored and varied from 1 bar (surface pressure) to 15 bars (pressure of the deepest site). At each dive, the divers went to the lift-module, which deposited them at the site to be explored (Figure 4). At each site, fragments of ~20cm were collected from 6 colonies per species (see Figure 6 and table 1). Fragments were individually placed in a plastic bag filled with ambient seawater and brought back to the surface.

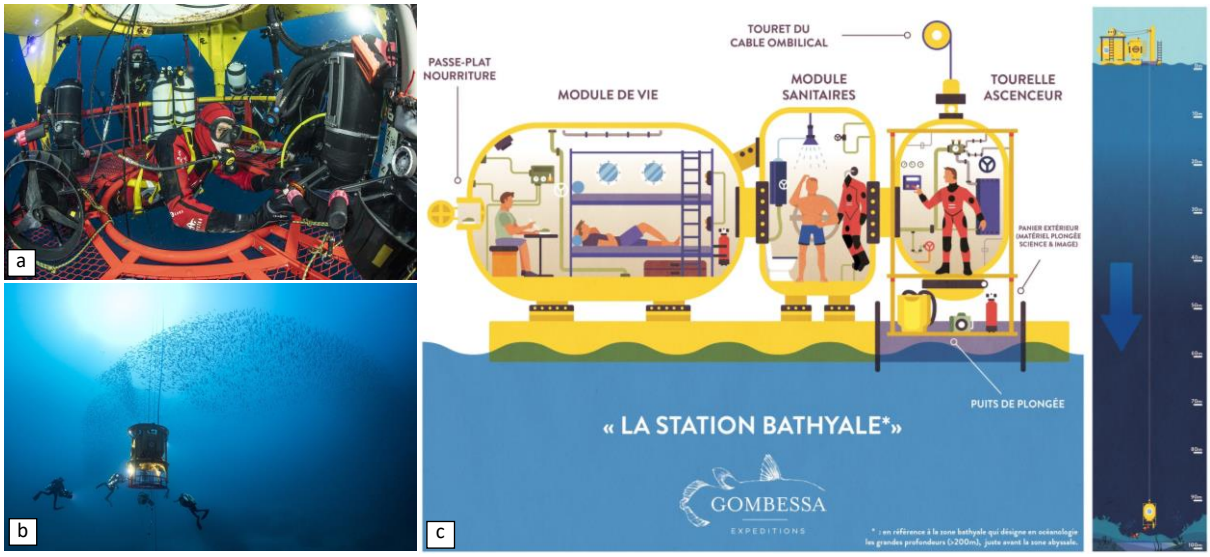

Figure 4: Images from the Gombessa expeditions a. Diver in the lift module, b. The lift module that lowered the divers to the desired depth, c. The "Bathyal station" (Source: L. Ballesta)

b. ENCOR expedition

Corals were sampled near Eilat (Israel) in October 2019 between 65 and 120 m depths (see Figure 6 and Table 1), under the permits of the Israel Nature and Parks Authority. Colonies of around 25–30 cm^2 were collected for each species with a ROV (ECA H800), equipped with an HD video camera (VS300 Eca Robotics), and a manipulative arm for sampling (Figure 5). The ROV was operated from a boat using a fiber-optics umbilical cable.

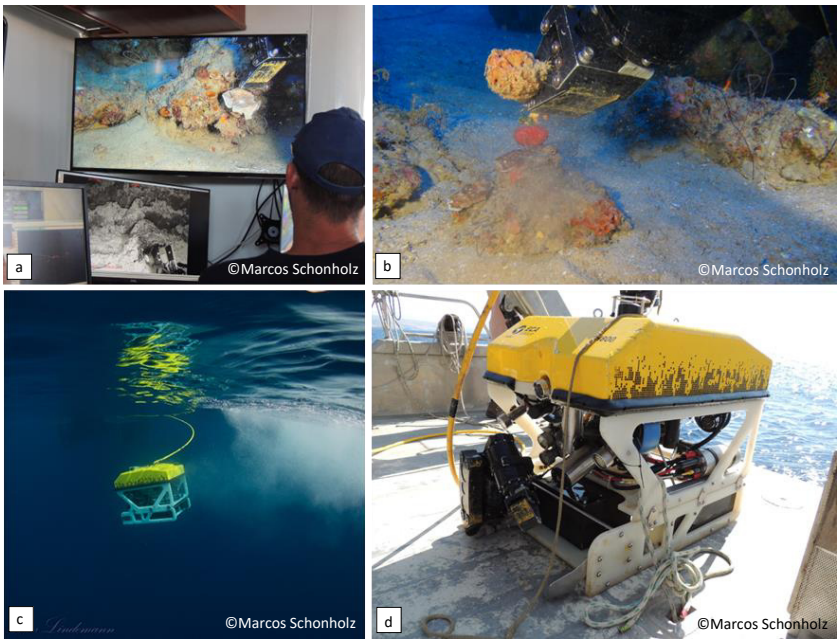

Figure 5: Images from the ENCOR expedition a. ROV operated from the boat, b. Manipulative arm of the ROV taking a coral sample, c. ROV going down from the boat, d. ROV reboarded after use

All samples were rinsed twice with 0.2-µm filtered seawater to remove exogenous, loosely associated microorganisms and stored in RNAlater (an aqueous storage solution from ThermoFisher Scientific) at 4 °C. In addition, between 2-30L of seawater were collected next to each octocoral colony and filtered sequentially through 0.2-µm Whatman Nuclepore Track-Etched filters (Sigma-Aldrich), and the retentate was kept in RNAlater at 4 °C.

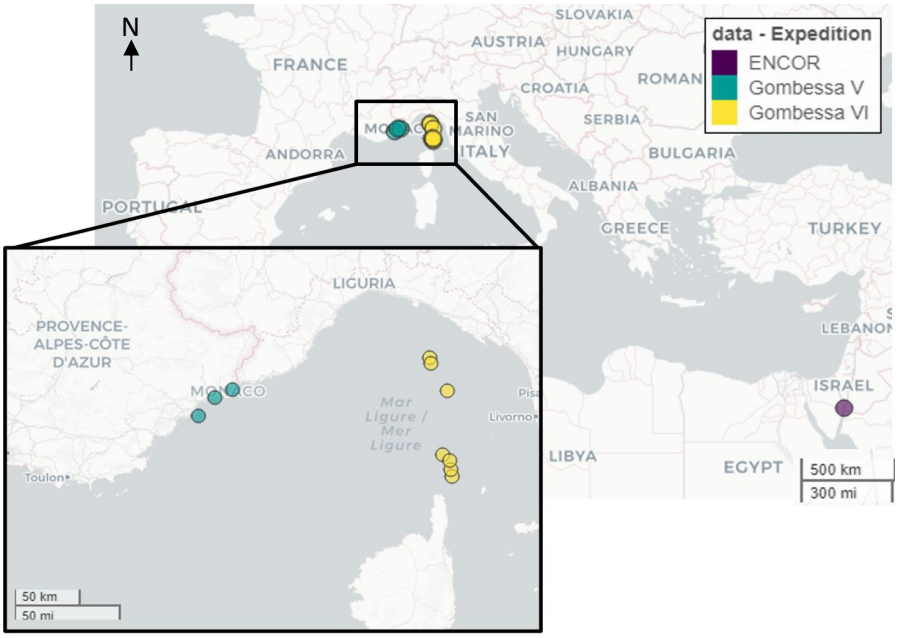

Figure 6: Map of the sampling sites for each survey (Source: Personal illustration)

Table 2: Summary table of the survey sample's information

Survey	Date	Sampling site	Species	Number of samples
Gombessa V	July 2019	- Le massif du Raventurier (Antibes) (70 m) *43°33'13.6"N 7°08'54.0"E* - St Martin (77 m) *43°44'15.1"N 7°28'17.2"E* - Le tombant des Américains Est (103 m) *43°41'04.5"N 7°18'18.7"E*	- *Corallium rubrum* - *Paramuricea clavata* - *P. clavata bicolor* - *Eunicella cavolini* - *Eunicella verrucosa*	10 10 13 14 14
Gombessa VI	July 2021	- Capense (80 m) *43°57'30.5856"N 9°18'57.5928"E* - Scalo (100 m) *43°55'20.1504"N 9°19'57.8712"E* - Palagaccio (100 m) *43°43'45.3828"N 9°29'4.362"E* - Cap Corse 8A (90 m) *43°7'50.9592"N 9°31'14.952"E* - Nord 1 site 1 (100 m) *43°17'10.8888"N 9°26'0.3228"E* - Anneaux site A (105 m) *43° 10' 59.4588"N 9° 30' 50.1588"E* - Anneaux DC (90 m) *43° 14' 43.3788"N 9° 29' 56.1588"E*	- *Corallium rubrum* - *Paramuricea clavata* - *Eunicella cavolini* - *Callogorgia verticillata* - *Alcyonium coralloides*	11 16 16 12 5
ENCOR	October 2019	Eilat (65-120m) *29°30'03.1"N 34°55'20.4"E*	- *Klyxum utinomii* - *Sinularia eilatensis* - *Sinularia loyai* - *Sinularia mesophotica* - *Sinularia vrijmoethi* - *Sinularia polydactyla* - *Paralemnalia thyrsoides* - *Ovabunda spp.* - *Sarcophyton glaucum*	4 9 3 3 13 2 10 15 12

Metadata for each sample (location, species and depth) is available in supplementary table 1.

3. DNA extraction and sequencing

The most commonly used method for microbes' identification and classification is *16S rRNA* gene sequencing (Weisburg et al. 1991; Bharti, Grimm 2021). This gene encodes the RNA of the small ribosomal subunit of prokaryotic cells. While highly conserved in all bacterial organisms, the 16S rRNA gene also presents 9 variable regions that are used to distinguish bacterial species (Figure 7). Extraction of DNA from samples and subsequent sequencing of variable regions of the *16S rRNA* gene allow the identification of bacterial species from complex bacterial communities.

Figure 7: Schematic representation of the 16S rRNA gene (Source: Personal illustration)

a. DNA extraction

DNA was extracted using the DNeasy PowerBiofilm kit (Qiagen) with the following modifications: during the cell lysis step, 2 µL of Proteinase K (600 U/ml) was added to the sample and incubated at 60 °C for 2 hours, followed by 2 min of bead beating using the CryoMill (Retch, Germany) at a frequency of 30 Hz. Negative extraction control samples (*i.e.,* extraction without sample material) were processed at the same time as the coral samples in order to account for contaminants. DNA concentration was measured using a fluorimeter (BioTek) and DNA was stored at −20°C.

b. Sequencing

There are many sequencing techniques available today. However, it is important to distinguish the old Sanger sequencing method and the newer NGS (Next-generation sequencing) methods such as Illumina. In principle, the concepts behind the 2 technologies are similar: sequencing-by-synthesis. Here, a DNA polymerase is used to sequentially attach fluorescent complementary nucleotides to a growing DNA template strand. Then the instrument can determine the nucleotide sequence based on the fluorescent signal emitted at each sequencing cycle. The main difference between Sanger sequencing and NGS is the number of samples that can be processed simultaneously. While the Sanger method can only process a single DNA sequence at a time, NGS can sequence millions of different sequences simultaneously. To investigate multiple microbial species in a sample, Illumina sequencing is the most appropriate, efficient and cost-effective method. However, to construct a phylogenetic tree of the hosts, Sanger sequencing of some specific genes of the corals is sufficient.

- *Illumina MiSeq sequencing of the 16S rRNA gene*

The V3-V4 region (~ 460 base pairs) of the 16S rRNA gene of the coral samples and negative control samples were sequenced using the NGS Illumina MiSeq technology. Amplicon library (amplification of the region of interest) was prepared using Illumina's standard "16S Metagenomic Sequencing Library Preparation" protocol (Illumina I. 2013). Primers 341F 5'-CCTACGGGNGGCWGCAG-3' and 785R 5'-GACTACHVGGGTATCTAATCC-3 were bonded to the sequence of interest, to specifically target the V3-V4 region with Polymerase Chain Reaction (PCR). Then Illumina barcodes, to label the samples for the company were attached to the sequenced region in a second PCR process.

A summary chart of the principle and steps of the protocol is presented below (Figure 8). DNA was sent to STAB VIDA sequencing company (Portugal). The amplicon library was paired-end (2x300 bp (base pairs), forward and reverse) sequenced on an Illumina MiSeq platform with the V3 chemistry. Base call data were converted to fastq files containing the raw sequencing data and sequence quality information.

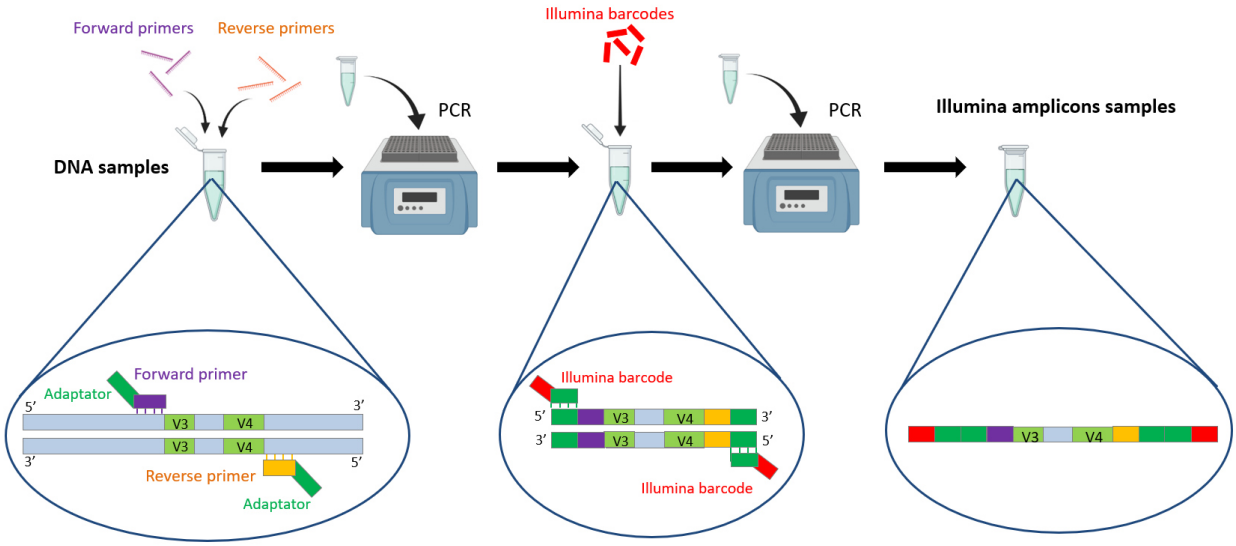

Figure 8: Summary chart of the Illumina amplicons preparation (Source: Personal illustration made in Biorender.com)

- *Sanger sequencing of specific genes of the octocoral species*

Exploring whether an evolutionary link between the corals and their microbiota exists requires studying the phylogeny of the octocoral hosts. To this end, the sequences of 3 different genes present in the genomes of all coral species were used to establish the phylogenetic relationships between the different hosts (McFadden et al. 2011; McFadden, van Ofwegen 2013). PCRs on these 3 genes were done on three samples per species and negative control samples were processed at the same time to check for the absence of contaminants. Primers used to specifically target the 3 genes and their respective hybridization temperature (The temperature required to ensure proper bonding of the primer to the DNA) are given in the table below (Table 2).

Table 2: Information table on the Sanger sequencing conducted

Gene	Sequence length	Primers	Hybridization temperature
COI	~1080 bp	COII8068xF 5'-CCATAACAGGRCTWGCAGCATC-3' COIOCTR 5'-ATCATAGCATAGACCATA-3'	46°C
MutS	~870 bp	ND42599F 5'-GCCATTATGGTTAACTATTAC-3' MUT3458R 5'-TSGAGCAAAAGCCACTC-3'	58°C
12S	~600 bp	12SF 5'-GTGCCAGCHNAHGCGGTYA-3' 12SR 5'-RAGDYGACGGGCRRTTTGT-3'	62°C

DNA samples were amplified following the 3-steps protocol recommended by the Phusion™ High-Fidelity DNA Polymerase kit (ThermoFisher™). The Table 3 and Figure 9 below summarize the PCR steps.

Table 3: PCR steps following the ThermoFisher kit guidelines

Cycle steps	Temperature	Time	Number of cycles
Initial denaturation	98°C	30 s	1
Denaturation	98°C	10 s	30
Annealing	Hybridization °C	30 s	
Extension	72°C	15-30 s/kb	
Final extension	72°C	5-10 min	1
Hold	4°C	Hold	Hold

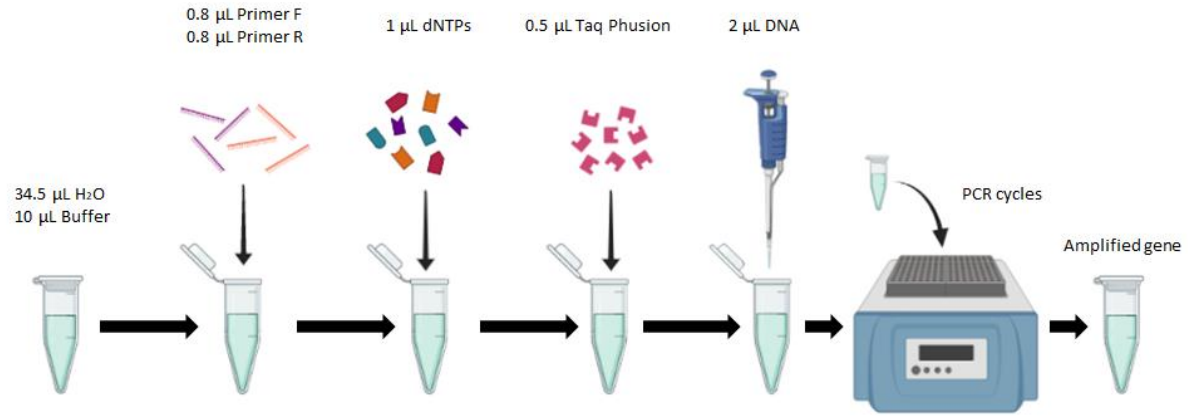

Figure 9: PCR protocol (Source: Personal illustration made in Biorender.com)

An electrophoresis was performed on the PCR products to check if the PCR reactions worked. DNA fragments with the expected size were excised from gel and purified using the GFX™ PCR DNA and Gel Band Purification kit (Illustra™). DNA amplicons were sent to Eurofins Genomics (Germany) for Sanger sequencing.

4. Bioinformatic data processing

a. Illumina sequences processing

The 16S rRNA gene amplicon data were processed using the USEARCH v11 software (64-bit version, https://drive5.com/usearch/). MiSeq technology produced 300 bp fragments called reads. Because the length of the gene region of interest is usually longer than this, it is sequenced in both directions, forward (from 5' to 3') and reverse (from 3' to 5') to get the entire sequence of interest by merging them. On the 198 samples, a total number of 22, 911, 242 reads were produced ranging from 158 to 508, 818 reads per sample. Negative controls produced 29, 535 reads ranging from 82 to 7, 030 reads per sample.

Illumina sequencing technology provides fastq files, which contain both the read sequences and the sequencing quality for each base. The base quality is given in the form of a score called the "Phred score" or "Quality (Q) score". The Q score is an integer ranging from 2 to 40 that is related to the probability that the base call is incorrect using this relation:

$$P = 10^{-\frac{Q}{10}} \Leftrightarrow Q = -10.\log\ (P)$$

As an example, Q=2 corresponds to an error probability of 63 %, meaning that the designated base is more likely to be wrong than right. Quality of the reads was checked before any further data manipulation. Figure 10 shows an example of quality check graphs that can be produced with the FastQC program.

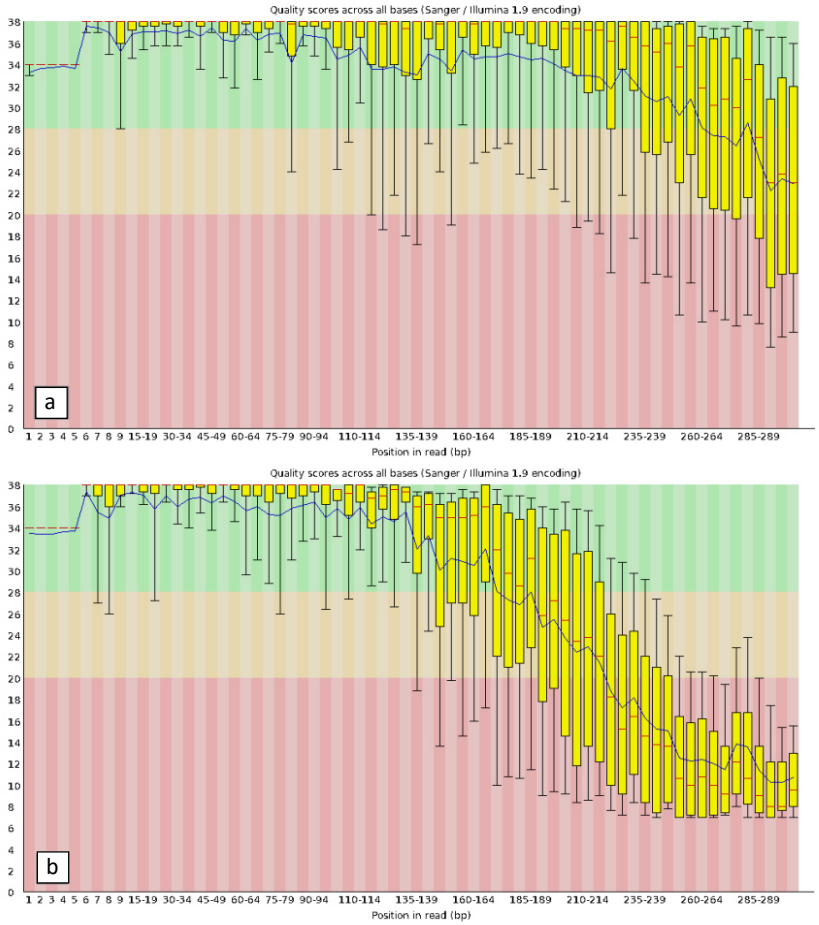

Figure 10: Average Q score for each base of (a) the forward reads and (b) reverse reads in a Corallium rubrum sample

To ensure that high quality reads were used for the following steps, reads were truncated when the quality of the reads dropped below Q=20, corresponding to an error probability of 1 %. Reads were truncated using the USEARCH -fastx_truncate function. No base pairs were cut from the forward reads and 90 bp were cut at the end of the reverse reads (3'). Forward (also called R1) and reverse (R2) reads overlap and can be merged together in order to get the entire sequence of interest. It was made using the USEARCH -fastq_mergepairs function. The quality was a bit low for some samples and the following parameters were added to ensure a satisfying merging ratio: a minimum and maximum length of the merged sequence of 400 bp and 510 bp,

respectively, and a minimum and maximum base-pair difference of 15 bp. Final merging ratios are available in supplementary table 2.

The forward and reverse primer sequences (~23 bp) were removed from the merged sequences using -fastq_truncate. The resulting sequences were quality filtered based on the expected number of errors (E). It is defined as the mean number of errors that would be observed in a very large collection of sequences where the error rate at each position is given by its quality score (Q_i), assuming that errors at different positions occur independently. According to the demonstration in Edgar and Flyvbjerg (2015) (Edgar, Flyvbjerg 2015), E is the sum of error probabilities (p_i):

$$E = \sum_i p_i = \sum_i 10^{-\frac{Q_i}{10}}$$

As recommended in their publication, the sequences were filtered allowing a maximum of one expected error using -fastq_filter, obtaining a total of 15, 862, 422 sequences with a range of sequences per sample of 3, 028 to 379, 407 sequences.

Unique sequences (identical over the full length) were identified using the USEARCH -fastx_uniques command and then denoised (removing sequence errors from amplicon reads) using the UNOISE3 algorithm, obtaining 17, 474 unique sequences. Operational Taxonomic Units' (OTUs) can be defined here as groups of bacterial sequences closely similar to one another. For this study, an OTU will be considered as an approximation of a bacterial species found in the sample. An OTU table, relating the number of reads of each OTU found in every sample, was generated by clustering sequences with an identity similarity value of 99 % using -otu_tab command. Then the OTUs in the table were taxonomically annotated using the SINTAX algorithm and the SILVA reference database (version 138) with an assignment confidence cutoff of 0.8. The bioinformatic pipeline is available as supplementary script 1.

b. Sanger sequences processing

For the 3 different genes, Sanger sequences were first aligned, *i.e.*, arranged to identify regions of similarity that may be a consequence of functional, structural, or evolutionary relationships, using the ClustalW Multiple Alignment program in the BioEdit software. Due to technical limits of the sequencer, beginnings and ends of a sequence are often unreliable as the machine cannot detect with certainty the right nucleotide. Approximately 20-25 nucleotides were cut on each sequence on both sides to ensure a good quality. As we had 3 replicates per species, a consensus sequence of each species was created by selecting for each nucleotide position the one base which occurs most frequently in the 3 sequences. For each species, the consensus sequence of COI (746 bp), MutS (779 bp) and 12S (583 bp) were concatenated to create a single sequence to use for the construction of the phylogenetic tree. The phylogeny software PhyML (Guindon et al. 2010) was used to create the host phylogenetic tree on the maximum-likelihood principle. Maximum likelihood method searches for the tree with the highest probability to look like the dataset given an evolutionary distance model. It first computed the best fitted nucleotides' substitution model. Indeed, the evolutionary distance between the sequences is not

exactly equal to the number of observed substitutions between nucleotides as they might have been substituted more than one time. Such models allow to estimate the actual evolutionary divergence from the observed substitutions. They use the distribution of the nucleotide frequencies π_A , π_T , π_G , π_C and Q, a 4x4 transition matrix giving the rate for each nucleotides transition. Akaike's Information Criteria (AIC) was used to choose the Gamma-distributed General Time-Reversible (GTR) model for a range of adjusted models (Supplementary table 3). It allows exchangeability rates to differ from one another. To ensure statistical consistency, 1000 bootstrap replications of the test were done, giving access to a bootstrap value for each split, defined as the proportion of the replicate trees that recovered that particular split.

5. Bacterial community analysis

The following analysis was run in the R environment under version 4.1.2 (2021-11-01). The R script is available in supplementary information (Script 2).

a. Data preparation

The R-package *decontam* (Davis et al. 2018) was used to identify contaminant OTUs in the samples based on the negative control samples (isContaminant function). 2, 386 of the 17, 474 OTUs were identified as contaminants and were removed. 4244 OTUs annotated "k_Unknown", "f_Mitochondria" and "o_Chloroplast" were removed from the dataset as it was not possible to identify clearly if it was from bacterial origin.

b. α-diversity analysis

First, species richness of each sample was evaluated (α-diversity). Sequencing methods do not give an exhaustive vision of the bacterial community diversity so α-diversity was estimated using Chao1 estimator, calculated using the R-package *vegan* (Oksanen et al. Version 2.6-2, 2022). Chao1 index is a nonparametric estimator based on mark-release-recapture methods. It considers the proportion of species that have been observed before ("recaptured") to those that are observed only once. A correction factor to the observed number of species is added as described in the following formula (Hughes et al. 2001):

$$S_{Chao1} = S_{obs} + \frac{n_1^2}{2n_2}$$

An ANOVA model was built to test if α-diversity was similar between species. Homoscedasticity was checked and did not give satisfying results (see in supplementary Figure 1). A log transformation was used to fit the model assumptions (see normality graphs in supplementary Figure 2). Post-hoc Tukey's test was performed to identify potential pair-wise differences.

c. Bacterial community composition analysis

To go further in the analysis, we examined β-diversity to quantify differences among the coral's bacterial compositions, detect unique OTUs and similarities between related species and locations. Because the samples were not sequenced with the same depth (the same number of times that a nucleotide in the given sequence has been read), the dataset was rarefied, *i.e.* cutting

the same number of sequences per sample using the R function *phyloseq_mult_raref_avg* with a threshold of 9000 reads. *Sinularia mesophotica* was removed from the dataset for this section as the number of sequences obtained after sequencing was below 9000. Then a distance matrix was generated by calculating the Bray-Curtis dissimilarity index (Bray, Curtis 1957) on the composition of the samples. It can be defined as:

$$BC_{ij} = 1 - \frac{2C_{ij}}{S_i + S_j}$$

Where C_{ij} is the sum of the lesser values between the 2 compared coral samples for only OTUs in common between both samples. S_i and S_j are the total number of specimens counted in both samples.

Based on the distance matrix, principal component analyses (PCA), as well as permutational multivariate analysis of variance (PERMANOVA) and dispersion analysis (PERMDISP) were used to assess differences in bacterial community diversity and dispersion between the coral species using 9999 permutations (*vegan* R-package). A pairwise test was also performed to identify species having significantly different bacterial community compositions. In anticipation of the search for phylosymbiosis and to better visualize similarities and differences in the bacterial community composition between species, hierarchical cluster analyses were used to create a dendrogram (*pvclust* R-package) using the Bray-Curtis distance and averaging agglomeration method (also known as UPGMA). P-values were computed for each of the clusters via multiscale bootstrap resampling. To identify OTUs that were differentially abundant between species, analyses were performed using the R-package *Aldex2*. OTU relative abundance was considered significantly different considering an expected Benjamini-Hochberg corrected p-value of < 0.1.

6. Phylosymbiotic signal detection

To assess the existence of a co-evolutive signal between the host phylogenetic tree and the clustering based on the bacterial community composition, the most commonly used methods are topological comparison metrics, such as the Robinson–Foulds distance and the more robust and sensitive matching cluster distance (Brooks et al. 2016; Kohl, Dearing, Bordenstein 2018; 2018; 2018; Claverie, Abergel 2018; Leigh et al. 2018; O'Brien et al. 2020; Ross et al. 2018). Robinson–Foulds calculates the distance between two trees as the smallest number of operations required to convert one topology (i.e. tree structure) to the other (Robinson, Foulds 1981). Matching cluster metric is a more refined computation considering congruency at the subtree level and therefore taking into account small topological changes that can affect incongruence (Bogdanowicz, Giaro 2013). The two metrics have been computed and normalized by dividing the result by the total possible congruency scores for the two trees, giving values ranking from 0 (complete congruence) to 1 (complete incongruence). Statistical significance of the distances was evaluated by comparing the host phylogenetic tree to 100 000 randomized dendrograms with equivalent topologies and estimating the p-value as the proportion of random trees giving an equivalent or more congruent result than the bacterial dendrogram. Distances, random trees and p-values were computed with an adapted Python

script (supplementary information Script 3) from Brooks and al. (Brooks et al. 2016) and the TreeCmp program (Bogdanowicz, Giaro, Wróbel 2012). Mantel tests were also performed to assess significance of the correlation between the bacterial composition distance matrix and the cophenetic distance matrix of the host tree, *i.e.*, the matrix of the height of the tree where the two branches that include two species merges into a single branch. A positive r-value, *i.e.,* a positive correlation between the matrices, indicates a potential phylosymbiosis link.

III. Results

1. Differences in the composition of the bacterial communities between corals and seawater

Before any further analysis, bacterial composition of the seawater samples was compared to the composition of the rest of the dataset. A significant difference allowed to assert that the observed bacterial composition is not from the surrounding water of the coral samples. PERMANOVA results showed that there is a significant difference in bacterial composition between seawater and coral samples (p-value = 0.001 < 0.05). Considering this, water samples were removed for the following analysis, removing 2287 OTUs (13 % of the total) being exclusively present in seawater. Principal Coordinates Analysis (PCoA) was used to plot an ordination plot on Bray-Curtis matrix distance presented below (Figure 11) and illustrates the compositional differences between seawater and coral samples. Seawater samples from the Red Sea and the Mediterranean Sea are noteworthy separated on the ordination plot.

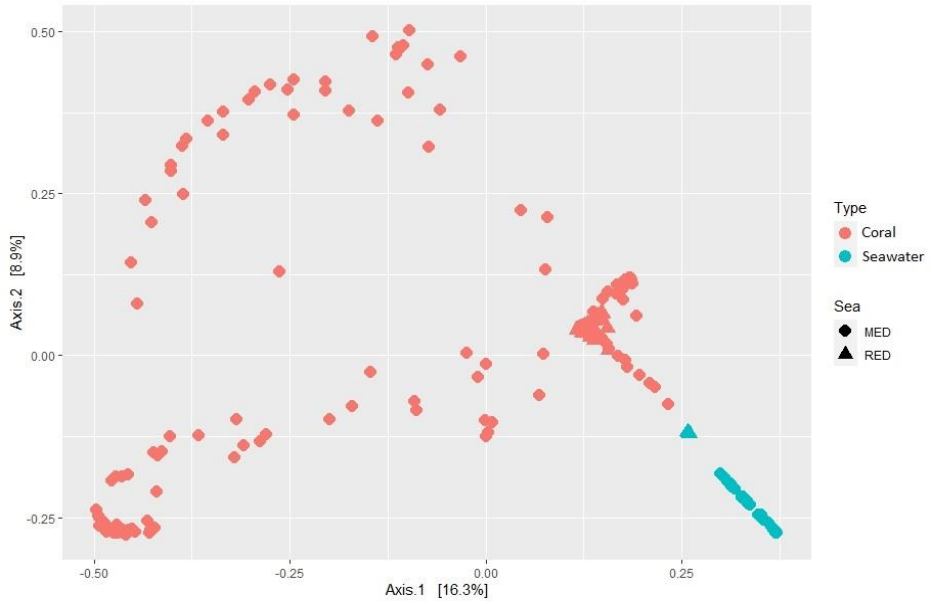

Figure 11: PCoA on Bray-Curtis distance matrix showing ordination of seawater and coral samples

2. Estimation of bacterial richness

The number of microbial species (α-diversity) within the microbiome of each coral species was estimated using the Chao1 index (Figure 12). Significant differences in α-diversity between species were observed (p-value = $5.588.10^{-10}$). Overall, α-diversity was low and did not differ significantly between coral species. However, Tukey's HSD test (Supplementary table 4) showed that the bacterial microbiome of *Sinularia polydactyla*, was more diverse than the bacterial microbiome of other species except *Alcyonium coralloides*, *Klyxum utinomii*, *Ovabunda sp.* and *Callogorgia verticillata*.

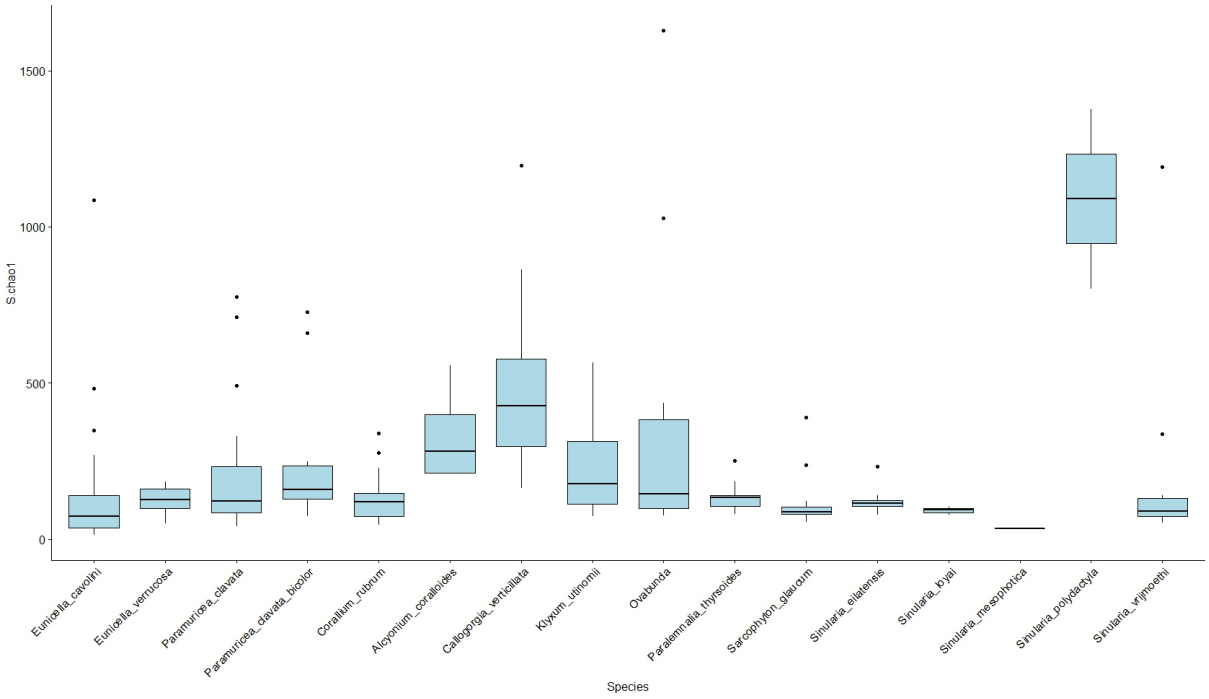

Figure 12: Bacterial richness estimation (Chao1) per coral species

3. Analysis of the bacterial community composition

Taking both the number of OTUs and their relative abundances into account, the β diversity of the bacterial microbiota of corals was investigated.

a. Differential composition between seas and coral species

Overall, the composition of the coral-associated bacterial communities differed between the Red and Mediterranean Seas (p-value = 1.10^{-4}) and between coral species (p-value = 1.10^{-4}). Non-metric multidimensional scaling (NMDS) was used to plot an ordination plot on Bray-Curtis matrix distance presented below (Figure 13). It illustrates the compositional differences between Mediterranean and Red Seas as well as between species.

Figure 13: NMDS on Bray-Curtis distance matrix showing ordination of coral samples (MED = Mediterranean Sea and RED = Red Sea)

Pairwise PERMANOVAs (supplementary table 5) were then used to test between which species the microbiota composition differed. All species from the Mediterranean Sea had significantly different bacterial community composition (p-value < 0.05) except for *Callogorgia verticillata* and *Corallium rubrum* (p-value = 0.063) even if they belong to different suborders according to WORMS taxonomy (see Figure 2 in the previous chapter II). In corals from the Red Sea, some species had no significant differences between their composition, especially between *Klyxum utinomii*, *Paralemnalia thyrsoides*, *Sarcophyton glaucum* and some of the *Sinularia* genus. *Alcyonium corralloides*, a Mediterranean species from the suborder Alcyoniina did not have a significant different composition than *Sinularia loyai* and *Sinularia polydactyla*, two Red Sea species also belonging to this suborder.

b. Dendrogram classification of the dataset

To better identify (dis)similarities in the composition of the coral-associated bacterial communities, a dendrogram (Figure 14) was built. Most of the dendrogram clusters matched with the octocoral taxonomy presented in II (Figure 2) as overall, the suborders Holaxonia, Calcaxonia, Scleraxonia and Alcyoniina are clustered separately. It is especially the case for the Mediterranean species. The sub-order of Holaxonia, *Eunicella verrucosa, Eunicella cavolini and Paramuricea clavata* clustered in the same branch. *Callorgorgia verticillata* from the Calcaxonia sub-order and *Corallium rubrum*, belonging to the sub-order of Scleraxonia were separated from the rest of the gorgonians. *Alcyonium coralloides* from the Alcyoniina sub-order was surprisingly not clustered in the same branch as the tropical Red Sea soft corals but with the red coral, a completely different taxonomic group. This correlation between bacterial communities' composition and taxonomy is further investigated in a later section after the construction of the phylogeny of the species based on the coral samples.

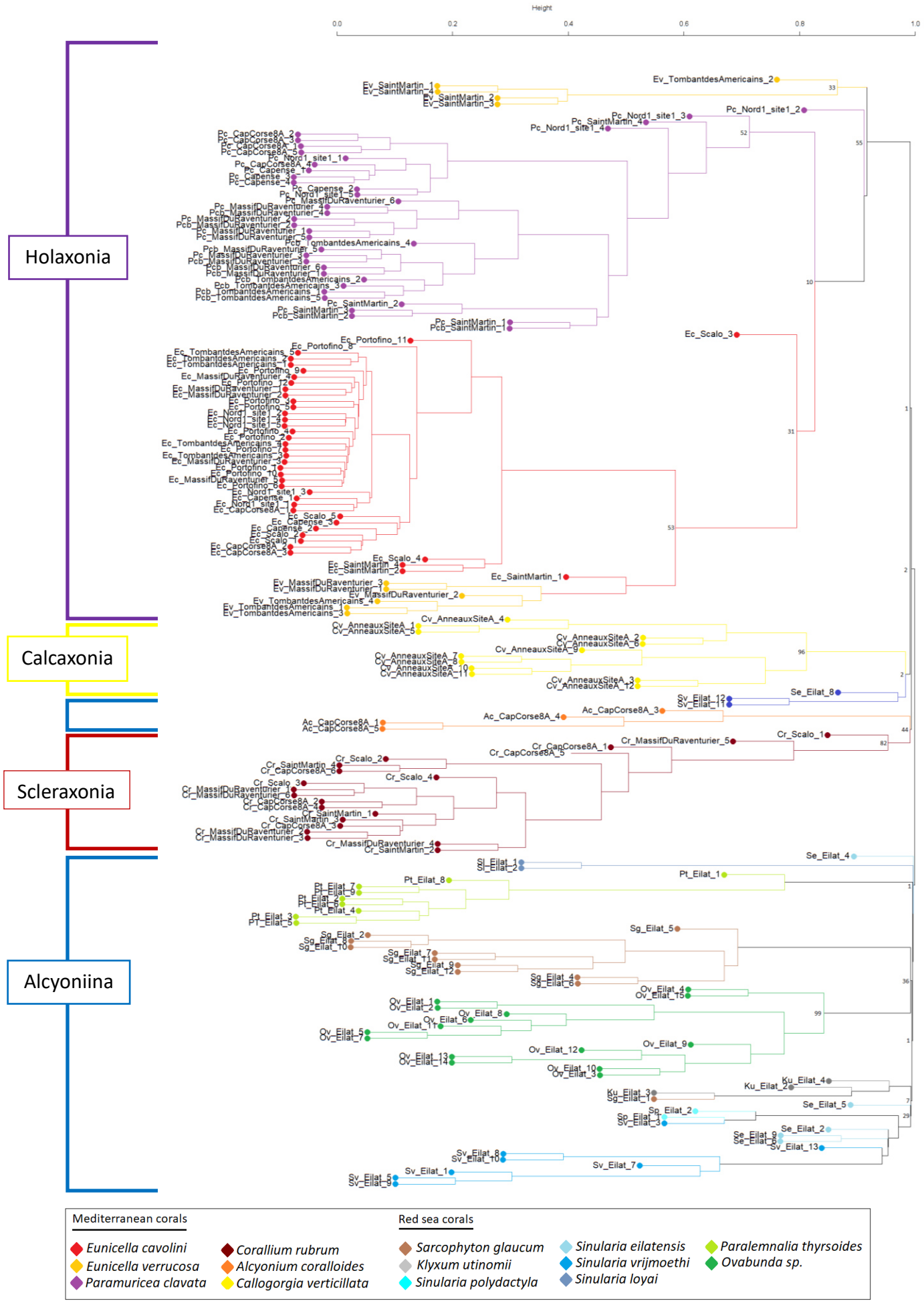

Figure 14: UPGMA hierarchical cluster analysis of the Bray-Curtis dissimilarity matrix based on the bacterial community composition of the coral samples

c. *Bacterial community composition*

Specific composition of the bacterial community has been investigated by grouping OTUs belonging to the same taxonomic classification (Figure 15).

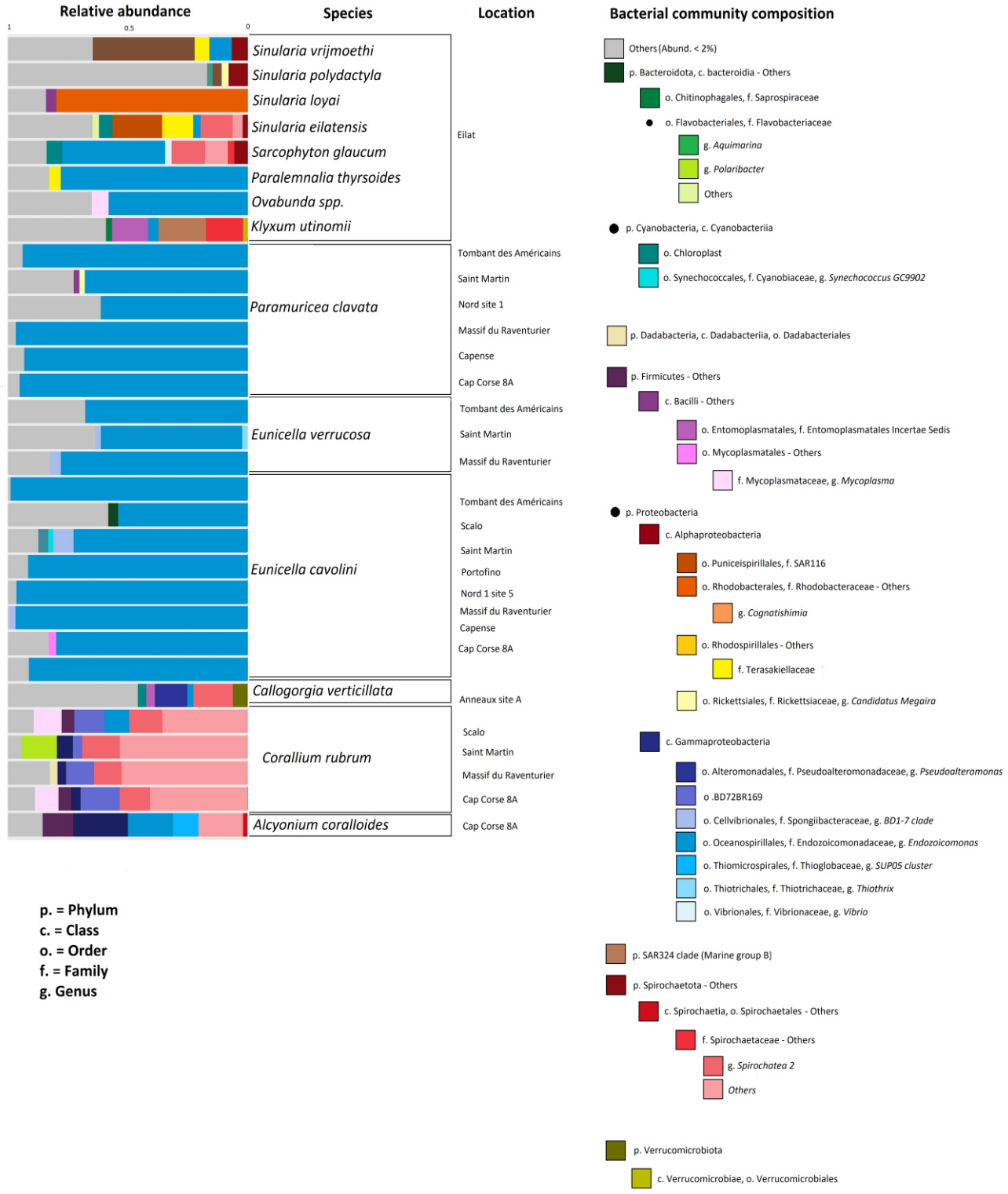

Figure 15: Bacterial community composition for each species per location

The Mediterranean gorgonians from the Holaxonia suborder had a very specific bacterial community, mostly dominated by members of the genus *Endozoicomonas (*52 % to 98 % of the bacterial composition), which are Gammaproteobacteria from the order Oceanospirillales. These bacteria were also found in the microbiota of some other Mediterranean and Red Sea octocoral species but in smaller proportions. In contrast, the composition of the microbiota of *Corallium rubrum* was driven by the phylum Spirochaetota especially from the Spirochaetaceae family (48 % to 67 % of the bacterial composition). Smaller proportions of Spirochaetota were found in *Callogorgia verticillata* (21 %), *Alcyonium corralloides* (15 %) and some Red Sea species. We also noted the presence of Firmicutes in *Corallium rubrum*, *Alcyonium coralloides*, *Callogorgia verticillata* and some Red Sea species. In the Red Sea species, the taxonomic diversity seemed higher than in the Mediterranean species as many different taxonomic groups are composing their bacterial communities.

4. Identification of differentially abundant OTUs

Because some species were clustering together, we investigated their similarity in bacterial community composition at the OTU level to determine on how many OTUs they differed. We first looked for differences in OTUs in the surprising cluster between *Corallium rubrum* and *Alcyonium coralloides* but also between the gorgonians *Eunicella* and *Paramuricea*. The abreviations p., c., o., f., and g. correspond respectively to Phylum, Class, Order, Family and Genus taxonomic levels.

a. Differences in OTUs abundance between Corallium rubrum and Alcyonium coralloides

Aldex t-test and Benjamini-Hochberg corrected p-value < 0.1 highlighted the presence of 5 OTUS significantly less abundant in *Corallium rubrum* (-) than *Alcyonium coralloides* and 2 OTUs significantly more abundant (+) as presented in table 4.

Table 4: List of OTU significantly different between C.rubrum and A.coralloides, (-) less abundant in Corallium rubrum than Alcyonium coralloides and (+) the opposite

OTU	Taxonomy	B-H p-value	Effect
OTU 73	p.Proteobacteria, c.Gammaproteobacteria, o.Thiomicrospirales, f.Thioglobaceae, g.*SUP05_cluster*	$1, 9.10^{-9}$	-
OTU 382	p.Proteobacteria, c.Gammaproteobacteria, o.Oceanospirillales, f.Endozoicomonadaceae, g.*Endozoicomonas*	0.08	-
OTU 1476	p.Spirochaetota, c.Spirochaetia, o.Spirochaetales, f.Spirochaetaceae, g.*Spirochaeta_2*	$1, 3.10^{-2}$	-
OTU 3022	p.Firmicutes, c.Bacilli, o.Mycoplasmatales, f.Mycoplasmataceae, g.*Mycoplasma*	$1, 6.10^{-2}$	-
OTU 10169	p.Proteobacteria, c.Gammaproteobacteria, o.Thiomicrospirales, f.Thioglobaceae, g.*SUP05_cluster*	$2, 6.10^{-4}$	-
OTU 4	p.Spirochaetota, c.Spirochaetia, o.Spirochaetales, f.Spirochaetaceae	0.09	+
OTU 16	p.Proteobacteria, c.Gammaproteobacteria, f.BD72BR169	0.09	+

The 2 high abundant Spirochaetaceae and Gammaproteobacteria BD72BR169 OTUs were significantly higher in *Corallium rubrum* than is *Alcyonium coralloides*. A *SUP05_cluster* genus was found higher abundant in *Alcyonium coralloides*. The other OTUs were relatively low abundant (OTU identification number indicates the relative abundance). We noted the significant higher presence of a low abundant Spirochaeta_2 genus in *Alcyonium coralloides.*

b. Differences in OTU abundance between Eunicella cavolini and Eunicella verrucosa

Aldex t-test and Benjamini-Hochberg corrected p-value highlighted the presence of 3 OTU that were significantly more abundant (+) in *Eunicella verrucosa* than *Eunicella cavolini* as presented in table 5.

Table 5: List of OTU significantly different between E.verrucosa and E.cavolini, (+) : significantly more abundant in Eunicella verrucosa than Eunicella cavolini

OTU	Taxonomy	B-H corrected p-value	Effect
OTU 8	p.Proteobacteria, c.Gammaproteobacteria, o.Oceanospirillales, f.Endozoicomonadaceae, g. *Endozoicomonas*	0.043	+
OTU 45	p.Cyanobacteria, c.Cyanobacteriia, o.Synechococcales, f.Cyanobiaceae, g.*Synechococcus_CC9902*	0.006	+
OTU 50	p.Cyanobacteria, c.Cyanobacteriia, o.Synechococcales, f.Cyanobiaceae, g.*Synechococcus_CC9902*	0.08	+

We noted the presence of a differentially higher abundant taxa *Endozoicomonas* in *Eunicella verrucosa* which was not present in *Eunicella cavolini*. The 2 other OTUs, from the genus *Synechococcus* were also relatively high abundant.

c. OTU differences between Paramuricea clavata and Paramuricea clavata bicolor

Only one very low abundant *Endozoicomonas* (OTU 16757) was found significantly higher abundant in *Paramuricea clavata bicolor.*

d. OTU differences between Paramuricea clavata and Eunicella cavolini

Both *Paramuricea* and *Eunicella* species had a high abundance of *Endozoicomonas*. It was interesting to compare if the same OTUs were found in their bacterial compositions. Aldex t-test and Benjamini-Hochberg corrected p-value highlighted the presence of 8 *Endozoicomonas* OTUs that were significantly more abundant (+) in *Paramuricea clavata* than *Eunicella cavolini* and 2 OTUs less abundant (-) as presented in table 6.

Table 6: List of OTU significantly different between Paramuricea clavata and Eunicella cavolini, (+) : OTUs significantly more abundant in Paramuricea clavata than Eunicella cavolini, (-) : the opposite

OTU	Taxonomy	B-H corrected p-value	Effect
OTU 2	p.Proteobacteria, c.Gammaproteobacteria, o.Oceanospirillales, f.Endozoicomonadaceae, g.*Endozoicomonas*	$4, 0.10^{-10}$	+
OTU 3	p.Proteobacteria, c.Gammaproteobacteria, o.Oceanospirillales, f.Endozoicomonadaceae, g.*Endozoicomonas*	$2, 0.10^{-8}$	+
OTU 8	p.Proteobacteria, c.Gammaproteobacteria, o.Oceanospirillales, f.Endozoicomonadaceae, g. *Endozoicomonas*	$4, 4.10^{-6}$	+
OTU 12	p.Proteobacteria, c.Gammaproteobacteria, o.Oceanospirillales, f.Endozoicomonadaceae, g.*Endozoicomonas*	$1, 8.10^{-12}$	+
OTU 5255	p.Proteobacteria, c.Gammaproteobacteria, o.Oceanospirillales, f.Endozoicomonadaceae, g.*Endozoicomonas*	0.03	+
OTU 8992	p.Proteobacteria, c.Gammaproteobacteria o.Oceanospirillales, f.Endozoicomonadaceae, g.*Endozoicomonas*	$1, 2.10^{-4}$	+
OTU 9277	p.Proteobacteria, c.Gammaproteobacteria, o.Oceanospirillales, f.Endozoicomonadaceae, g.*Endozoicomonas*	$4, 5.10^{-4}$	+
OTU 15611	p.Proteobacteria, c.Gammaproteobacteria, o.Oceanospirillales, f.Endozoicomonadaceae, g.*Endozoicomonas*	0.02	+
OTU 5	p.Proteobacteria, c.Gammaproteobacteria, o.Oceanospirillales, f.Endozoicomonadaceae, g.*Endozoicomonas*	$1, 3.10^{-4}$	-
OTU 35	p.Proteobacteria, c.Gammaproteobacteria, o.Cellvibrionales, f.Spongiibacteraceae, g.*BD1-7_clade*	0.02	-

5. Phylogenetic tree construction

Overall, the phylogenetic tree constructed from the sequencing of the 3 genes COI, MutS and 12S seemed to be consistent with the taxonomy defined in chapter II (Figure 2). The suborders were correctly separated except for the Scleraxonia (*Corallium rubrum*) and Calcaxonia (*Callogorgia verticillata*). Inside the Alcyoniina suborder, species distribution did not well follow the taxonomy especially *Ovabunda spp*. and *Paralemnalia thyrsoides* that should have been separated from the other species as they belong to different families. The tree is presented on the left part (1) of the figure 15 in the following part 6.

6. Phylosymbiosis signal detection

a. Search for phylosymbiosis considering all coral species

Abundance of each OTUs was averaged for samples from the same species to get a consensus bacterial composition for each species and build a simplified dendrogram to compare with the phylogenetic tree of the coral hosts as presented in the figure 16.

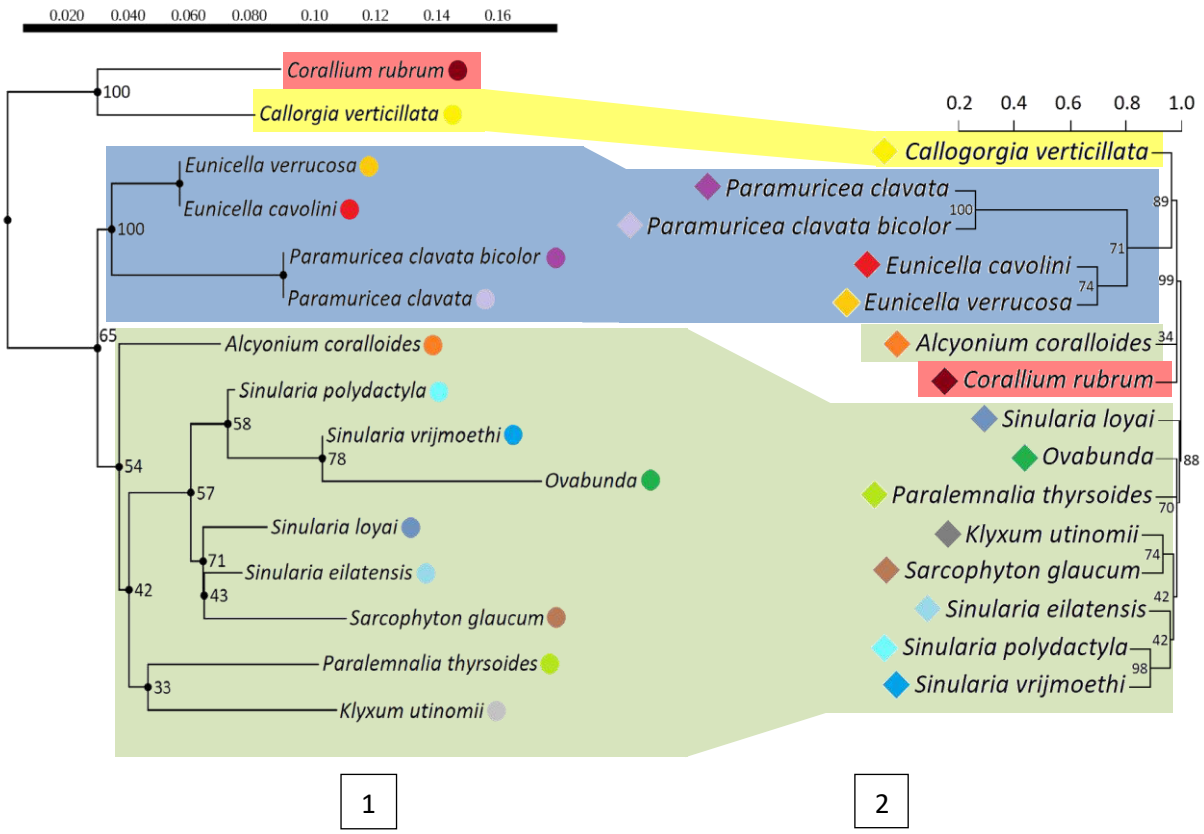

Figure 16: Juxtaposition of species phylogeny (1) and microbiome dendrogram (2)

Robinson-Foulds distance (0.68 with a p-value = 3.3.10-4) and matching cluster distance (0.85 with a p-value=0.045) were close to 1 and suggested that there were no signal of phylosymbiosis considering all coral species. Mantel test between the cophenetic distance matrix gave similar results with a r-value= -0.024 close to 0, indicating no significant correlation in the structure of the 2 matrices. As the structure of the data suggests more correlation within some suborders, such as for the Mediterranean gorgonians, a phylosymbiosis signal was also studied considering separately the Mediterranean and Red Sea coral species.

b. Search for phylosymbiosis within the Mediterranean Sea coral species

Robinson-Foulds distance (0.28 with a p-value = 0.01) and matching cluster distance (0.32 with a p-value=0.001) were closer to 0, suggesting a phylosymbiotic signal within the Mediterranean coral species. Mantel test between the cophenetic distance matrix gave similar results with a r-value of 0.44 (p-value = 0.05), indicating a better correlation in the structure of the two matrices.

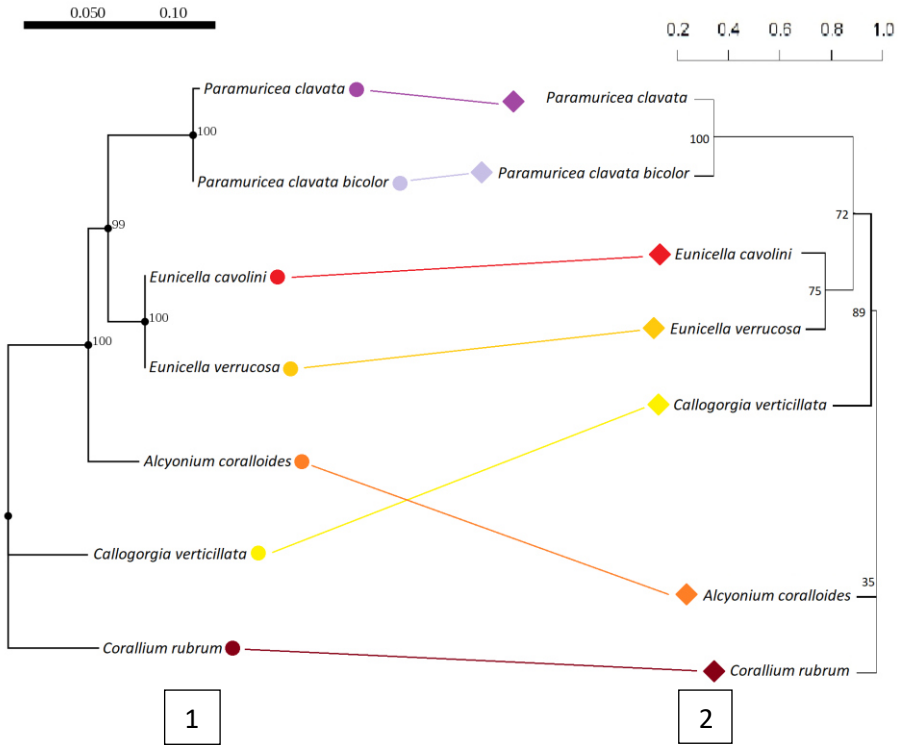

Figure 17: Juxtaposition of Mediterranean species phylogeny (1) and microbiome dendrogram (2)

A phylosymbiotic pattern was thus observed within the Mediterranean coral species, as most of the species matched their microbiome composition, except *Alcyonium coralloides* and *Callogorgia verticillata* whose position between the host phylogeny and microbial composition was "reversed". *Corallium rubrum* and *Alcyonium coralloides* bacterial community compositions were still clustered together even if their position was distant in the phylogeny (Figure 17).

c. *Search for phylosymbiosis within the Red Sea coral species*

There is no clear identification of a phylosymbiosis pattern within the Red Sea species. Both phylogenetic tree and microbiome dendrogram are shown in supplementary figure 3. Robinson-Foulds distance (1.08 with a p-value = 0.99) and matching cluster distance (0.85 with a p-value=0.11) were close to 1, potentially indicating no phylosymbiotic signal within the Red Sea species but regarding the p-values, no conclusion can be provided. Mantel test between the cophenetic distance matrix gave similar results with a r-value= -0.23 closer to 0, indicating no strong correlation in the structure of the 2 matrices.

IV. Discussion

1. Octocorals are associated to specific bacterial communities

The α-diversity was measured for each coral species, and summarized the structure of the bacterial community in terms of its richness (number of taxonomic groups). The low index obtained for most species means that only a small number of OTUs (around 1500-3000 OTUs) was present in the community composition of each coral. In comparison, the seawater samples had around 6800 OTUs. PERMANOVA confirmed that the bacterial community composition of corals differed from that of seawater, as shown previously (van de Water et al. 2018; Haydon et al. 2022), suggesting that corals have a specific bacterial community and exert some control over it (van de Water, Allemand, Ferrier-Pagès 2018; Dunphy et al. 2019). Although corals are associated with a restricted community of bacteria, differences in the number of associated bacterial species (or OTUs) can be observed among different coral species. For example, in the Mediterranean Sea (Chao1 mean = 235.22), *Callogorgia verticillata* had the most diverse bacterial microbiome (Chao1 = 497.046 ± 299.659). Compared to the other species, it is a depth specialist and the only representative of the suborder Calcaxonia. Therefore, its bacterial association could be due to a different evolutionary pattern than the other Mediterranean species. *Sinularia polydactyla* had the highest α-diversity index (Chao1=1089.53 ± 407.05), with most bacterial taxa representing less than 2% of the total abundance. This species is known for its strong antimicrobial defense against colonizing marine organisms (Eskander et al. 2018). This antimicrobial activity could increase competition among potential bacterial associations and explain the high bacterial diversity of this species. Overall, Red Sea octocorals had a broader range of taxa in their bacterial communities than Mediterranean octocorals, with many taxa occurring at very low abundance. This could be explained by a thick layer of mucus around their tissues, which has its own bacterial community, that differs from that of the animal tissue (Glasl, Herndl, Frade 2016; Hadaidi et al. 2017; Kooperman et al. 2007). Indeed, the mucus is composed of polymeric glycoproteins and lipids (Bythell, Wild 2011), which provide a highly nutritious medium on which a diverse assemblage of microbes can grow.

Detailed analysis of the bacterial community showed that mesophotic octocorals from the Mediterranean, particularly gorgonians of the Holaxonia family, had a high abundance of *Endozoicomonas*, as observed in shallow populations at different locations and seasons (van de Water et al. 2017c; Bayer et al. 2013b; La Rivière, Garrabou, Bally 2015; Ransome et al. 2014). *Endozoicomonas* OTUs were present in gorgonians at varying abundances, as also observed previously (van de Water et al. 2017c), with some OTUs very abundant and present in all samples (OTU 1, OTU 2, OTU 5, OTU 6) and some very rare and present only in some samples. Some soft corals of the Red Sea, *Klyxum utinomii, Ovabunda* spp., *Paralemnalia thyrsoides*, *Sarcophyton glaucum*, *Sinularia eilatensis* and S. *vrijmoethi* had also some *Endozoicomonas* OTUs but much less abundant than in gorgonians. Their constant presence in the core microbiome of most octocoral species (Haydon et al. 2022; Keller-Costa et al. 2022; Park et al. 2022) underscores their importance as symbionts. *Endozoicomonas* bacteria are symbiotic organisms of numerous marine hosts, from simple invertebrates such as corals to complex vertebrates such as fish. Yet, their function in the holobiont remains poorly understood (Neave et al. 2016). They may be involved in the digestion of complex molecules (Speck,

Donachie 2012), nutrient cycling (Pogoreutz et al. 2022) and sulfur cycling (dimethylsulfoniopropionate transformation, Tandon et al. 2020). They may also play a role in coral health, as lower abundance of Endozoicomonadaceae has been found in diseased corals compared to healthy corals (Ransome et al. 2014; La Rivière et al. 2013). It has also been hypothesized that *Endozoicomonas*, as important architectural microbes, may structure the composition of the microbiome by regulating bacterial colonization of the host through the production of bioactive secondary metabolites or probiotics to eliminate competing pathogenic bacteria (Jessen et al. 2013; Porporato et al. 2013b; Morrow et al. 2015).

Another bacterial taxon, Spirochaetaceae dominated the community of the Mediterranean *Corallium rubrum* and was also abundant in the tropical *Klyxum utinomii*, *Sarcophyton glaucum*, *Sinularia polydactyla*, *S. eilatensis* and *S. vrimoethi*. The exceptionally high abundance and persistence of these bacteria in the microbiome of *Corallium rubrum* distinguished this species within the Anthozoans class (van de Water et al. 2016b). These bacteria may also play an important role in host physiology, although their function in the holobiont is still not well understood. Some Spirochaetes have been shown to be involved in nitrogen fixation in termite guts and freshwater sediments (Lilburn et al. 2001), but this remains to be investigated for corals.

The other low abundant bacteria (less than 2 %), which may represent all together up to 82 % of the total bacterial community depending on the coral species, are largely unknown. These low-abundant bacteria may also have important functions in the holobiont, or may present different tolerance levels to environmental factors (van de Water et al. 2017). This range of different bacteria available could allow corals to switch OTUs to maintain certain functions in response to changing conditions that affect their physiological needs.

2. Octocorals present similarities and dissimilarities in their bacterial community composition according to their location and taxonomy

The dendrogram based on the composition of the bacterial communities showed a clear separation between the Mediterranean and Red Sea samples (bootstrap value of 0.88), which was confirmed by the PERMANOVA results. These findings suggest that the bacterial microbiome of octocorals, even within the same suborder, may have evolved differently depending on environmental conditions. For example, species of the same suborder Alcyoniina exhibited a different bacterial community composition depending on their origin (Mediterranean Sea-*Alcyonium coralloides* and Red Sea - Eilat samples). The Mediterranean and Red Sea were separated for millions of years before the opening of the Suez Canal in 1869 (Hamza, Abdel-Latif 2003) and their connection remains tenuous today. The light, temperature and salinity conditions in these two seas are completely different, which may contribute to the observed differences in the microbiome. A significant effect of the environmental conditions on coral microbiome has often been observed in studies on tropical coral species (Lima et al. 2020; Roder et al. 2015), favoring the occurrence of different bacterial taxa according to the conditions (Pantos et al. 2015).

The dendrogram however showed similarities in the bacterial composition of several coral species, namely between the two *Eunicella* spp (only 0.1% difference in OTUs) between *Corallium rubrum* and *Alcyonium coralloides* (only 0.4% difference in OTUs) and between the two *Paramuricea clavata* colormorphs. The colormorphs shared a very similar bacterial community composition, with only one (out of 2676 shared bacterial taxa) significantly more abundant *Endozoicomonas* in the *bicolor* colormorph. Overall, very similar OTUs in these groups of coral species explained their close grouping in the dendrogram (Figure 14) and suggests that the microbiome was conserved during their evolution. The presence of similar OTUs between *Corallium rubrum* and *Alcyonium coralloides* and the close clustering of their bacterial community compositions in the dendrogram (Figure 13) is however surprising. The two species belong to very different taxonomic groups with no clear relationship in their habitat and physiology (*Alcyonium coralloides* is an encrusting epibiont of gorgonians (McFadden 1999) while *Corallium rubrum* grows its colonies directly on rocky surfaces).

Although the taxonomic composition of the bacterial community of *Eunicella cavolini* and *Paramuricea clavata* appeared similar, with a strong dominance of *Endozoicomonas*, differences in the *Endozoicomonas* genus, resulted in separate clustering in the dendrogram (72% of bootstrap replications). Since these two species are phylogenetically close, this fits the idea expressed above of ancient conservation of their bacterial microbiome, this time within the suborder Holaxonia.

3. Unclear signals of phylosymbiosis in octocorals are driven by multiple factors

Composition of the bacterial communities of the octocorals appeared to be species-specific, with taxa systematically associated with the same species (core microbiome). However, similarities among suborders were also found. This suggests the existence of a phylosymbiotic signal, *i.e.* a link between host evolutionary history and microbiome diversity (Lim, Bordenstein 2020). Such signal have already been observed between Scleractinians in Australian reefs (Pollock et al. 2018). According to the topological comparisons and Mantel tests based on both microbial communities and host genotypes, there is however no clear phylosymbiotic signal between the octocoral species studied here when all species are considered. However, signs of phylosymbiosis were evident to some degree in the temperate Mediterranean octocorals, and even to the species level in the suborder Holaxonia, suggesting that the bacterial communities might structure their composition in concordance with their host phylogeny. As these Mediterranean species, especially gorgonians, have a very specific microbiome stable in time and space as previously described, they are probably among the "microbiome regulators", which exert a strong control on their microbial community (Ziegler et al. 2019). As their microbiome probably evolved closely with the host phylogeny, this type of behavior could have contributed to the clear pattern of phylosymbiosis observed in the Mediterranean group. This also suggests possible vertical transmission (maternal inheritance) of bacterial communities between coral generations, as suggested by van de Water et al. (2018). Vertical transmission of the microbiota has already been observed in brooding scleractinian octocorals such as *Porites astreoides* (Sharp et al. 2012), as well as for photosynthetic octocoral symbionts belonging to the Symbiodiniaceae (Forcioli et al. 2011)+. The vertical transmission

of the microbiota in octocorals is favored by the fact that octocorals are brooders (larval development inside the colony), and larvae are in direct contact with the mother colony and its microbiome. Further studies on this topic in gorgonians would greatly contribute to understanding the evolutionary relationship of octocoral symbiosis.

Unlike Mediterranean octocorals, tropical octocorals do not exhibit any phylosymbiotic relationship with their microbiome. These species, particularly *Sinularia spp.*, may belong to what has been defined as "microbiome conformers" (Ziegler et al. 2019; Lu et al. 2020; Haydon et al. 2022). Conformers are flexible in their choice of microbial partners and therefore have the potential for dynamic adaptation of the microbiome to environmental change. The fact that tropical soft corals can readily change the composition of their microbiome depending on location, time and environmental conditions explains why there is likely no link between host phylogeny and bacterial community evolution. Tropical octocorals also produce large amounts of mucus. Coral mucus harbours a dynamic microbial community that changes in composition between new and aged mucus (Glasl, Herndl, Frade 2016) and under environmental changes (Kooperman et al. 2007). Coral tissue samples are often contaminated by coral mucus, which could affect the bacterial community composition of the Red Sea octocorals. It would be interesting to conduct different studies with the same octocoral species, specifically targeting different anatomical regions of the coral hosts to determine if this would result in different phylosymbiosis patterns.

Another reason for the lack of phylosymbiosis could be the underrepresentation of the Red Sea octocoral suborders. All Red Sea species belong to the suborder Alcyoniina and originate from the same location, whereas Mediterranean species have a wider geographical range and include three suborders. Debelius et al. (2016) and Lim and Bordenstein (2020) emphasized the importance of the size of the dataset for studying microbial ecology and advocated for large-scale studies that shed light on which variables have broad effects on the microbiome. Expanding the dataset to include more octocoral species from different locations and suborders in the dataset could improve the analysis.

In addition, the phylogenetic tree of the coral hosts does not agree with the known taxonomy concerning the suborder Alcyoniina. In particular, some gene sequences of *Ovabunda spp*. have been identified as belonging to *Sinularia vrijmoethi*. These species are closely related genetically, and the sequenced genes COI, MutS and 12S may not be well suited for the identification of species in the Alcyoniina suborder.

V. Conclusion

The bacterial microbiome of Mediterranean octocorals was relatively stable at mesophotic depth, and was found to be dominated by two taxonomic groups, *Endozoicomonas* in the gorgonians and Spirochaetaceae in the red coral *Corallium rubrum*. Mediterranean Octocorals probably behave as "microbiome regulators", which exert a strong control over their bacterial communities. Therefore, a phylosymbiotic signal was observed among these Mediterranean samples.

A higher taxonomic diversity in the bacterial communities was observed in Red Sea octocorals species, suggesting that they are more "microbiome conformers", flexible in the composition of their microbiome. As a consequence, among other factors, no phylosymbiotic signal could be observed, either within Red Sea octocorals or between all samples. Expansion of the dataset to include more diverse samples, encompassing representatives of multiple Red Sea suborders, would be necessary to improve our understanding of host-symbiont dynamics and phylosymbiosis associations in tropical octocorals. It would also be interesting to sample several sites in order to have a more representative view of the bacterial communities of the Red Sea.

The bioinformatics methods used in this study are part of the standard approach in microbial ecology. Recent publications have proposed new approaches, particularly in relation to the statistical treatment of microbial diversity and composition, that takes into account the compositional nature of microbiome datasets (CoDa *i.e* Compositional Data Analysis) and propose tools to get rid of methods such as the questionable rarefaction principle (Gloor et al. 2017). Bioinformaticians are increasingly using denoising methods that generate amplicon sequence variants (ASVs) to replace the sequence identity-based clustering approach that generates OTUs. The choice of method to study microbial biodiversity appears to have a major impact on diversity measurement, even more important than the threshold for rarefaction and OTU identity (Chiarello et al. 2022; Jeske, Gallert 2022). It would be interesting to apply these new methods in the future in the frame of a publication.

Beyond phylosymbiosis, finer tests of host-microbe cophylogeny, as proposed in Lawler et al. (2016), could allow the identification of specific microbial lineages (e.g., in Endozoicomonas or Spirochaetacae) that may have co-evolved with their hosts. This would support the notion that these microbial families perform important host functions and have formed stable symbiotic relationships over time.

Bibliography

AINSWORTH, Tracy D, KRAUSE, Lutz, BRIDGE, Thomas, TORDA, Gergely, RAINA, Jean-Baptise, ZAKRZEWSKI, Martha, GATES, Ruth D, PADILLA-GAMIÑO, Jacqueline L, SPALDING, Heather L, SMITH, Celia, WOOLSEY, Erika S, BOURNE, David G, BONGAERTS, Pim, HOEGH-GULDBERG, Ove et LEGGAT, William, 2015. The coral core microbiome identifies rare bacterial taxa as ubiquitous endosymbionts. *The ISME Journal*. octobre 2015. Vol. 9, n° 10, pp. 2261-2274. DOI 10.1038/ismej.2015.39.

BARLOW, Jos, FRANÇA, Filipe, GARDNER, Toby A., HICKS, Christina C., LENNOX, Gareth D., BERENGUER, Erika, CASTELLO, Leandro, ECONOMO, Evan P., FERREIRA, Joice, GUÉNARD, Benoit, GONTIJO LEAL, Cecília, ISAAC, Victoria, LEES, Alexander C., PARR, Catherine L., WILSON, Shaun K., YOUNG, Paul J. et GRAHAM, Nicholas A. J., 2018. The future of hyperdiverse tropical ecosystems. *Nature*. juillet 2018. Vol. 559, n° 7715, pp. 517-526. DOI 10.1038/s41586-018-0301-1.

BAYER, T, ARIF, C, FERRIER-PAGÈS, C, ZOCCOLA, D, ARANDA, M et VOOLSTRA, Cr, 2013a. Bacteria of the genus Endozoicomonas dominate the microbiome of the Mediterranean gorgonian coral Eunicella cavolini. *Marine Ecology Progress Series*. 8 avril 2013. Vol. 479, pp. 75-84. DOI 10.3354/meps10197.

BAYER, T, ARIF, C, FERRIER-PAGÈS, C, ZOCCOLA, D, ARANDA, M et VOOLSTRA, Cr, 2013b. Bacteria of the genus Endozoicomonas dominate the microbiome of the Mediterranean gorgonian coral Eunicella cavolini. *Marine Ecology Progress Series*. 8 avril 2013. Vol. 479, pp. 75-84. DOI 10.3354/meps10197.

BHARTI, Richa et GRIMM, Dominik G, 2021. Current challenges and best-practice protocols for microbiome analysis. *Briefings in Bioinformatics*. 18 janvier 2021. Vol. 22, n° 1, pp. 178-193. DOI 10.1093/bib/bbz155.

BOGDANOWICZ, Damian et GIARO, Krzysztof, 2013. On a matching distance between rooted phylogenetic trees. *International Journal of Applied Mathematics and Computer Science*. 1 septembre 2013. Vol. 23, n° 3, pp. 669-684. DOI 10.2478/amcs-2013-0050.

BOGDANOWICZ, Damian, GIARO, Krzysztof et WRÓBEL, Borys, 2012. TreeCmp: Comparison of Trees in Polynomial Time. *Evolutionary Bioinformatics*. janvier 2012. Vol. 8, pp. EBO.S9657. DOI 10.4137/EBO.S9657.

BOURNE, David G., GARREN, Melissa, WORK, Thierry M., ROSENBERG, Eugene, SMITH, Garriet W. et HARVELL, C. Drew, 2009. Microbial disease and the coral holobiont. *Trends in Microbiology*. décembre 2009. Vol. 17, n° 12, pp. 554-562. DOI 10.1016/j.tim.2009.09.004.

BRAY, J. Roger et CURTIS, J. T., 1957. An Ordination of the Upland Forest Communities of Southern Wisconsin. *Ecological Monographs*. octobre 1957. Vol. 27, n° 4, pp. 325-349. DOI 10.2307/1942268.

BROOKS, Andrew W., KOHL, Kevin D., BRUCKER, Robert M., VAN OPSTAL, Edward J. et BORDENSTEIN, Seth R., 2016. Phylosymbiosis: Relationships and Functional Effects of Microbial Communities across Host Evolutionary History. RELMAN, David (éd.), *PLOS Biology*. 18 novembre 2016. Vol. 14, n° 11, pp. e2000225. DOI 10.1371/journal.pbio.2000225.

BYTHELL, John C. et WILD, Christian, 2011. Biology and ecology of coral mucus release. *Journal of Experimental Marine Biology and Ecology*. novembre 2011. Vol. 408, n° 1-2, pp. 88-93. DOI 10.1016/j.jembe.2011.07.028.

CASAS-GÜELL, Edgar, TEIXIDÓ, Núria, GARRABOU, Joaquim et CEBRIAN, Emma, 2015. Structure and biodiversity of coralligenous assemblages over broad spatial and temporal scales. *Marine Biology*. avril 2015. Vol. 162, n° 4, pp. 901-912. DOI 10.1007/s00227-015-2635-7.

CLAVERIE, Jean-Michel et ABERGEL, Chantal, 2018. Mimiviridae: An Expanding Family of Highly Diverse Large dsDNA Viruses Infecting a Wide Phylogenetic Range of Aquatic Eukaryotes. *Viruses*. 18 septembre 2018. Vol. 10, n° 9, pp. 506. DOI 10.3390/v10090506.

COLL, Marta, PIRODDI, Chiara, STEENBEEK, Jeroen, KASCHNER, Kristin, BEN RAIS LASRAM, Frida, AGUZZI, Jacopo, BALLESTEROS, Enric, BIANCHI, Carlo Nike, CORBERA, Jordi, DAILIANIS, Thanos, DANOVARO, Roberto, ESTRADA, Marta, FROGLIA, Carlo, GALIL, Bella S., GASOL, Josep M., GERTWAGEN, Ruthy, GIL, João, GUILHAUMON, François, KESNER-REYES, Kathleen, KITSOS, Miltiadis-Spyridon, KOUKOURAS, Athanasios, LAMPADARIOU, Nikolaos, LAXAMANA, Elijah, LÓPEZ-FÉ DE LA CUADRA, Carlos M., LOTZE, Heike K., MARTIN, Daniel, MOUILLOT, David, ORO, Daniel, RAICEVICH, Saša, RIUS-BARILE, Josephine, SAIZ-SALINAS, Jose Ignacio, SAN VICENTE, Carles, SOMOT, Samuel, TEMPLADO, José, TURON, Xavier, VAFIDIS, Dimitris, VILLANUEVA, Roger et VOULTSIADOU, Eleni, 2010. The Biodiversity of the Mediterranean Sea: Estimates, Patterns, and Threats. BOGRAD, Steven J. (éd.), *PLoS ONE*. 2 août 2010. Vol. 5, n° 8, pp. e11842. DOI 10.1371/journal.pone.0011842.

DAVIS, Nicole M., PROCTOR, Diana M., HOLMES, Susan P., RELMAN, David A. et CALLAHAN, Benjamin J., 2018. Simple statistical identification and removal of contaminant sequences in marker-gene and metagenomics data. *Microbiome*. décembre 2018. Vol. 6, n° 1, pp. 226. DOI 10.1186/s40168-018-0605-2.

DAVY, Simon K., ALLEMAND, Denis et WEIS, Virginia M., 2012. Cell Biology of Cnidarian-Dinoflagellate Symbiosis. *Microbiology and Molecular Biology Reviews*. juin 2012. Vol. 76, n° 2, pp. 229-261. DOI 10.1128/MMBR.05014-11.

DEBELIUS, Justine, SONG, Se Jin, VAZQUEZ-BAEZA, Yoshiki, XU, Zhenjiang Zech, GONZALEZ, Antonio et KNIGHT, Rob, 2016. Tiny microbes, enormous impacts: what matters in gut microbiome studies? *Genome Biology*. décembre 2016. Vol. 17, n° 1, pp. 217. DOI 10.1186/s13059-016-1086-x.

DUNPHY, Courtney M., GOUHIER, Tarik C., CHU, Nathaniel D. et VOLLMER, Steven V., 2019. Structure and stability of the coral microbiome in space and time. *Scientific Reports*. décembre 2019. Vol. 9, n° 1, pp. 6785. DOI 10.1038/s41598-019-43268-6.

EDGAR, Robert C. et FLYVBJERG, Henrik, 2015. Error filtering, pair assembly and error correction for next-generation sequencing reads. *Bioinformatics*. 1 novembre 2015. Vol. 31, n° 21, pp. 3476-3482. DOI 10.1093/bioinformatics/btv401.

ESKANDER, Rehab, AL-SOFYANI, Abdulmohsin A., EL-SHERBINY, Mohsen M. O., BA-AKDAH, Mohammad Abdulaziz et SATHEESH, Sathianeson, 2018. Chemical Defense of Soft Coral Sinularia polydactyla from the Red Sea Against Marine Biofilm-Forming Bacteria. *Journal of Ocean University of China*. décembre 2018. Vol. 17, n° 6, pp. 1451-1457. DOI 10.1007/s11802-018-3657-9.

FISHER, Rebecca, O'LEARY, Rebecca A., LOW-CHOY, Samantha, MENGERSEN, Kerrie, KNOWLTON, Nancy, BRAINARD, Russell E. et CALEY, M. Julian, 2015. Species Richness on Coral Reefs and the Pursuit of Convergent Global Estimates. *Current Biology*. février 2015. Vol. 25, n° 4, pp. 500-505. DOI 10.1016/j.cub.2014.12.022.

FORCIOLI, D, MERLE, Pl, CALIGARA, C, CIOSI, M, MUTI, C, FRANCOUR, P, CERRANO, C et ALLEMAND, D, 2011. Symbiont diversity is not involved in depth acclimation in the Mediterranean sea whip

Eunicella singularis. *Marine Ecology Progress Series*. 20 octobre 2011. Vol. 439, pp. 57-71. DOI 10.3354/meps09314.

GLASL, Bettina, HERNDL, Gerhard J et FRADE, Pedro R, 2016. The microbiome of coral surface mucus has a key role in mediating holobiont health and survival upon disturbance. *The ISME Journal*. septembre 2016. Vol. 10, n° 9, pp. 2280-2292. DOI 10.1038/ismej.2016.9.

GRAY, Michael A., STONE, Robert P., MCLAUGHLIN, Molly R. et KELLOGG, Christina A., 2011. Microbial consortia of gorgonian corals from the Aleutian islands: Microbial consortia of Aleutian gorgonians. *FEMS Microbiology Ecology*. avril 2011. Vol. 76, n° 1, pp. 109-120. DOI 10.1111/j.1574-6941.2010.01033.x.

GUINDON, Stéphane, DUFAYARD, Jean-François, LEFORT, Vincent, ANISIMOVA, Maria, HORDIJK, Wim et GASCUEL, Olivier, 2010. New Algorithms and Methods to Estimate Maximum-Likelihood Phylogenies: Assessing the Performance of PhyML 3.0. *Systematic Biology*. 29 mars 2010. Vol. 59, n° 3, pp. 307-321. DOI 10.1093/sysbio/syq010.

HADAIDI, Ghaida, RÖTHIG, Till, YUM, Lauren K., ZIEGLER, Maren, ARIF, Chatchanit, RODER, Cornelia, BURT, John et VOOLSTRA, Christian R., 2017. Stable mucus-associated bacterial communities in bleached and healthy corals of Porites lobata from the Arabian Seas. *Scientific Reports*. juin 2017. Vol. 7, n° 1, pp. 45362. DOI 10.1038/srep45362.

HAMZA, M et ABDEL-LATIF, M, 2003. The construction of the Suez canal. [en ligne]. 2003. DOI 10.2495/MH030111. Disponible à l'adresse : https://www.witpress.com/Secure/elibrary/papers/MH03/MH03011FU.pdf

HAYDON, Trent D., SUGGETT, David J., SIBONI, Nachshon, KAHLKE, Tim, CAMP, Emma F. et SEYMOUR, Justin R., 2022. Temporal Variation in the Microbiome of Tropical and Temperate Octocorals. *Microbial Ecology*. mai 2022. Vol. 83, n° 4, pp. 1073-1087. DOI 10.1007/s00248-021-01823-7.

HERNANDEZ-AGREDA, Alejandra, LEGGAT, William, BONGAERTS, Pim et AINSWORTH, Tracy D., 2016. The Microbial Signature Provides Insight into the Mechanistic Basis of Coral Success across Reef Habitats. ROSENBERG, Eugene et AZAM, Farooq (éd.), *mBio* [en ligne]. 7 septembre 2016. Vol. 7, n° 4. [Consulté le 17 février 2022]. DOI 10.1128/mBio.00560-16. Disponible à l'adresse : https://journals.asm.org/doi/10.1128/mBio.00560-16

HUGHES, Jennifer B., HELLMANN, Jessica J., RICKETTS, Taylor H. et BOHANNAN, Brendan J. M., 2001. Counting the Uncountable: Statistical Approaches to Estimating Microbial Diversity. *Applied and Environmental Microbiology*. octobre 2001. Vol. 67, n° 10, pp. 4399-4406. DOI 10.1128/AEM.67.10.4399-4406.2001.

ILLUMINA I., 2013. *16S Metagenomic Sequencing Library Preparation.* 2013.

JESSEN, Christian, VILLA LIZCANO, Javier Felipe, BAYER, Till, RODER, Cornelia, ARANDA, Manuel, WILD, Christian et VOOLSTRA, Christian R, 2013. In-situ Effects of Eutrophication and Overfishing on Physiology and Bacterial Diversity of the Red Sea Coral Acropora hemprichii. GILBERT, Jack Anthony (éd.), *PLoS ONE*. 22 avril 2013. Vol. 8, n° 4, pp. e62091. DOI 10.1371/journal.pone.0062091.

KAHNG, S. E., GARCIA-SAIS, J. R., SPALDING, H. L., BROKOVICH, E., WAGNER, D., WEIL, E., HINDERSTEIN, L. et TOONEN, R. J., 2010. Community ecology of mesophotic coral reef ecosystems. *Coral Reefs*. juin 2010. Vol. 29, n° 2, pp. 255-275. DOI 10.1007/s00338-010-0593-6.

KELLER-COSTA, Tina, KOZMA, Lydia, SILVA, Sandra G., TOSCAN, Rodolfo, GONÇALVES, Jorge, LAGO-LESTÓN, Asunción, KYRPIDES, Nikos C., ROCHA, Ulisses Nunes et COSTA, Rodrigo, 2022. *Evidence for cross-feeding, metabolic specialization, and niche partitioning in the octocoral holobiont* [en ligne]. preprint. In Review. [Consulté le 13 juillet 2022]. Disponible à l'adresse : https://www.researchsquare.com/article/rs-1630933/v1

KELLOGG, Christina A., LISLE, John T. et GALKIEWICZ, Julia P., 2009. Culture-Independent Characterization of Bacterial Communities Associated with the Cold-Water Coral *Lophelia pertusa* in the Northeastern Gulf of Mexico. *Applied and Environmental Microbiology*. 15 avril 2009. Vol. 75, n° 8, pp. 2294-2303. DOI 10.1128/AEM.02357-08.

KNOWLTON, Nancy et ROHWER, Forest, 2003. Multispecies Microbial Mutualisms on Coral Reefs: The Host as a Habitat. *The American Naturalist*. octobre 2003. Vol. 162, n° S4, pp. S51-S62. DOI 10.1086/378684.

KOHL, Kevin D., DEARING, M. Denise et BORDENSTEIN, Seth R., 2018. Microbial communities exhibit host species distinguishability and phylosymbiosis along the length of the gastrointestinal tract. *Molecular Ecology*. avril 2018. Vol. 27, n° 8, pp. 1874-1883. DOI 10.1111/mec.14460.

KOOPERMAN, Netta, BEN-DOV, Eitan, KRAMARSKY-WINTER, Esti, BARAK, Zeev et KUSHMARO, Ariel, 2007. Coral mucus-associated bacterial communities from natural and aquarium environments. *FEMS Microbiology Letters*. novembre 2007. Vol. 276, n° 1, pp. 106-113. DOI 10.1111/j.1574-6968.2007.00921.x.

KVENNEFORS, E. Charlotte E., SAMPAYO, Eugenia, KERR, Caroline, VIEIRA, Genyess, ROFF, George et BARNES, Andrew C., 2012. Regulation of Bacterial Communities Through Antimicrobial Activity by the Coral Holobiont. *Microbial Ecology*. avril 2012. Vol. 63, n° 3, pp. 605-618. DOI 10.1007/s00248-011-9946-0.

LA RIVIÈRE, Marie, GARRABOU, Joaquim et BALLY, Marc, 2015. Evidence for host specificity among dominant bacterial symbionts in temperate gorgonian corals. *Coral Reefs*. décembre 2015. Vol. 34, n° 4, pp. 1087-1098. DOI 10.1007/s00338-015-1334-7.

LA RIVIÈRE, Marie, ROUMAGNAC, Marie, GARRABOU, Joaquim et BALLY, Marc, 2013. Transient Shifts in Bacterial Communities Associated with the Temperate Gorgonian Paramuricea clavata in the Northwestern Mediterranean Sea. THOMPSON, Fabiano (éd.), *PLoS ONE*. 20 février 2013. Vol. 8, n° 2, pp. e57385. DOI 10.1371/journal.pone.0057385.

LEIGH, Brittany A., BORDENSTEIN, Sarah R., BROOKS, Andrew W., MIKAELYAN, Aram et BORDENSTEIN, Seth R., 2018. Finer-Scale Phylosymbiosis: Insights from Insect Viromes. HECK, Michelle (éd.), *mSystems*. 30 octobre 2018. Vol. 3, n° 6, pp. e00131-18. DOI 10.1128/mSystems.00131-18.

LEMA, Kimberley A., WILLIS, Bette L. et BOURNE, David G., 2012. Corals Form Characteristic Associations with Symbiotic Nitrogen-Fixing Bacteria. *Applied and Environmental Microbiology*. 1 mai 2012. Vol. 78, n° 9, pp. 3136-3144. DOI 10.1128/AEM.07800-11.

LILBURN, T. G., KIM, K. S., OSTROM, N. E., BYZEK, K. R., LEADBETTER, J. R. et BREZNAK, J. A., 2001. Nitrogen Fixation by Symbiotic and Free-Living Spirochetes. *Science*. 29 juin 2001. Vol. 292, n° 5526, pp. 2495-2498. DOI 10.1126/science.1060281.

LIM, Shen Jean et BORDENSTEIN, Seth R., 2020a. An introduction to phylosymbiosis. *Proceedings of the Royal Society B: Biological Sciences*. 11 mars 2020. Vol. 287, n° 1922, pp. 20192900. DOI 10.1098/rspb.2019.2900.

LIM, Shen Jean et BORDENSTEIN, Seth R., 2020b. An introduction to phylosymbiosis. *Proceedings of the Royal Society B: Biological Sciences*. 11 mars 2020. Vol. 287, n° 1922, pp. 20192900. DOI 10.1098/rspb.2019.2900.

LIMA, Laís F. O., WEISSMAN, Maya, REED, Micheal, PAPUDESHI, Bhavya, ALKER, Amanda T., MORRIS, Megan M., EDWARDS, Robert A., DE PUTRON, Samantha J., VAIDYA, Naveen K. et DINSDALE, Elizabeth A., 2020. Modeling of the Coral Microbiome: the Influence of Temperature and Microbial Network. MEDINA, Monica et MCFALL-NGAI, Margaret J. (éd.), *mBio*. 28 avril 2020. Vol. 11, n° 2, pp. e02691-19. DOI 10.1128/mBio.02691-19.

LU, Hao, ASEM, Alireza, WANG, Lu, LI, Weidong et WANG, PeiZheng, 2020. Comparison of Symbiotic Bacterial Community of Soft Corals Sarcophyton and Sinularia of the Hainan Province, (South China Sea, China). *Genetics of Aquatic Organisms*. 30 novembre 2020. Vol. 5, n° 1, pp. 19-28. DOI 10.4194/2459-1831-v5_1_03.

MATTHEWS, Jennifer L., RAINA, Jean-Baptiste, KAHLKE, Tim, SEYMOUR, Justin R., OPPEN, Madeleine J. H. et SUGGETT, David J., 2020. Symbiodiniaceae-bacteria interactions: rethinking metabolite exchange in reef-building corals as multi-partner metabolic networks. *Environmental Microbiology*. mai 2020. Vol. 22, n° 5, pp. 1675-1687. DOI 10.1111/1462-2920.14918.

MCFADDEN, C. S., 1999. Genetic and taxonomic relationships among Northeastern Atlantic and Mediterranean populations of the soft coral Alcyonium coralloides. *Marine Biology*. 9 mars 1999. Vol. 133, n° 2, pp. 171-184. DOI 10.1007/s002270050456.

MCFADDEN, Catherine S., BENAYAHU, Yehuda, PANTE, Eric, THOMA, Jana N., NEVAREZ, P. Andrew et FRANCE, Scott C., 2011. Limitations of mitochondrial gene barcoding in Octocorallia. *Molecular Ecology Resources*. janvier 2011. Vol. 11, n° 1, pp. 19-31. DOI 10.1111/j.1755-0998.2010.02875.x.

MCFADDEN, Catherine et VAN OFWEGEN, Leen, 2013. Molecular phylogenetic evidence supports a new family of octocorals and a new genus of Alcyoniidae (Octocorallia, Alcyonacea). *ZooKeys*. 1 novembre 2013. Vol. 346, pp. 59-83. DOI 10.3897/zookeys.346.6270.

MORROW, Kathleen M, BOURNE, David G, HUMPHREY, Craig, BOTTÉ, Emmanuelle S, LAFFY, Patrick, ZANEVELD, Jesse, UTHICKE, Sven, FABRICIUS, Katharina E et WEBSTER, Nicole S, 2015. Natural volcanic CO2 seeps reveal future trajectories for host–microbial associations in corals and sponges. *The ISME Journal*. avril 2015. Vol. 9, n° 4, pp. 894-908. DOI 10.1038/ismej.2014.188.

MUSCATINE, L., R. MCCLOSKEY, L. et E. MARIAN, R., 1981. Estimating the daily contribution of carbon from zooxanthellae to coral animal respiration. *Limnology and Oceanography*. juillet 1981. Vol. 26, n° 4, pp. 601-611. DOI 10.4319/lo.1981.26.4.0601.

NEAVE, Matthew J., APPRILL, Amy, FERRIER-PAGÈS, Christine et VOOLSTRA, Christian R., 2016. Diversity and function of prevalent symbiotic marine bacteria in the genus Endozoicomonas. *Applied Microbiology and Biotechnology*. octobre 2016. Vol. 100, n° 19, pp. 8315-8324. DOI 10.1007/s00253-016-7777-0.

NISSIMOV, Jozef, ROSENBERG, Eugene et MUNN, Colin B., 2009. Antimicrobial properties of resident coral mucus bacteria of Oculina patagonica. *FEMS Microbiology Letters*. mars 2009. Vol. 292, n° 2, pp. 210-215. DOI 10.1111/j.1574-6968.2009.01490.x.

O'BRIEN, Paul A., TAN, Shangjin, YANG, Chentao, FRADE, Pedro R., ANDREAKIS, Nikos, SMITH, Hillary A., MILLER, David J., WEBSTER, Nicole S., ZHANG, Guojie et BOURNE, David G., 2020. Diverse coral reef invertebrates exhibit patterns of phylosymbiosis. *The ISME Journal*. septembre 2020. Vol. 14, n° 9, pp. 2211-2222. DOI 10.1038/s41396-020-0671-x.

OKSANEN, J, BLANCHET, FG, KINDT, R, LEGENDRE, P, MINCHIN, P, O'HARA, B, SIMPSON, G, SOLYMOS, P, STEVENS, H et WAGNER, H, [sans date]. Vegan: Community Ecology Package. R Package Version 22-1 2:1-2. [en ligne]. Disponible à l'adresse : https://cran.r-project.org/web/packages/vegan/index.html

PANTOS, Olga, BONGAERTS, Pim, DENNIS, Paul G, TYSON, Gene W et HOEGH-GULDBERG, Ove, 2015. Habitat-specific environmental conditions primarily control the microbiomes of the coral Seriatopora hystrix. *The ISME Journal*. septembre 2015. Vol. 9, n° 9, pp. 1916-1927. DOI 10.1038/ismej.2015.3.

PARK, Joon Sang, HAN, Jeonghoon, SUH, Sung-Suk, KIM, Hyun-Jung, LEE, Taek-Kyun et JUNG, Seung Won, 2022. Characterization of bacterial community structure in two alcyonacean soft corals (Litophyton sp. and Sinularia sp.) from Chuuk, Micronesia. *Coral Reefs*. juin 2022. Vol. 41, n° 3, pp. 563-574. DOI 10.1007/s00338-021-02176-w.

PEIXOTO, Raquel S., ROSADO, Phillipe M., LEITE, Deborah Catharine de Assis, ROSADO, Alexandre S. et BOURNE, David G., 2017. Beneficial Microorganisms for Corals (BMC): Proposed Mechanisms for Coral Health and Resilience. *Frontiers in Microbiology* [en ligne]. 7 mars 2017. Vol. 8. [Consulté le 3 mars 2022]. DOI 10.3389/fmicb.2017.00341. Disponible à l'adresse : http://journal.frontiersin.org/article/10.3389/fmicb.2017.00341/full

PENN, Kevin, WU, Dongying, EISEN, Jonathan A. et WARD, Naomi, 2006. Characterization of Bacterial Communities Associated with Deep-Sea Corals on Gulf of Alaska Seamounts. *Applied and Environmental Microbiology*. février 2006. Vol. 72, n° 2, pp. 1680-1683. DOI 10.1128/AEM.72.2.1680-1683.2006.

PIAZZI, Luigi, ATZORI, Fabrizio, CADONI, Nicoletta, CINTI, Maria Francesca, FRAU, Francesca, PANSINI, Arianna, PINNA, Federico, STIPCICH, Patrizia et CECCHERELLI, Giulia, 2021. Animal Forest Mortality: Following the Consequences of a Gorgonian Coral Loss on a Mediterranean Coralligenous Assemblage. *Diversity*. 19 mars 2021. Vol. 13, n° 3, pp. 133. DOI 10.3390/d13030133.

POGOREUTZ, Claudia, OAKLEY, Clinton A., RÄDECKER, Nils, CÁRDENAS, Anny, PERNA, Gabriela, XIANG, Nan, PENG, Lifeng, DAVY, Simon K., NGUGI, David K. et VOOLSTRA, Christian R., 2022. Coral holobiont cues prime Endozoicomonas for a symbiotic lifestyle. *The ISME Journal*. août 2022. Vol. 16, n° 8, pp. 1883-1895. DOI 10.1038/s41396-022-01226-7.

POLLOCK, F. Joseph, MCMINDS, Ryan, SMITH, Styles, BOURNE, David G., WILLIS, Bette L., MEDINA, Mónica, THURBER, Rebecca Vega et ZANEVELD, Jesse R., 2018. Coral-associated bacteria demonstrate phylosymbiosis and cophylogeny. *Nature Communications*. décembre 2018. Vol. 9, n° 1, pp. 4921. DOI 10.1038/s41467-018-07275-x.

PORPORATO, E. M. D., LO GIUDICE, A., MICHAUD, L., DE DOMENICO, E. et SPANÒ, N., 2013a. Diversity and Antibacterial Activity of the Bacterial Communities Associated with Two Mediterranean Sea Pens, Pennatula phosphorea and Pteroeides spinosum (Anthozoa: Octocorallia). *Microbial Ecology*. octobre 2013. Vol. 66, n° 3, pp. 701-714. DOI 10.1007/s00248-013-0260-x.

PORPORATO, E. M. D., LO GIUDICE, A., MICHAUD, L., DE DOMENICO, E. et SPANÒ, N., 2013b. Diversity and Antibacterial Activity of the Bacterial Communities Associated with Two Mediterranean

Sea Pens, Pennatula phosphorea and Pteroeides spinosum (Anthozoa: Octocorallia). *Microbial Ecology*. octobre 2013. Vol. 66, n° 3, pp. 701-714. DOI 10.1007/s00248-013-0260-x.

RAINA, Jean-Baptiste, TAPIOLAS, Dianne, WILLIS, Bette L. et BOURNE, David G., 2009. Coral-Associated Bacteria and Their Role in the Biogeochemical Cycling of Sulfur. *Applied and Environmental Microbiology*. juin 2009. Vol. 75, n° 11, pp. 3492-3501. DOI 10.1128/AEM.02567-08.

RANSOME, Emma, ROWLEY, Sonia J., THOMAS, Simon, TAIT, Karen et MUNN, Colin B., 2014. Disturbance to conserved bacterial communities in the cold-water gorgonian coral *Eunicella verrucosa*. *FEMS Microbiology Ecology*. août 2014. pp. n/a-n/a. DOI 10.1111/1574-6941.12398.

RITCHIE, Kb, 2006. Regulation of microbial populations by coral surface mucus and mucus-associated bacteria. *Marine Ecology Progress Series*. 20 septembre 2006. Vol. 322, pp. 1-14. DOI 10.3354/meps322001.

ROBERTS, Callum M., MCCLEAN, Colin J., VERON, John E. N., HAWKINS, Julie P., ALLEN, Gerald R., MCALLISTER, Don E., MITTERMEIER, Cristina G., SCHUELER, Frederick W., SPALDING, Mark, WELLS, Fred, VYNNE, Carly et WERNER, Timothy B., 2002. Marine Biodiversity Hotspots and Conservation Priorities for Tropical Reefs. *Science*. 15 février 2002. Vol. 295, n° 5558, pp. 1280-1284. DOI 10.1126/science.1067728.

ROBINSON, D.F. et FOULDS, L.R., 1981. Comparison of phylogenetic trees. *Mathematical Biosciences*. février 1981. Vol. 53, n° 1-2, pp. 131-147. DOI 10.1016/0025-5564(81)90043-2.

RODER, Cornelia, BAYER, Till, ARANDA, Manuel, KRUSE, Maren et VOOLSTRA, Christian R., 2015. Microbiome structure of the fungid coral C tenactis echinata aligns with environmental differences. *Molecular Ecology*. juillet 2015. Vol. 24, n° 13, pp. 3501-3511. DOI 10.1111/mec.13251.

ROSS, Ashley A., MÜLLER, Kirsten M., WEESE, J. Scott et NEUFELD, Josh D., 2018. Comprehensive skin microbiome analysis reveals the uniqueness of human skin and evidence for phylosymbiosis within the class Mammalia. *Proceedings of the National Academy of Sciences* [en ligne]. 19 juin 2018. Vol. 115, n° 25. [Consulté le 23 juin 2022]. DOI 10.1073/pnas.1801302115. Disponible à l'adresse : https://pnas.org/doi/full/10.1073/pnas.1801302115

ROSSI, Sergio et RIZZO, Lucia, 2021. The Importance of Food Pulses in Benthic-Pelagic Coupling Processes of Passive Suspension Feeders. *Water*. 4 avril 2021. Vol. 13, n° 7, pp. 997. DOI 10.3390/w13070997.

RYPIEN, Krystal L., WARD, Jessica R. et AZAM, Farooq, 2010. Antagonistic interactions among coral-associated bacteria. *Environmental Microbiology*. janvier 2010. Vol. 12, n° 1, pp. 28-39. DOI 10.1111/j.1462-2920.2009.02027.x.

SCHUBERT, Nadine, BROWN, Darren et ROSSI, Sergio, 2017. Symbiotic Versus Nonsymbiotic Octocorals: Physiological and Ecological Implications. ROSSI, Sergio, BRAMANTI, Lorenzo, GORI, Andrea et OREJAS, Covadonga (éd.), *Marine Animal Forests*. 2017. pp. 887-918. DOI 10.1007/978-3-319-21012-4_54.

SHALTOUT, Mohamed et OMSTEDT, Anders, 2014. Recent sea surface temperature trends and future scenarios for the Mediterranean Sea. *Oceanologia*. juin 2014. Vol. 56, n° 3, pp. 411-443. DOI 10.5697/oc.56-3.411.

SHARP, Koty H, DISTEL, Dan et PAUL, Valerie J, 2012. Diversity and dynamics of bacterial communities in early life stages of the Caribbean coral Porites astreoides. *The ISME Journal*. avril 2012. Vol. 6, n° 4, pp. 790-801. DOI 10.1038/ismej.2011.144.

SPECK, Mark D. et DONACHIE, Stuart P., 2012. Widespread Oceanospirillaceae Bacteria in *Porites* spp. *Journal of Marine Biology*. 2012. Vol. 2012, pp. 1-7. DOI 10.1155/2012/746720.

TANDON, Kshitij, LU, Chih-Ying, CHIANG, Pei-Wen, WADA, Naohisa, YANG, Shan-Hua, CHAN, Ya-Fan, CHEN, Ping-Yun, CHANG, Hsiao-Yu, CHIOU, Yu-Jing, CHOU, Ming-Shean, CHEN, Wen-Ming et TANG, Sen-Lin, 2020. Comparative genomics: Dominant coral-bacterium Endozoicomonas acroporae metabolizes dimethylsulfoniopropionate (DMSP). *The ISME Journal*. mai 2020. Vol. 14, n° 5, pp. 1290-1303. DOI 10.1038/s41396-020-0610-x.

VAN DE WATER, Jeroen A. J. M., ALLEMAND, Denis et FERRIER-PAGÈS, Christine, 2018. Host-microbe interactions in octocoral holobionts - recent advances and perspectives. *Microbiome*. décembre 2018. Vol. 6, n° 1, pp. 64. DOI 10.1186/s40168-018-0431-6.

VAN DE WATER, Jeroen A. J. M., MELKONIAN, Rémy, JUNCA, Howard, VOOLSTRA, Christian R., REYNAUD, Stéphanie, ALLEMAND, Denis et FERRIER-PAGÈS, Christine, 2016a. Spirochaetes dominate the microbial community associated with the red coral Corallium rubrum on a broad geographic scale. *Scientific Reports*. juin 2016. Vol. 6, n° 1, pp. 27277. DOI 10.1038/srep27277.

VAN DE WATER, Jeroen A. J. M., MELKONIAN, Rémy, JUNCA, Howard, VOOLSTRA, Christian R., REYNAUD, Stéphanie, ALLEMAND, Denis et FERRIER-PAGÈS, Christine, 2016b. Spirochaetes dominate the microbial community associated with the red coral Corallium rubrum on a broad geographic scale. *Scientific Reports*. juin 2016. Vol. 6, n° 1, pp. 27277. DOI 10.1038/srep27277.

VAN DE WATER, Jeroen A. J. M., MELKONIAN, Rémy, VOOLSTRA, Christian R., JUNCA, Howard, BERAUD, Eric, ALLEMAND, Denis et FERRIER-PAGÈS, Christine, 2017a. Comparative Assessment of Mediterranean Gorgonian-Associated Microbial Communities Reveals Conserved Core and Locally Variant Bacteria. *Microbial Ecology*. février 2017. Vol. 73, n° 2, pp. 466-478. DOI 10.1007/s00248-016-0858-x.

VAN DE WATER, Jeroen A. J. M., MELKONIAN, Rémy, VOOLSTRA, Christian R., JUNCA, Howard, BERAUD, Eric, ALLEMAND, Denis et FERRIER-PAGÈS, Christine, 2017b. Comparative Assessment of Mediterranean Gorgonian-Associated Microbial Communities Reveals Conserved Core and Locally Variant Bacteria. *Microbial Ecology*. février 2017. Vol. 73, n° 2, pp. 466-478. DOI 10.1007/s00248-016-0858-x.

VAN DE WATER, Jeroen A. J. M., MELKONIAN, Rémy, VOOLSTRA, Christian R., JUNCA, Howard, BERAUD, Eric, ALLEMAND, Denis et FERRIER-PAGÈS, Christine, 2017c. Comparative Assessment of Mediterranean Gorgonian-Associated Microbial Communities Reveals Conserved Core and Locally Variant Bacteria. *Microbial Ecology*. février 2017. Vol. 73, n° 2, pp. 466-478. DOI 10.1007/s00248-016-0858-x.

VAN DE WATER, Jeroen A. J. M., VOOLSTRA, Christian R., ROTTIER, Cecile, COCITO, Silvia, PEIRANO, Andrea, ALLEMAND, Denis et FERRIER-PAGÈS, Christine, 2018. Seasonal Stability in the Microbiomes of Temperate Gorgonians and the Red Coral Corallium rubrum Across the Mediterranean Sea. *Microbial Ecology*. janvier 2018. Vol. 75, n° 1, pp. 274-288. DOI 10.1007/s00248-017-1006-y.

WEISBURG, W G, BARNS, S M, PELLETIER, D A et LANE, D J, 1991. 16S ribosomal DNA amplification for phylogenetic study. *Journal of Bacteriology*. janvier 1991. Vol. 173, n° 2, pp. 697-703. DOI 10.1128/jb.173.2.697-703.1991.

WILKINSON, Clive, 2008. Status of coral reefs of the world :2008. *Global Coral Reef Monitoring Network and Reef and Rainforest Research Centre, Townsville, Australia*. 2008. pp. 296.

WORM, Boris, BARBIER, Edward B., BEAUMONT, Nicola, DUFFY, J. Emmett, FOLKE, Carl, HALPERN, Benjamin S., JACKSON, Jeremy B. C., LOTZE, Heike K., MICHELI, Fiorenza, PALUMBI, Stephen R., SALA, Enric, SELKOE, Kimberley A., STACHOWICZ, John J. et WATSON, Reg, 2006. Impacts of Biodiversity Loss on Ocean Ecosystem Services. *Science*. 3 novembre 2006. Vol. 314, n° 5800, pp. 787-790. DOI 10.1126/science.1132294.

ZIEGLER, Maren, GRUPSTRA, Carsten G. B., BARRETO, Marcelle M., EATON, Martin, BAOMAR, Jaafar, ZUBIER, Khalid, AL-SOFYANI, Abdulmohsin, TURKI, Adnan J., ORMOND, Rupert et VOOLSTRA, Christian R., 2019. Coral bacterial community structure responds to environmental change in a host-specific manner. *Nature Communications*. décembre 2019. Vol. 10, n° 1, pp. 3092. DOI 10.1038/s41467-019-10969-5.

Supplementary data

Table 1: Metadata for the samples (location, species and depth)

Sample	Depth	ExactDepth	Location	Species	Expedition
AC1S4	deep	81	CapCorse8A	Alcyonium_coralloides	GombessaVI
AC2S4	deep	81	CapCorse8A	Alcyonium_coralloides	GombessaVI
AC3S4	deep	81	CapCorse8A	Alcyonium_coralloides	GombessaVI
AC4S4	deep	81	CapCorse8A	Alcyonium_coralloides	GombessaVI
AC6S4	deep	81	CapCorse8A	Alcyonium_coralloides	GombessaVI
CR1S2	deep	62	Scalo	Corallium_rubrum	GombessaVI
CR2S2	deep	62	Scalo	Corallium_rubrum	GombessaVI
CR4S2	deep	62	Scalo	Corallium_rubrum	GombessaVI
CR5S2	deep	62	Scalo	Corallium_rubrum	GombessaVI
CR1S4	deep	81	CapCorse8A	Corallium_rubrum	GombessaVI
CR2S4	deep	81	CapCorse8A	Corallium_rubrum	GombessaVI
CR3S4	deep	81	CapCorse8A	Corallium_rubrum	GombessaVI
CR4S4	deep	81	CapCorse8A	Corallium_rubrum	GombessaVI
CR5S4	deep	81	CapCorse8A	Corallium_rubrum	GombessaVI
CR6S4	deep	81	CapCorse8A	Corallium_rubrum	GombessaVI
CV01S11	deep	116	AnneauxSiteA	Callogorgia_verticillata	GombessaVI
CV03S11	deep	116	AnneauxSiteA	Callogorgia_verticillata	GombessaVI
CV04S11	deep	116	AnneauxSiteA	Callogorgia_verticillata	GombessaVI
CV05S11	deep	116	AnneauxSiteA	Callogorgia_verticillata	GombessaVI
CV16S11	deep	116	AnneauxSiteA	Callogorgia_verticillata	GombessaVI
CV21S11	deep	116	AnneauxSiteA	Callogorgia_verticillata	GombessaVI
CV1S12	deep	105	AnneauxDC	Callogorgia_verticillata	GombessaVI
CV2S12	deep	105	AnneauxDC	Callogorgia_verticillata	GombessaVI
CV3S12	deep	105	AnneauxDC	Callogorgia_verticillata	GombessaVI
CV4S12	deep	105	AnneauxDC	Callogorgia_verticillata	GombessaVI
CV5S12	deep	105	AnneauxDC	Callogorgia_verticillata	GombessaVI
CV6S12	deep	105	AnneauxDC	Callogorgia_verticillata	GombessaVI
EC2S1	deep	72	Capense	Eunicella_cavolini	GombessaVI
EC3S1	deep	72	Capense	Eunicella_cavolini	GombessaVI
EC6S1	deep	72	Capense	Eunicella_cavolini	GombessaVI
EC1S2	deep	62	Scalo	Eunicella_cavolini	GombessaVI
EC2S2	deep	62	Scalo	Eunicella_cavolini	GombessaVI
EC3S2	deep	62	Scalo	Eunicella_cavolini	GombessaVI
EC4S2	deep	62	Scalo	Eunicella_cavolini	GombessaVI
EC5S2	deep	62	Scalo	Eunicella_cavolini	GombessaVI
EC2S4	deep	81	CapCorse8A	Eunicella_cavolini	GombessaVI
EC4S4	deep	81	CapCorse8A	Eunicella_cavolini	GombessaVI
EC6S4	deep	81	CapCorse8A	Eunicella_cavolini	GombessaVI
EC1S5	deep	95	Nord1_site1	Eunicella_cavolini	GombessaVI
EC2S5	deep	95	Nord1_site1	Eunicella_cavolini	GombessaVI

EC3S5	deep	95	Nord1_site1	Eunicella_cavolini	GombessaVI
EC4S5	deep	95	Nord1_site1	Eunicella_cavolini	GombessaVI
EC6S5	deep	95	Nord1_site1	Eunicella_cavolini	GombessaVI
NC1H3	Negative	Negative	Negative	Negative	GombessaVI
NC2D8	Negative	Negative	Negative	Negative	GombessaVI
NC3E10	Negative	Negative	Negative	Negative	GombessaVI
NC4F10	Negative	Negative	Negative	Negative	GombessaVI
PC3S1	deep	72	Capense	Paramuricea_clavata	GombessaVI
PC4S1	deep	72	Capense	Paramuricea_clavata	GombessaVI
PC5S1	deep	72	Capense	Paramuricea_clavata	GombessaVI
PC6S1	deep	72	Capense	Paramuricea_clavata	GombessaVI
PC2S4	deep	81	CapCorse8A	Paramuricea_clavata	GombessaVI
PC3S4	deep	81	CapCorse8A	Paramuricea_clavata	GombessaVI
PC4S4	deep	81	CapCorse8A	Paramuricea_clavata	GombessaVI
PC5S4	deep	81	CapCorse8A	Paramuricea_clavata	GombessaVI
PC6S4	deep	81	CapCorse8A	Paramuricea_clavata	GombessaVI
PC1S5	deep	95	Nord1_site1	Paramuricea_clavata	GombessaVI
PC2S5	deep	95	Nord1_site1	Paramuricea_clavata	GombessaVI
PC3S5	deep	95	Nord1_site1	Paramuricea_clavata	GombessaVI
PC4S5	deep	95	Nord1_site1	Paramuricea_clavata	GombessaVI
PC5S5	deep	95	Nord1_site1	Paramuricea_clavata	GombessaVI
Seawater1S1	deep	72	Capense	Seawater	GombessaVI
Seawater2S1	deep	72	Capense	Seawater	GombessaVI
Seawater3S1	deep	72	Capense	Seawater	GombessaVI
Seawater4S1	deep	72	Capense	Seawater	GombessaVI
Seawater1S2	deep	62	Scalo	Seawater	GombessaVI
Seawater2S2	deep	62	Scalo	Seawater	GombessaVI
Seawater3S2	deep	62	Scalo	Seawater	GombessaVI
Seawater4S2	deep	62	Scalo	Seawater	GombessaVI
SeawaterS3	deep	88	Palagaccio	Seawater	GombessaVI
Seawater1S4	deep	81	CapCorse8A	Seawater	GombessaVI
Seawater2S4	deep	81	CapCorse8A	Seawater	GombessaVI
Seawater4S4	deep	81	CapCorse8A	Seawater	GombessaVI
Seawater3S4	deep	81	CapCorse8A	Seawater	GombessaVI
Seawater5S4	deep	81	CapCorse8A	Seawater	GombessaVI
Seawater6S4	deep	81	CapCorse8A	Seawater	GombessaVI
Seawater1S5	deep	95	Nord1_site1	Seawater	GombessaVI
Seawater2S5	deep	95	Nord1_site1	Seawater	GombessaVI
Seawater3S5	deep	95	Nord1_site1	Seawater	GombessaVI
Seawater4S5	deep	95	Nord1_site1	Seawater	GombessaVI
Seawater5S5	deep	95	Nord1_site1	Seawater	GombessaVI
Seawater6S5	deep	95	Nord1_site1	Seawater	GombessaVI
Seawater1S12	deep	105	AnneauxDC	Seawater	GombessaVI
Seawater2S12	deep	105	AnneauxDC	Seawater	GombessaVI
Seawater3S12	deep	105	AnneauxDC	Seawater	GombessaVI
Ovabunda1	deep	44	Eilat	Ovabunda	ENCOR

Ovabunda2	deep	44	Eilat	Ovabunda	ENCOR
Ovabunda3	deep	44	Eilat	Ovabunda	ENCOR
Ovabunda4	deep	44	Eilat	Ovabunda	ENCOR
Klyxumutinomii5	deep	44	Eilat	Klyxum_utinomii	ENCOR
Sarcophytonglaucum6	deep	44	Eilat	Sarcophyton_glaucum	ENCOR
Sarcophytonglaucum7	deep	44	Eilat	Sarcophyton_glaucum	ENCOR
Sarcophytonglaucum8	deep	44	Eilat	Sarcophyton_glaucum	ENCOR
Klyxumutinomii9	deep	44	Eilat	Klyxum_utinomii	ENCOR
Sinulariavrijmoethi10	deep	43	Eilat	Sinularia_vrijmoethi	ENCOR
Sinulariaeilatensis11	deep	43	Eilat	Sinularia_eilatensis	ENCOR
Sinulariavrijmoethi12	deep	40	Eilat	Sinularia_vrijmoethi	ENCOR
Ovabunda13	shallow	12	Eilat	Ovabunda	ENCOR
Ovabunda14	shallow	12	Eilat	Ovabunda	ENCOR
Ovabunda15	shallow	12	Eilat	Ovabunda	ENCOR
Ovabunda16	shallow	6	Eilat	Ovabunda	ENCOR
Sinulariavrijmoethi17	deep	44	Eilat	Sinularia_vrijmoethi	ENCOR
Sinulariavrijmoethi18	deep	44	Eilat	Sinularia_vrijmoethi	ENCOR
Sarcophytonglaucum19	deep	44	Eilat	Sarcophyton_glaucum	ENCOR
Ovabunda20	deep	44	Eilat	Ovabunda	ENCOR
Sinulariapolydactyla21	deep	44	Eilat	Sinularia_polydactyla	ENCOR
Paralemnalia22	deep	43	Eilat	Paralemnalia_thyrsoides	ENCOR
Klyxumutinomii23	deep	43	Eilat	Klyxum_utinomii	ENCOR
Sinulariapolydactyla24	shallow	18	Eilat	Sinularia_polydactyla	ENCOR
Ovabunda25	shallow	18	Eilat	Ovabunda	ENCOR
Ovabunda26	shallow	12	Eilat	Ovabunda	ENCOR
Sinulariavrijmoethi32	shallow	18	Eilat	Sinularia_vrijmoethi	ENCOR
Sarcophytonglaucum33	shallow	18	Eilat	Sarcophyton_glaucum	ENCOR
Sinulariaeilatensis34	shallow	18	Eilat	Sinularia_eilatensis	ENCOR
Sarcophytonglaucum35	shallow	17	Eilat	Sarcophyton_glaucum	ENCOR
Sarcophytonglaucum36	shallow	17	Eilat	Sarcophyton_glaucum	ENCOR
Sarcophytonglaucum37	shallow	18	Eilat	Sarcophyton_glaucum	ENCOR
Sinulariaeilatensis38	shallow	18	Eilat	Sinularia_eilatensis	ENCOR
Sarcophytonglaucum40	shallow	7	Eilat	Sarcophyton_glaucum	ENCOR
Sinulariavrijmoethi41	shallow	20	Eilat	Sinularia_vrijmoethi	ENCOR
Sinulariavrijmoethi42	shallow	21	Eilat	Sinularia_vrijmoethi	ENCOR
Sinulariavrijmoethi43	shallow	21	Eilat	Sinularia_vrijmoethi	ENCOR
Sinulariavrijmoethi44	shallow	21	Eilat	Sinularia_vrijmoethi	ENCOR
Paralemnaliathyrsoides45	shallow	20	Eilat	Paralemnalia_thyrsoides	ENCOR
Paralemnaliathyrsoides46	shallow	18	Eilat	Paralemnalia_thyrsoides	ENCOR
Paralemnaliathyrsoides47	shallow	18	Eilat	Paralemnalia_thyrsoides	ENCOR
Paralemnaliathyrsoides48	shallow	17	Eilat	Paralemnalia_thyrsoides	ENCOR
Paralemnaliathyrsoides49	shallow	7	Eilat	Paralemnalia_thyrsoides	ENCOR
Sinularialoyai51	shallow	7	Eilat	Sinularia_loyai	ENCOR
Sarcophytonglaucum52	shallow	6	Eilat	Sarcophyton_glaucum	ENCOR
Sarcophytonglaucum53	shallow	6	Eilat	Sarcophyton_glaucum	ENCOR
Sarcophytonglaucum54	shallow	8	Eilat	Sarcophyton_glaucum	ENCOR

Sinularialoyai55	shallow	5	Eilat	Sinularia_loyai	ENCOR
Sinularialoyai56	shallow	5	Eilat	Sinularia_loyai	ENCOR
Sinulariavrijmoethi57	shallow	9	Eilat	Sinularia_vrijmoethi	ENCOR
Ovabunda61	shallow	19	Eilat	Ovabunda	ENCOR
Ovabunda62	shallow	18	Eilat	Ovabunda	ENCOR
Ovabunda63	shallow	19	Eilat	Ovabunda	ENCOR
Sinulariaeilatensis64	shallow	12	Eilat	Sinularia_eilatensis	ENCOR
Paralemnaliathyrsoides65	shallow	11	Eilat	Paralemnalia_thyrsoides	ENCOR
Paralemnaliathyrsoides66	shallow	10	Eilat	Paralemnalia_thyrsoides	ENCOR
Paralemnaliathyrsoides67	shallow	10	Eilat	Paralemnalia_thyrsoides	ENCOR
Leptoseris1	deep	79	Eilat	Leptoseris	ENCOR
Leptoseris2	deep	81	Eilat	Leptoseris	ENCOR
Leptoseris3	deep	82	Eilat	Leptoseris	ENCOR
Leptoseris4	deep	79	Eilat	Leptoseris	ENCOR
Leptoseris5	deep	81	Eilat	Leptoseris	ENCOR
Leptoseris6	deep	92	Eilat	Leptoseris	ENCOR
NC9E	Negative	Negative	Negative	Negative	ENCOR
SinulariaeilatensisS1	deep	67	Eilat	Sinularia_eilatensis	ENCOR
SinulariaeilatensisS2	deep	67	Eilat	Sinularia_eilatensis	ENCOR
SinularialeptocladusS3	deep	64	Eilat	Sinularia_leptocladus	ENCOR
SinulariamesophoticaS4	deep	61	Eilat	Sinularia_mesophotica	ENCOR
SinulariavrijmoethiS5	deep	60	Eilat	Sinularia_vrijmoethi	ENCOR
SinulariaeilatensisS6	deep	63	Eilat	Sinularia_eilatensis	ENCOR
SinularialeptocladusS7	deep	64	Eilat	Sinularia_leptocladus	ENCOR
KlyxumutinomiiS8	deep	53	Eilat	Klyxum_utinomii	ENCOR
OvabundaS9	deep	54	Eilat	Ovabunda	ENCOR
SinulariavrijmoethiS10	deep	50	Eilat	Sinularia_vrijmoethi	ENCOR
SinulariavrijmoethiS11	deep	43	Eilat	Sinularia_vrijmoethi	ENCOR
ParalemnaliathyrsoidesS12	deep	48	Eilat	Paralemnalia_thyrsoides	ENCOR
SinulariaeilatensisS13	deep	56	Eilat	Sinularia_eilatensis	ENCOR
SinulariaeilatensisS14	deep	59	Eilat	Sinularia_eilatensis	ENCOR
SinulariamesophoticaS15	deep	62	Eilat	Sinularia_mesophotica	ENCOR
SinulariamesophoticaS16	deep	65	Eilat	Sinularia_mesophotica	ENCOR
Seawater1E	deep	80	Eilat	Seawater	ENCOR
Seawater2E	deep	80	Eilat	Seawater	ENCOR
Seawater3E	deep	80	Eilat	Seawater	ENCOR
Seawater4E	deep	80	Eilat	Seawater	ENCOR
Seawater5E	deep	80	Eilat	Seawater	ENCOR
Seawater6E	deep	80	Eilat	Seawater	ENCOR
CR1AntibesS89	deep	70	MassifDuRaventurier	Corallium_rubrum	GombessaV
CR4MonacoS97	deep	77	SaintMartin	Corallium_rubrum	GombessaV
EV6AntibesS105	deep	70	MassifDuRaventurier	Eunicella_verrucosa	GombessaV
PC2AntibesS113	deep	70	MassifDuRaventurier	Paramuricea_clavata	GombessaV
PCb4AntibesS121	deep	70	MassifDuRaventurier	Paramuricea_clavata_bicolor	GombessaV
EC4MonacoS129	deep	77	SaintMartin	Eunicella_cavolini	GombessaV
EV1NiceS137	deep	103	TombantdesAmericains	Eunicella_verrucosa	GombessaV

EC5NiceS145	deep	103	TombantdesAmericains	Eunicella_cavolini	GombessaV
NC1S153	Negative	Negative	Negative	Negative	GombessaV
CR2AntibesS90	deep	70	MassifDuRaventurier	Corallium_rubrum	GombessaV
CR5MonacoS98	deep	77	SaintMartin	Corallium_rubrum	GombessaV
EC1AntibesS106	deep	70	MassifDuRaventurier	Eunicella_cavolini	GombessaV
PC3AntibesS114	deep	70	MassifDuRaventurier	Paramuricea_clavata	GombessaV
PCb5AntibesS122	deep	70	MassifDuRaventurier	Paramuricea_clavata_bicolor	GombessaV
EC5MonacoS130	deep	77	SaintMartin	Eunicella_cavolini	GombessaV
EV2NiceS138	deep	103	TombantdesAmericains	Eunicella_verrucosa	GombessaV
PCb1NiceS146	deep	103	TombantdesAmericains	Paramuricea_clavata_bicolor	GombessaV
NC2S154	Negative	Negative	Negative	Negative	GombessaV
CR3AntibesS91	deep	70	MassifDuRaventurier	Corallium_rubrum	GombessaV
ESAntibesS99	deep	70	MassifDuRaventurier	Eunicella_singularis	GombessaV
EC2AntibesS107	deep	70	MassifDuRaventurier	Eunicella_cavolini	GombessaV
PC4AntibesS115	deep	70	MassifDuRaventurier	Paramuricea_clavata	GombessaV
EV1MonacoS123	deep	77	SaintMartin	Eunicella_verrucosa	GombessaV
PC1MonacoS131	deep	77	SaintMartin	Paramuricea_clavata	GombessaV
EV3NiceS139	deep	103	TombantdesAmericains	Eunicella_verrucosa	GombessaV
PCb2NiceS147	deep	103	TombantdesAmericains	Paramuricea_clavata_bicolor	GombessaV
NC3S155	Negative	Negative	Negative	Negative	GombessaV
CR4AntibesS92	deep	70	MassifDuRaventurier	Corallium_rubrum	GombessaV
EV1AntibesS100	deep	70	MassifDuRaventurier	Eunicella_verrucosa	GombessaV
EC3AntibesS108	deep	70	MassifDuRaventurier	Eunicella_cavolini	GombessaV
PC5AntibesS116	deep	70	MassifDuRaventurier	Paramuricea_clavata	GombessaV
EV2MonacoS124	deep	77	SaintMartin	Eunicella_verrucosa	GombessaV
PC2MonacoS132	deep	77	SaintMartin	Paramuricea_clavata	GombessaV
EV4NiceS140	deep	103	TombantdesAmericains	Eunicella_verrucosa	GombessaV
PCb3NiceS148	deep	103	TombantdesAmericains	Paramuricea_clavata_bicolor	GombessaV
NC4S156	Negative	Negative	Negative	Negative	GombessaV
CR5AntibesS93	deep	70	MassifDuRaventurier	Corallium_rubrum	GombessaV
EV2AntibesS101	deep	70	MassifDuRaventurier	Eunicella_verrucosa	GombessaV
EC4AntibesS109	deep	70	MassifDuRaventurier	Eunicella_cavolini	GombessaV
PCbAntibesS117	deep	70	MassifDuRaventurier	Paramuricea_clavata_bicolor	GombessaV
EV3MonacoS125	deep	77	SaintMartin	Eunicella_verrucosa	GombessaV
PC3MonacoS133	deep	77	SaintMartin	Paramuricea_clavata	GombessaV
EC1NiceS141	deep	103	TombantdesAmericains	Eunicella_cavolini	GombessaV
PCb4NiceS149	deep	103	TombantdesAmericains	Paramuricea_clavata_bicolor	GombessaV
NC5S157	Negative	Negative	Negative	Negative	GombessaV
CR6AntibesS94	deep	70	MassifDuRaventurier	Corallium_rubrum	GombessaV
EV3AntibesS102	deep	70	MassifDuRaventurier	Eunicella_verrucosa	GombessaV
EC5AntibesS110	deep	70	MassifDuRaventurier	Eunicella_cavolini	GombessaV
PCb1AntibesS118	deep	70	MassifDuRaventurier	Paramuricea_clavata_bicolor	GombessaV
EV5MonacoS126	deep	77	SaintMartin	Eunicella_verrucosa	GombessaV
PC5MonacoS134	deep	77	SaintMartin	Paramuricea_clavata	GombessaV
EC2NiceS142	deep	103	TombantdesAmericains	Eunicella_cavolini	GombessaV
PCb5NiceS150	deep	103	TombantdesAmericains	Paramuricea_clavata_bicolor	GombessaV

NC6S158	Negative	Negative	Negative	Negative	GombessaV
CR1MonacoS95	deep	77	SaintMartin	Corallium_rubrum	GombessaV
EV4AntibesS103	deep	70	MassifDuRaventurier	Eunicella_verrucosa	GombessaV
PCAntibesS111	deep	70	MassifDuRaventurier	Paramuricea_clavata	GombessaV
PCb2AntibesS119	deep	70	MassifDuRaventurier	Paramuricea_clavata_bicolor	GombessaV
EC1MonacoS127	deep	77	SaintMartin	Eunicella_cavolini	GombessaV
PCb1MonacoS135	deep	77	SaintMartin	Paramuricea_clavata_bicolor	GombessaV
EC3NiceS143	deep	103	TombantdesAmericains	Eunicella_cavolini	GombessaV
NC7S159	Negative	Negative	Negative	Negative	GombessaV
CR2MonacoS96	deep	77	SaintMartin	Corallium_rubrum	GombessaV
EV5AntibesS104	deep	70	MassifDuRaventurier	Eunicella_verrucosa	GombessaV
PC1AntibesS112	deep	70	MassifDuRaventurier	Paramuricea_clavata	GombessaV
PCb3AntibesS120	deep	70	MassifDuRaventurier	Paramuricea_clavata_bicolor	GombessaV
EC3MonacoS128	deep	77	SaintMartin	Eunicella_cavolini	GombessaV
PCb3MonacoS136	deep	77	SaintMartin	Paramuricea_clavata_bicolor	GombessaV
EC4NiceS144	deep	103	TombantdesAmericains	Eunicella_cavolini	GombessaV
NC8S160	Negative	Negative	Negative	Negative	GombessaV
EcPortMay1	deep	70	Portofino	Eunicella_cavolini	PortofinoSurvey
EcPortMay2	deep	70	Portofino	Eunicella_cavolini	PortofinoSurvey
EcPortMay3	deep	70	Portofino	Eunicella_cavolini	PortofinoSurvey
EcPortMay4	deep	70	Portofino	Eunicella_cavolini	PortofinoSurvey
EcPortMay5	deep	70	Portofino	Eunicella_cavolini	PortofinoSurvey
EcPortMay6	deep	70	Portofino	Eunicella_cavolini	PortofinoSurvey
EcPortNov1	deep	63	Portofino	Eunicella_cavolini	PortofinoSurvey
EcPortNov2	deep	63	Portofino	Eunicella_cavolini	PortofinoSurvey
EcPortNov3	deep	63	Portofino	Eunicella_cavolini	PortofinoSurvey
EcPortNov4	deep	63	Portofino	Eunicella_cavolini	PortofinoSurvey
EcPortNov5	deep	63	Portofino	Eunicella_cavolini	PortofinoSurvey
EcPortNov6	deep	63	Portofino	Eunicella_cavolini	PortofinoSurvey
SeawaterPortMay1	deep	70	Portofino	Seawater	PortofinoSurvey
SeawaterPortMay2	deep	70	Portofino	Seawater	PortofinoSurvey
SeawaterPortMay3	deep	70	Portofino	Seawater	PortofinoSurvey
SeawaterPortNov1	deep	63	Portofino	Seawater	PortofinoSurvey
SeawaterPortNov2	deep	63	Portofino	Seawater	PortofinoSurvey
SeawaterPortNov3	deep	63	Portofino	Seawater	PortofinoSurvey

Table 2: Final merging ratios after bioinformatic treatment to the dataset

Number of pairs	Percentage of merged sequences	Percentage of alignments with zero differences	Percentage of alignments with > 15 differences	No alignment found	Mean alignment length
22.9M	78.66 %	39.27 %	15.41 % (> 15)	3.82 %	52.81 bp

Table 3: Table with the AIC and BIC criterion for a range of nucleotides' substitution models

Model	Decoration	K	Llk	AIC	BIC
GTR	"+R"	44	-8135,5433	16359,0867	16610,3554
GTR	"+G"	39	-8140,8579	16359,7158	16582,4313
GTR	"+G+I"	40	-8140,8681	16361,7362	16590,1624
TN93	"+R"	41	-8142,7543	16367,5085	16601,6453
GTR	"+I"	39	-8247,033	16572,0659	16794,7814
GTR		38	-8448,7505	16973,501	17190,5058

Table 4: Tukey's HSD test results after ANOVA on Chao1 index

Comparison	Species.diff	Species.lwr	Species.upr	Species.p.adj
Callogorgia_verticillata-Alcyonium_coralloides	0,331416	-1,17512	1,837951	0,999993
Corallium_rubrum-Alcyonium_coralloides	-1,03112	-2,46034	0,398104	0,471138
Eunicella_cavolini-Alcyonium_coralloides	-1,39492	-2,76033	-0,02951	0,039746
Eunicella_verrucosa-Alcyonium_coralloides	-0,97331	-2,4527	0,506073	0,634146
Klyxum_utinomii-Alcyonium_coralloides	-0,49621	-2,34133	1,348913	0,999902
Ovabunda-Alcyonium_coralloides	-0,39353	-1,86192	1,074854	0,999906
Paralemnalia_thyrsoides-Alcyonium_coralloides	-0,84183	-2,40988	0,726218	0,887679
Paramuricea_clavata-Alcyonium_coralloides	-0,7846	-2,19384	0,62463	0,856079
Paramuricea_clavata_bicolor-Alcyonium_coralloides	-0,4702	-1,96218	1,021773	0,99933
Sarcophyton_glaucum-Alcyonium_coralloides	-1,07033	-2,57686	0,436209	0,499066
Sinularia_eilatensis-Alcyonium_coralloides	-0,94164	-2,53956	0,656277	0,79463
Sinularia_loyai-Alcyonium_coralloides	-1,22196	-3,21492	0,770996	0,742767
Sinularia_mesophotica-Alcyonium_coralloides	-2,19449	-5,11188	0,722905	0,395678
Sinularia_polydactyla-Alcyonium_coralloides	1,23649	-1,02331	3,496291	0,871902
Sinularia_vrijmoethi-Alcyonium_coralloides	-0,97057	-2,46255	0,52141	0,652802
Corallium_rubrum-Callogorgia_verticillata	-1,36254	-2,31535	-0,40972	0,000174
Eunicella_cavolini-Callogorgia_verticillata	-1,72634	-2,58046	-0,87221	5,1E-09
Eunicella_verrucosa-Callogorgia_verticillata	-1,30473	-2,33126	-0,2782	0,001795
Klyxum_utinomii-Callogorgia_verticillata	-0,82762	-2,33416	0,678911	0,868388
Ovabunda-Callogorgia_verticillata	-0,72495	-1,73556	0,285664	0,48155
Paralemnalia_thyrsoides-Callogorgia_verticillata	-1,17325	-2,32388	-0,02261	0,040592
Paramuricea_clavata-Callogorgia_verticillata	-1,11602	-2,03858	-0,19346	0,004122
Paramuricea_clavata_bicolor-Callogorgia_verticillata	-0,80162	-1,84621	0,242973	0,360363
Sarcophyton_glaucum-Callogorgia_verticillata	-1,40174	-2,46702	-0,33646	0,000953
Sinularia_eilatensis-Callogorgia_verticillata	-1,27306	-2,46408	-0,08204	0,023496
Sinularia_loyai-Callogorgia_verticillata	-1,55338	-3,23774	0,130978	0,10754
Sinularia_mesophotica-Callogorgia_verticillata	-2,5259	-5,24185	0,190041	0,10004
Sinularia_polydactyla-Callogorgia_verticillata	0,905074	-1,08788	2,898031	0,970294
Sinularia_vrijmoethi-Callogorgia_verticillata	-1,30198	-2,34658	-0,25739	0,002519
Eunicella_cavolini-Corallium_rubrum	-0,3638	-1,07272	0,345119	0,919141
Eunicella_verrucosa-Corallium_rubrum	0,057806	-0,85148	0,967091	1
Klyxum_utinomii-Corallium_rubrum	0,534912	-0,89431	1,964136	0,995457
Ovabunda-Corallium_rubrum	0,637586	-0,25369	1,528863	0,486564

Paralemnalia_thyrsoides-Corallium_rubrum	0,189287	-0,85809	1,236663	0,999999
Paramuricea_clavata-Corallium_rubrum	0,246516	-0,54352	1,036549	0,999404
Paramuricea_clavata_bicolor-Corallium_rubrum	0,560915	-0,36871	1,490545	0,764626
Sarcophyton_glaucum-Corallium_rubrum	-0,03921	-0,99202	0,91361	1
Sinularia_eilatensis-Corallium_rubrum	0,089476	-1,00211	1,181064	1
Sinularia_loyai-Corallium_rubrum	-0,19084	-1,80642	1,424736	1
Sinularia_mesophotica-Corallium_rubrum	-1,16337	-3,8372	1,510467	0,979824
Sinularia_polydactyla-Corallium_rubrum	2,26761	0,332431	4,202788	0,006746
Sinularia_vrijmoethi-Corallium_rubrum	0,060552	-0,86908	0,990182	1
Eunicella_verrucosa-Eunicella_cavolini	0,421605	-0,38367	1,226882	0,906182
Klyxum_utinomii-Eunicella_cavolini	0,898712	-0,4667	2,264124	0,633434
Ovabunda-Eunicella_cavolini	1,001385	0,216498	1,786271	0,001679
Paralemnalia_thyrsoides-Eunicella_cavolini	0,553086	-0,40538	1,511557	0,819108
Paramuricea_clavata-Eunicella_cavolini	0,610315	-0,05738	1,278015	0,115897
Paramuricea_clavata_bicolor-Eunicella_cavolini	0,924714	0,096534	1,752894	0,013404
Sarcophyton_glaucum-Eunicella_cavolini	0,324593	-0,52953	1,178718	0,99467
Sinularia_eilatensis-Eunicella_cavolini	0,453275	-0,55332	1,459871	0,972443
Sinularia_loyai-Eunicella_cavolini	0,172957	-1,38645	1,732368	1
Sinularia_mesophotica-Eunicella_cavolini	-0,79957	-3,43984	1,840708	0,999582
Sinularia_polydactyla-Eunicella_cavolini	2,631409	0,742868	4,51995	0,000304
Sinularia_vrijmoethi-Eunicella_cavolini	0,424351	-0,40383	1,252531	0,92007
Klyxum_utinomii-Eunicella_verrucosa	0,477107	-1,00228	1,956494	0,999124
Ovabunda-Eunicella_verrucosa	0,57978	-0,3899	1,549461	0,776497
Paralemnalia_thyrsoides-Eunicella_verrucosa	0,131481	-0,98337	1,246336	1
Paramuricea_clavata-Eunicella_verrucosa	0,18871	-0,68882	1,06624	0,999995
Paramuricea_clavata_bicolor-Eunicella_verrucosa	0,503109	-0,50194	1,508155	0,933177
Sarcophyton_glaucum-Eunicella_verrucosa	-0,09701	-1,12354	0,929518	1
Sinularia_eilatensis-Eunicella_verrucosa	0,03167	-1,12482	1,188161	1
Sinularia_loyai-Eunicella_verrucosa	-0,24865	-1,90877	1,411472	1
Sinularia_mesophotica-Eunicella_verrucosa	-1,22117	-3,92215	1,479807	0,971439
Sinularia_polydactyla-Eunicella_verrucosa	2,209804	0,237287	4,18232	0,012811
Sinularia_vrijmoethi-Eunicella_verrucosa	0,002746	-1,0023	1,007792	1
Ovabunda-Klyxum_utinomii	0,102673	-1,36571	1,571061	1
Paralemnalia_thyrsoides-Klyxum_utinomii	-0,34563	-1,91368	1,222426	0,999993
Paramuricea_clavata-Klyxum_utinomii	-0,2884	-1,69763	1,120837	0,999997
Paramuricea_clavata_bicolor-Klyxum_utinomii	0,026003	-1,46598	1,517981	1
Sarcophyton_glaucum-Klyxum_utinomii	-0,57412	-2,08065	0,932416	0,994514
Sinularia_eilatensis-Klyxum_utinomii	-0,44544	-2,04336	1,152485	0,999847
Sinularia_loyai-Klyxum_utinomii	-0,72575	-2,71871	1,267203	0,996604
Sinularia_mesophotica-Klyxum_utinomii	-1,69828	-4,61567	1,219113	0,809158
Sinularia_polydactyla-Klyxum_utinomii	1,732697	-0,5271	3,992499	0,361848
Sinularia_vrijmoethi-Klyxum_utinomii	-0,47436	-1,96634	1,017618	0,999258
Paralemnalia_thyrsoides-Ovabunda	-0,4483	-1,54852	0,651919	0,989208
Paramuricea_clavata-Ovabunda	-0,39107	-1,24993	0,467787	0,969594
Paramuricea_clavata_bicolor-Ovabunda	-0,07667	-1,06545	0,912113	1
Sarcophyton_glaucum-Ovabunda	-0,67679	-1,68741	0,333823	0,604102

Sinularia_eilatensis-Ovabunda	-0,54811	-1,6905	0,594277	0,952485
Sinularia_loyai-Ovabunda	-0,82843	-2,47875	0,821898	0,931711
Sinularia_mesophotica-Ovabunda	-1,80095	-4,49592	0,894019	0,607744
Sinularia_polydactyla-Ovabunda	1,630024	-0,33426	3,594305	0,233698
Sinularia_vrijmoethi-Ovabunda	-0,57703	-1,56582	0,41175	0,806249
Paramuricea_clavata-Paralemnalia_thyrsoides	0,057229	-0,9627	1,077157	1
Paramuricea_clavata_bicolor-Paralemnalia_thyrsoides	0,371628	-0,75988	1,503137	0,99892
Sarcophyton_glaucum-Paralemnalia_thyrsoides	-0,22849	-1,37913	0,922142	0,999998
Sinularia_eilatensis-Paralemnalia_thyrsoides	-0,09981	-1,36775	1,168126	1
Sinularia_loyai-Paralemnalia_thyrsoides	-0,38013	-2,11973	1,359466	0,999993
Sinularia_mesophotica-Paralemnalia_thyrsoides	-1,35265	-4,1032	1,397889	0,941926
Sinularia_polydactyla-Paralemnalia_thyrsoides	2,078322	0,038465	4,11818	0,040941
Sinularia_vrijmoethi-Paralemnalia_thyrsoides	-0,12874	-1,26024	1,002774	1
Paramuricea_clavata_bicolor-Paramuricea_clavata	0,314399	-0,58419	1,212993	0,997802
Sarcophyton_glaucum-Paramuricea_clavata	-0,28572	-1,20828	0,636838	0,999454
Sinularia_eilatensis-Paramuricea_clavata	-0,15704	-1,22232	0,908241	1
Sinularia_loyai-Paramuricea_clavata	-0,43736	-2,03528	1,160563	0,999878
Sinularia_mesophotica-Paramuricea_clavata	-1,40988	-4,07308	1,253319	0,898325
Sinularia_polydactyla-Paramuricea_clavata	2,021094	0,100632	3,941556	0,028324
Sinularia_vrijmoethi-Paramuricea_clavata	-0,18596	-1,08456	0,71263	0,999997
Sarcophyton_glaucum-Paramuricea_clavata_bicolor	-0,60012	-1,64471	0,444473	0,824005
Sinularia_eilatensis-Paramuricea_clavata_bicolor	-0,47144	-1,64399	0,701114	0,990542
Sinularia_loyai-Paramuricea_clavata_bicolor	-0,75176	-2,42311	0,919592	0,972722
Sinularia_mesophotica-Paramuricea_clavata_bicolor	-1,72428	-4,43218	0,983615	0,686898
Sinularia_polydactyla-Paramuricea_clavata_bicolor	1,706695	-0,27528	3,688672	0,182854
Sinularia_vrijmoethi-Paramuricea_clavata_bicolor	-0,50036	-1,52385	0,523126	0,944619
Sinularia_eilatensis-Sarcophyton_glaucum	0,128682	-1,06234	1,319702	1
Sinularia_loyai-Sarcophyton_glaucum	-0,15164	-1,83599	1,53272	1
Sinularia_mesophotica-Sarcophyton_glaucum	-1,12416	-3,8401	1,591783	0,98742
Sinularia_polydactyla-Sarcophyton_glaucum	2,306815	0,313858	4,299773	0,008088
Sinularia_vrijmoethi-Sarcophyton_glaucum	0,099758	-0,94484	1,144351	1
Sinularia_loyai-Sinularia_eilatensis	-0,28032	-2,04689	1,48625	1
Sinularia_mesophotica-Sinularia_eilatensis	-1,25284	-4,02052	1,514838	0,971131
Sinularia_polydactyla-Sinularia_eilatensis	2,178134	0,115226	4,241041	0,027244
Sinularia_vrijmoethi-Sinularia_eilatensis	-0,02892	-1,20148	1,143629	1
Sinularia_mesophotica-Sinularia_loyai	-0,97252	-3,98559	2,040545	0,999116
Sinularia_polydactyla-Sinularia_loyai	2,458452	0,076412	4,840492	0,035476
Sinularia_vrijmoethi-Sinularia_loyai	0,251394	-1,41996	1,922744	1
Sinularia_polydactyla-Sinularia_mesophotica	3,430976	0,235134	6,626818	0,022264
Sinularia_vrijmoethi-Sinularia_mesophotica	1,223918	-1,48398	3,931815	0,971518
Sinularia_vrijmoethi-Sinularia_polydactyla	-2,20706	-4,18903	-0,22508	0,013898

Table 5: Pairwise PERMANOVA results on bacterial composition

Comparison	R2	F	df	p	p.adj
Alcyonium_coralloides.Callogorgia_verticillata	0,381306	8,628294	1;14	0,0008	0,002471
Alcyonium_coralloides.Corallium_rubrum	0,175553	4,684569	1;22	0,0002	0,000875
Alcyonium_coralloides.Eunicella_cavolini	0,081021	3,791054	1;43	0,0001	0,000525
Alcyonium_coralloides.Eunicella_verrucosa	0,487967	12,38898	1;13	0,0006	0,001969
Alcyonium_coralloides.Klyxum_utinomii	0,492741	4,856904	1;5	0,028571	0,042254
Alcyonium_coralloides.Ovabunda	0,353977	9,314845	1;17	0,0001	0,000525
Alcyonium_coralloides.Paralemnalia_thyrsoides	0,252229	3,710382	1;11	0,0013	0,00325
Alcyonium_coralloides.Paramuricea_clavata	0,221947	7,416765	1;26	0,0001	0,000525
Alcyonium_coralloides.Paramuricea_clavata_bicolor	0,225613	4,370163	1;15	0,0013	0,00325
Alcyonium_coralloides.Sarcophyton_glaucum	0,279534	5,043882	1;13	0,0004	0,001448
Alcyonium_coralloides.Sinularia_eilatensis	0,328366	3,911242	1;8	0,0057	0,011735
Alcyonium_coralloides.Sinularia_loyai	0,63235	6,879925	1;4	0,066667	0,085366
Alcyonium_coralloides.Sinularia_polydactyla	0,712665	9,921012	1;4	0,066667	0,085366
Alcyonium_coralloides.Sinularia_vrijmoethi	0,288376	4,862838	1;12	0,0011	0,003122
Callogorgia_verticillata.Corallium_rubrum	0,068751	2,214801	1;30	0,0439	0,063144
Callogorgia_verticillata.Eunicella_cavolini	0,128205	7,500019	1;51	0,0001	0,000525
Callogorgia_verticillata.Eunicella_verrucosa	0,444497	16,80356	1;21	0,0001	0,000525
Callogorgia_verticillata.Klyxum_utinomii	0,282485	5,118081	1;13	0,0027	0,006163
Callogorgia_verticillata.Ovabunda	0,381675	15,43178	1;25	0,0001	0,000525
Callogorgia_verticillata.Paralemnalia_thyrsoides	0,241186	6,039078	1;19	0,0002	0,000875
Callogorgia_verticillata.Paramuricea_clavata	0,297018	14,36541	1;34	0,0001	0,000525
Callogorgia_verticillata.Paramuricea_clavata_bicolor	0,250871	7,702325	1;23	0,0001	0,000525
Callogorgia_verticillata.Sarcophyton_glaucum	0,285588	8,394821	1;21	0,0001	0,000525
Callogorgia_verticillata.Sinularia_eilatensis	0,261249	5,658171	1;16	0,0001	0,000525
Callogorgia_verticillata.Sinularia_loyai	0,298857	5,114915	1;12	0,0119	0,020484
Callogorgia_verticillata.Sinularia_polydactyla	0,33205	5,965405	1;12	0,0112	0,0196
Callogorgia_verticillata.Sinularia_vrijmoethi	0,283839	7,926666	1;20	0,0001	0,000525
Corallium_rubrum.Eunicella_cavolini	0,065953	4,165952	1;59	0,0001	0,000525
Corallium_rubrum.Eunicella_verrucosa	0,169744	5,92897	1;29	0,0007	0,002227
Corallium_rubrum.Klyxum_utinomii	0,094967	2,203578	1;21	0,0272	0,0408
Corallium_rubrum.Ovabunda	0,212346	8,896546	1;33	0,0002	0,000875
Corallium_rubrum.Paralemnalia_thyrsoides	0,109307	3,31348	1;27	0,0014	0,003419
Corallium_rubrum.Paramuricea_clavata	0,150863	7,462004	1;42	0,0001	0,000525
Corallium_rubrum.Paramuricea_clavata_bicolor	0,082263	2,778729	1;31	0,0133	0,021485
Corallium_rubrum.Sarcophyton_glaucum	0,140001	4,720958	1;29	0,0002	0,000875
Corallium_rubrum.Sinularia_eilatensis	0,10648	2,860073	1;24	0,0059	0,011913
Corallium_rubrum.Sinularia_loyai	0,117582	2,665007	1;20	0,0044	0,009429
Corallium_rubrum.Sinularia_polydactyla	0,116901	2,647517	1;20	0,0094	0,017017
Corallium_rubrum.Sinularia_vrijmoethi	0,128514	4,129045	1;28	0,0003	0,001167
Eunicella_cavolini.Eunicella_verrucosa	0,090822	4,994731	1;50	0,0001	0,000525
Eunicella_cavolini.Klyxum_utinomii	0,029499	1,276626	1;42	0,2006	0,226484
Eunicella_cavolini.Ovabunda	0,090524	5,37488	1;54	0,0001	0,000525
Eunicella_cavolini.Paralemnalia_thyrsoides	0,042086	2,108867	1;48	0,0077	0,0147

Eunicella_cavolini.Paramuricea_clavata	0,065985	4,450745	1;63	0,0004	0,001448
Eunicella_cavolini.Paramuricea_clavata_bicolor	0,037928	2,050025	1;52	0,0163	0,025545
Eunicella_cavolini.Sarcophyton_glaucum	0,052801	2,787211	1;50	0,0012	0,00325
Eunicella_cavolini.Sinularia_eilatensis	0,046119	2,175714	1;45	0,0073	0,014194
Eunicella_cavolini.Sinularia_loyai	0,049552	2,137533	1;41	0,0011	0,003122
Eunicella_cavolini.Sinularia_polydactyla	0,036998	1,575196	1;41	0,0479	0,06706
Eunicella_cavolini.Sinularia_vrijmoethi	0,05059	2,611	1;49	0,0019	0,004534
Eunicella_verrucosa.Klyxum_utinomii	0,296591	5,059775	1;12	0,004	0,00875
Eunicella_verrucosa.Ovabunda	0,347213	12,76542	1;24	0,0001	0,000525
Eunicella_verrucosa.Paralemnalia_thyrsoides	0,268525	6,607803	1;18	0,0001	0,000525
Eunicella_verrucosa.Paramuricea_clavata	0,148059	5,73508	1;33	0,0013	0,00325
Eunicella_verrucosa.Paramuricea_clavata_bicolor	0,100957	2,470477	1;22	0,0451	0,063993
Eunicella_verrucosa.Sarcophyton_glaucum	0,285026	7,97305	1;20	0,0001	0,000525
Eunicella_verrucosa.Sinularia_eilatensis	0,311829	6,796908	1;15	0,0005	0,001694
Eunicella_verrucosa.Sinularia_loyai	0,407793	7,574597	1;11	0,0123	0,020831
Eunicella_verrucosa.Sinularia_polydactyla	0,359947	6,186069	1;11	0,0133	0,021485
Eunicella_verrucosa.Sinularia_vrijmoethi	0,278213	7,323549	1;19	0,0001	0,000525
Klyxum_utinomii.Ovabunda	0,032958	0,545306	1;16	0,6517	0,657966
Klyxum_utinomii.Paralemnalia_thyrsoides	0,120258	1,366968	1;10	0,1473	0,175756
Klyxum_utinomii.Paramuricea_clavata	0,033773	0,873846	1;25	0,5602	0,582386
Klyxum_utinomii.Paramuricea_clavata_bicolor	0,122504	1,954495	1;14	0,0526	0,070808
Klyxum_utinomii.Sarcophyton_glaucum	0,082661	1,081321	1;12	0,3414	0,36162
Klyxum_utinomii.Sinularia_eilatensis	0,146833	1,204723	1;7	0,3018	0,328964
Klyxum_utinomii.Sinularia_loyai	0,501249	3,01503	1;3	0,2	0,226484
Klyxum_utinomii.Sinularia_polydactyla	0,172968	0,627431	1;3	0,6	0,617647
Klyxum_utinomii.Sinularia_vrijmoethi	0,047601	0,549778	1;11	0,7459	0,7459
Ovabunda.Paralemnalia_thyrsoides	0,139406	3,563735	1;22	0,0159	0,025295
Ovabunda.Paramuricea_clavata	0,056236	2,204736	1;37	0,0522	0,070808
Ovabunda.Paramuricea_clavata_bicolor	0,211832	6,987889	1;26	0,0003	0,001167
Ovabunda.Sarcophyton_glaucum	0,093793	2,48402	1;24	0,0552	0,073367
Ovabunda.Sinularia_eilatensis	0,197987	4,690391	1;19	0,0048	0,01008
Ovabunda.Sinularia_loyai	0,225974	4,379185	1;15	0,0295	0,043021
Ovabunda.Sinularia_polydactyla	0,029426	0,454774	1;15	0,6384	0,650796
Ovabunda.Sinularia_vrijmoethi	0,112897	2,927095	1;23	0,0259	0,039413
Paralemnalia_thyrsoides.Paramuricea_clavata	0,115339	4,041681	1;31	0,001	0,003
Paralemnalia_thyrsoides.Paramuricea_clavata_bicolor	0,11443	2,584322	1;20	0,0033	0,007372
Paralemnalia_thyrsoides.Sarcophyton_glaucum	0,089145	1,761661	1;18	0,0839	0,102436
Paralemnalia_thyrsoides.Sinularia_eilatensis	0,104441	1,516076	1;13	0,1046	0,126241
Paralemnalia_thyrsoides.Sinularia_loyai	0,122381	1,255016	1;9	0,2666	0,294663
Paralemnalia_thyrsoides.Sinularia_polydactyla	0,1634	1,757831	1;9	0,0715	0,089375
Paralemnalia_thyrsoides.Sinularia_vrijmoethi	0,10182	1,927165	1;17	0,0509	0,070322
Paramuricea_clavata.Paramuricea_clavata_bicolor	0,107859	4,231484	1;35	0,0013	0,00325
Paramuricea_clavata.Sarcophyton_glaucum	0,082006	2,947934	1;33	0,0129	0,021485
Paramuricea_clavata.Sinularia_eilatensis	0,141775	4,625485	1;28	0,0003	0,001167
Paramuricea_clavata.Sinularia_loyai	0,14841	4,18259	1;24	0,0021	0,0049
Paramuricea_clavata.Sinularia_polydactyla	0,033937	0,843113	1;24	0,3444	0,36162

Paramuricea_clavata.Sinularia_vrijmoethi	0,086896	3,045308	1;32	0,0089	0,016395
Paramuricea_clavata_bicolor.Sarcophyton_glaucum	0,144825	3,725741	1;22	0,0001	0,000525
Paramuricea_clavata_bicolor.Sinularia_eilatensis	0,129535	2,529792	1;17	0,0061	0,012085
Paramuricea_clavata_bicolor.Sinularia_loyai	0,160348	2,482606	1;13	0,0087	0,016313
Paramuricea_clavata_bicolor.Sinularia_polydactyla	0,153361	2,354834	1;13	0,0112	0,0196
Paramuricea_clavata_bicolor.Sinularia_vrijmoethi	0,136807	3,328265	1;21	0,0005	0,001694
Sarcophyton_glaucum.Sinularia_eilatensis	0,133846	2,317928	1;15	0,0224	0,034588
Sarcophyton_glaucum.Sinularia_loyai	0,144505	1,858055	1;11	0,1786	0,208367
Sarcophyton_glaucum.Sinularia_polydactyla	0,111693	1,383099	1;11	0,1667	0,196669
Sarcophyton_glaucum.Sinularia_vrijmoethi	0,066127	1,345389	1;19	0,2341	0,261495
Sinularia_eilatensis.Sinularia_loyai	0,237829	1,872252	1;6	0,0689	0,087163
Sinularia_eilatensis.Sinularia_polydactyla	0,285264	2,394708	1;6	0,0747	0,092276
Sinularia_eilatensis.Sinularia_vrijmoethi	0,073784	1,115268	1;14	0,3039	0,328964
Sinularia_loyai.Sinularia_polydactyla	0,856905	11,97675	1;2	0,333333	0,357143
Sinularia_loyai.Sinularia_vrijmoethi	0,205915	2,593113	1;10	0,0591	0,077569
Sinularia_polydactyla.Sinularia_vrijmoethi	0,130895	1,506096	1;10	0,1871	0,215885

Figure 1: Homoscedasticity checking graphs for the "raw data" ANOVA model

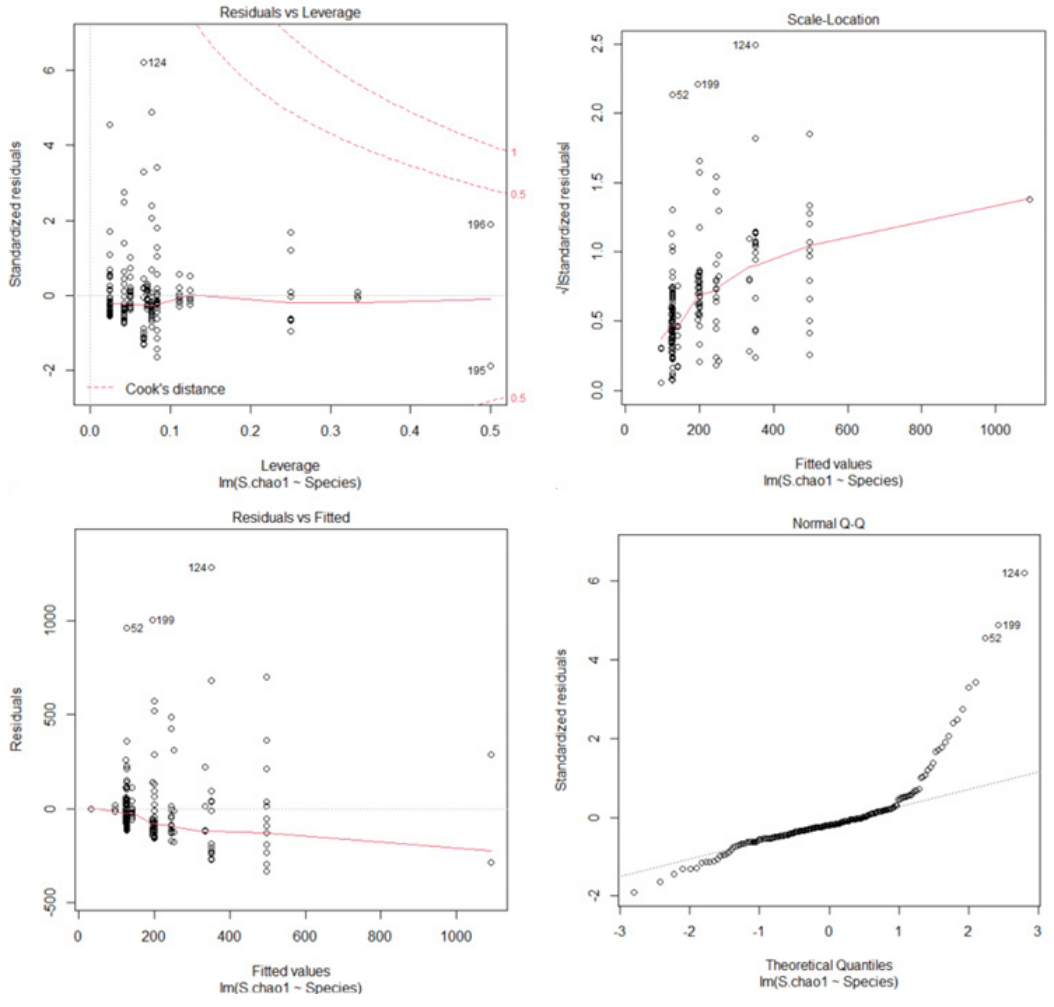

Figure 2: Homoscedasticity checking graphs for the log transformed ANOVA model

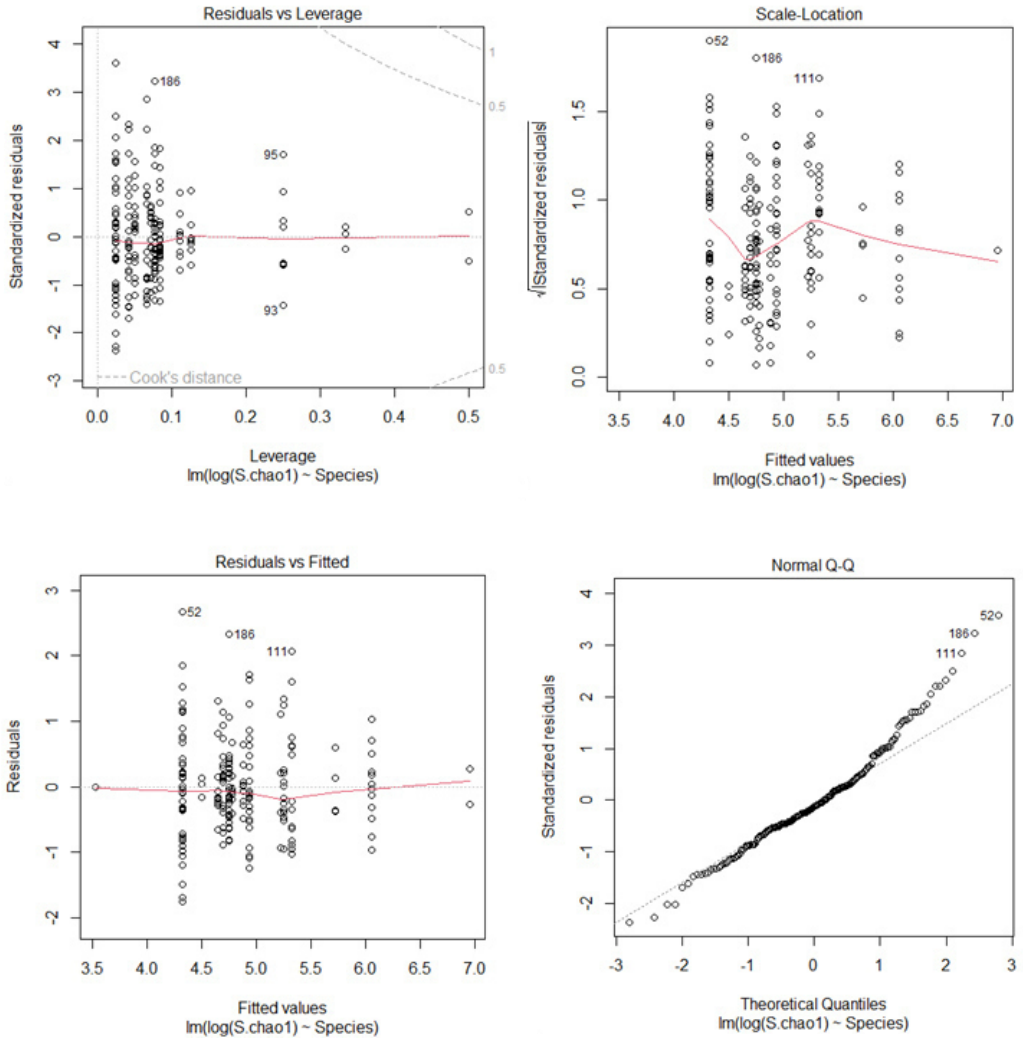

Figure 3: Juxtaposition of Red Sea species phylogeny (1) and microbiome dendrogram (2)

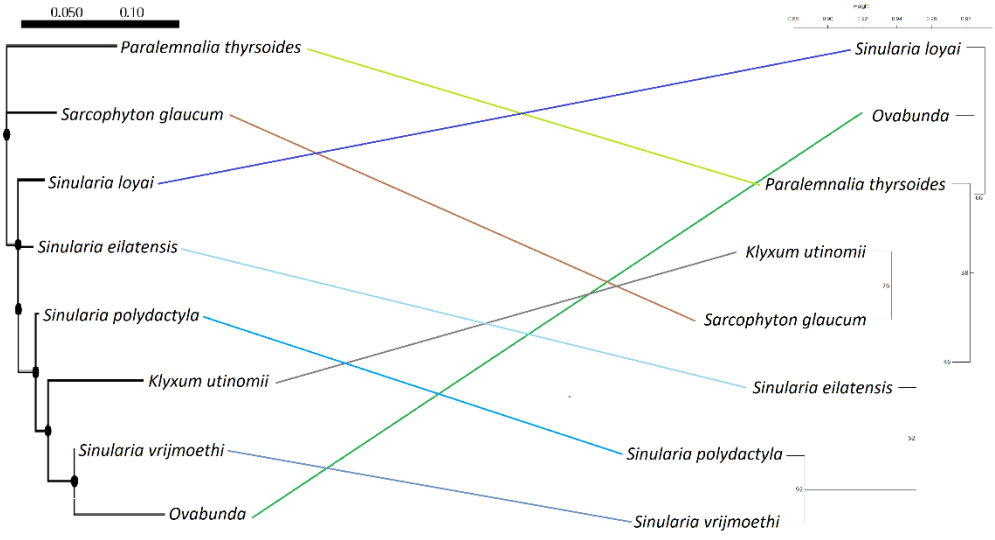

Figure 4: Poster presented during the International Coral Reef Symposium (ICRS) in Bremen (Germany) from 3rd to 8th July 2022

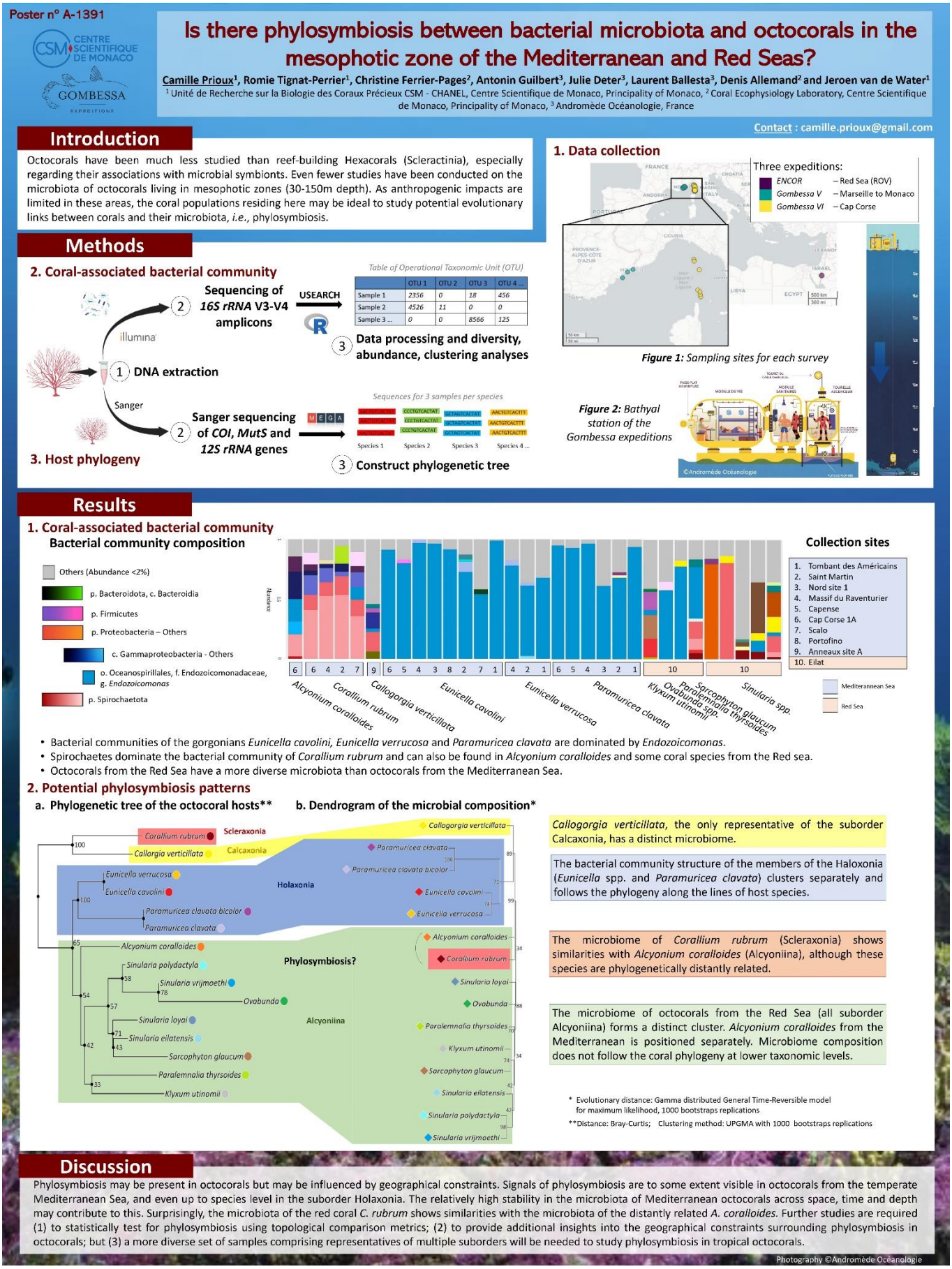

Script 1: Bioinformatic pipeline for the Illumina sequences

```
#!/bin/bash
#create a file to check if the steps are done or not
#touch 1checkpoints.txt

#Unzip the files
#gunzip *.gz

###Preparation des donnees
#rename the files (preparer un fichier names.txt avec le nom original a droite et en face le nom qu'on veut mettre)
if ! grep Rename "1checkpoints.txt" ;then
  while read a b; do mv "$a" "$b"; done < namesV3V4.txt
  for i in *.fastq*; do    #retirer les ? qui se mettent a la fin du fichier
     mv "$i" "${i%?}"
     done
  echo "Rename" >> 1checkpoints.txt
fi

#### quality check (sur Fastqc)

if ! grep QualityCheck "1checkpoints.txt" ;then
  for i in *.fastq ; do
    /media/ecolo/home/camille/usearchv11 -fastq_eestats2 ${i} -output
/media/ecolo/home/camille/dataset/V3V4/QualityCheck/"$i"eestats2.txt -length_cutoffs 50,*,50
    fastqc -f fastq ${i} -output /media/ecolo/home/camille/dataset/V3V4/QualityCheck/eestats.txt
    unzip $i
    done
    echo "QualityCheck" >> 1checkpoints.txt
fi

#juste une petite boucle pour regarder les infos sur les reads (le nombre de pb principalement)
#for i in *.fastq ; do
  #/media/ecolo/home/camille/usearchv11 -fastx_info ${i}
  #done

#### Truncate the sequence when the quality drops

if ! grep Truncate "1checkpoints.txt" ;then
  for i in *.fastq
    do
    if [[ $i =~ "_R2" ]]
      then
        /media/ecolo/home/camille/usearchv11 -fastx_truncate ${i} -stripright 90 -fastqout ${i/%.fastq/.fq}
      else
        /media/ecolo/home/camille/usearchv11 -fastx_truncate ${i} -stripright 0 -fastqout ${i/%.fastq/.fq}
    fi
    done
    echo "Truncate" >> 1checkpoints.txt
fi

#### Process

if ! grep Processing "1checkpoints.txt" ;then

  #### Merge R1/R2
```

```
  /media/ecolo/home/camille/usearchv11 -fastq_mergepairs *R1.fq -reverse *R2.fq -fastq_maxmergelen 510 -
fastq_minmergelen 400 -fastq_maxdiffs 15 -report
/media/ecolo/home/camille/dataset/V3V4/Process/ReportMerging.txt -fastqout
/media/ecolo/home/camille/dataset/V3V4/Process/merged.fq  -relabel @

  #### Cut the primers (faut couper des deux cotes selon la taille des primers)
  /media/ecolo/home/camille/usearchv11 -fastx_truncate
/media/ecolo/home/camille/dataset/V3V4/Process/merged.fq -stripright 23 -stripleft 23 -fastqout
/media/ecolo/home/camille/dataset/V3V4/Process/merged_truncate.fq

  #### Quality filtering
  /media/ecolo/home/camille/usearchv11 -fastq_filter
/media/ecolo/home/camille/dataset/V3V4/Process/merged_truncate.fq -fastq_maxee 1 -fastaout
/media/ecolo/home/camille/dataset/V3V4/Process/merged_truncate.fasta

  #### Uniques sequences (trouver les sequences uniques et en combien d'exemplaires elles sont)
  /media/ecolo/home/camille/usearchv11 -fastx_uniques
/media/ecolo/home/camille/dataset/V3V4/Process/merged_truncate.fasta -fastaout
/media/ecolo/home/camille/dataset/V3V4/Process/uniques.fasta -sizeout -relabel Uniq

  #### denoise the uniques sequences

  /media/ecolo/home/camille/usearchv11 -unoise3
/media/ecolo/home/camille/dataset/V3V4/Process/uniques.fasta -zotus
/media/ecolo/home/camille/dataset/V3V4/Results/zotus.fasta -tabbedout
/media/ecolo/home/camille/dataset/V3V4/Process/unoise3.txt

  #### OTU table construction
  /media/ecolo/home/camille/usearchv11 -otutab
/media/ecolo/home/camille/dataset/V3V4/Process/merged_truncate.fq -zotus
/media/ecolo/home/camille/dataset/V3V4/Results/zotus.fasta -otutabout
/media/ecolo/home/camille/dataset/V3V4/Results/otutab.txt -mapout
/media/ecolo/home/camille/dataset/V3V4/Results/zmap.txt -id 0.99

  /media/ecolo/home/camille/usearchv11 -otutab_stats
/media/ecolo/home/camille/dataset/V3V4/Results/otutab.txt -output
/media/ecolo/home/camille/dataset/V3V4/Results/report.txt
  echo "Processing" >> 1checkpoints.txt
fi

#### Taxonomy predictions

if ! grep Taxonomy "1checkpoints.txt" ;then
  /media/ecolo/home/camille/usearchv11 -sintax /media/ecolo/home/camille/dataset/V3V4/Results/zotus.fasta -
db /media/ecolo/home/camille/reference_databases/silva_16s_v138_NR99_noEuk_v11.udb -tabbedout
/media/ecolo/home/camille/dataset/V3V4/Results/taxonomy.txt \
  -strand both -sintax_cutoff 0.8
  echo "Taxonomy" >> 1checkpoints.txt
fi

#### Taxonomy predictions with eukaryotes

if ! grep Taxonomy "1checkpoints.txt" ;then
  /media/ecolo/home/camille/usearchv11 -sintax /media/ecolo/home/camille/dataset/V3V4/Results/zotus.fasta -
db /media/ecolo/home/camille/reference_databases/SILVA_138_ProEuk_v11.udb -tabbedout
/media/ecolo/home/camille/dataset/V3V4/Results/taxonomyPROEUK.txt \
```

```
  -strand both -sintax_cutoff 0.8
  echo "Taxonomy" >> 1checkpoints.txt
fi
#### Taxonomy predictions with eukaryotes

if ! grep Taxonomy "1checkpoints.txt" ;then
  /media/ecolo/home/camille/usearchv11 -sintax /media/ecolo/home/camille/dataset/V3V4/Results/zotus.fasta -
db /media/ecolo/home/camille/reference_databases/SILVA_138_Eukaryotes_v11.udb -tabbedout
/media/ecolo/home/camille/dataset/V3V4/Results/taxonomyEUK.txt \
  -strand both -sintax_cutoff 0.8
  echo "Taxonomy" >> 1checkpoints.txt
fi

#Tree building

/media/ecolo/home/camille/usearchv11 -calc_distmx
/media/ecolo/home/camille/dataset/V3V4/Results/zotus.fasta -tabbedout
/media/ecolo/home/camille/dataset/V3V4/Results/DMX.txt -maxdist 0.2 -termdist 0.3

/media/ecolo/home/camille/usearchv11 -calc_distmx
/media/ecolo/home/camille/dataset/V3V4/Results/zotus.fasta -tabbedout
/media/ecolo/home/camille/dataset/V3V4/Results/DIST.tree -format phylip_lower_triangular

/media/ecolo/home/camille/usearchv11 -cluster_aggd
/media/ecolo/home/camille/dataset/V3V4/Results/DMX.txt -treeout
/media/ecolo/home/camille/dataset/V3V4/Results/TREE.tree -clusterout
/media/ecolo/home/camille/dataset/V3V4/Results/CLUSTERS.txt -id 0.8 -linkage min

/media/ecolo/home/camille/usearchv11 -draw_tree /media/ecolo/home/camille/dataset/V3V4/Results/TREE.tree
-output /media/ecolo/home/camille/dataset/V3V4/Results/TREE.txt
```

Script 2: R script for bacterial communities' analysis

```
                                        #####Library loading#####

library(biomformat)
library("phyloseq")
library("plyr")
library("ggplot2")
library(decontam)
library(vegan)
library(tidyverse)
library(ggpubr)
library(rstatix)
library(MASS)
library(car)

                                        #####Dataset preparation#####

setwd("C:/Users/cprioux.CSM/Desktop/Bioinfo/Results/V3V4")

#import metadata
MD <- import_qiime_sample_data("MetaData.txt")

#import otutable with taxonomy
myData <- import_biom("otuMDProEuk.biom", "TREE.tree")
```

```
colnames(tax_table(myData)) <- c("Kingdom", "Phylum", "Class", "Order", "Family", "Genus", "Species")
taxtable <- as.data.frame(tax_table(myData))

#merge otu table with metadata
myData <- merge_phyloseq(myData, MD)

#decontamination of the dataset
OTU_dec <- otu_table(myData)
OTU_dec <- as.matrix(OTU_dec)
neg=c(rep(FALSE, 105), rep(TRUE, 13),  rep(FALSE, 134))
decontam <- isContaminant(myData, neg=neg, threshold=0.1)

indices_decontaminated <- which(decontam$contaminant==FALSE)
decontaminated_otu <- as.vector(rownames(OTU_dec)[indices_decontaminated])

#Prune negative controls
myDataD <- prune_taxa(decontaminated_otu, myData)
myDataD <- subset_samples(myDataD, Type != "Negative")
myDataD <- prune_taxa(taxa_sums(myDataD) > 0, myDataD)

                                    ####PERMANOVA sur abundance entre samples et SW####
#Rarefaction
library(metagMisc)
min(sample_sums(myDataD)) #choose minimum number of read as threshold : 3021
myDataDraw <- phyloseq_mult_raref_avg(myDataD, SampSize = 3021, MinSizeThreshold = 3021, iter = 10,
replace = T)

otu_table_decontamRaw <- as.data.frame(otu_table(myDataDraw))
otu_table_decontamRaw <- t(otu_table_decontamRaw)
otu_table_decontamRawMD <- merge(otu_table_decontamRaw, MD, by = 'row.names')

#Bray-curtis distance matrix
otutab_RawDist <- vegdist(otu_table_decontamRaw, method = "bray")

#Permanova
Perm_OTU_SW <- adonis2(otutab_RawDist~as.factor(otu_table_decontamRawMD$Type),
data=otu_table_decontamRawMD, permutations = 999)
plot(Perm_OTU_SW)

#Ordination with PcoA
Ord <- ordinate(myDataD, "NMDS", "bray")
plot_ordination(myDataD, Ord, type="samples", color="Type", shape="Sea") + geom_point(size=4)

####We can remove seawater samples and OTU that are not bacteria
myDataD <- subset_samples(myDataD, Type != "SW")
myDataD <- subset_taxa(myDataD, Order!="o__Chloroplast")
myDataD <- subset_taxa(myDataD, Kingdom!="k__Unknown")
myDataD <- subset_taxa(myDataD, Family!="f__Mitochondria")
myDataD <- prune_taxa(taxa_sums(myDataD) > 0, myDataD)

                                    #####Alpha diversity : Chao1 richness estimation#####

otu_table_decontam <- as.data.frame(otu_table(myDataD))
otu_table_decontam <- t(otu_table_decontam)

#Chao1 estimation
```

```
Richness <- as.data.frame(estimateR(otu_table_decontam), header=T)

#merge metadata to richness table
Richness <- as.data.frame(t(Richness))
Richness <- merge(Richness, MD, by = 'row.names')
Richness <- subset(Richness, select=c("samples","Species","S.chao1", "Type"))
Richness <- subset(Richness, Type == "sample")

#explore dataset

RichnessStatsSpecies <- Richness %>%
  group_by(Species) %>%
  get_summary_stats(S.chao1, type = "mean_sd")

library("writexl")
write_xlsx(RichnessStatsSpecies,"RichnessStatsSpecies.xlsx")

windows()
library(ggpubr)
g <- ggboxplot(Richness, x = "Species", y = "S.chao1", fill="lightblue")

#ANOVA to assess differences in Chao1 richness between species

#model.null  <- lm(S.chao1 ~ Species, data = Richness)
#anova(model.null)
#plot(model.null) #residuals are not normally distributed

model  <- lm(log(S.chao1) ~ Species, data = Richness)
ANOVA <- anova(model)
plot(model) #residuals are much more normally distributed

#Tukey test to see who is different
a1 <- aov(model)
posthoc <- TukeyHSD(x=a1, 'Species', conf.level=0.95)
Tukey <- as.data.frame(posthoc[1])
names <- rownames(Tukey)
rownames(Tukey) <- NULL
Tukey <- cbind(names,Tukey)
write_xlsx(Tukey,"Tukey_Chao1_ANOVA.xlsx")


                                    #####Beta diversity : Standard approach#####

#Rarefaction
library(metagMisc)
min(sample_sums(myDataD))
myDataD <- phyloseq_mult_raref_avg(myDataD, SampSize = 9000, MinSizeThreshold = 9000, iter = 10,
replace = T)

otu_table_decontam <- as.data.frame(otu_table(myDataD))
otu_table_decontam <- t(otu_table_decontam)
otu_table_decontamMD <- merge(otu_table_decontam, MD, by = 'row.names')

#Bray-curtis distance matrix
otu_table_Dist <- vegdist(otu_table_decontam, method = "bray")
otu_table_MD <- merge(otu_table_decontam, MD, by = 'row.names')
```

```
#Ordination plot of Bray-curtis distances
library(ggplot2)
ordu = ordinate(myDataD, "NMDS", "bray", weighted=TRUE)
p = plot_ordination(myDataD, ordu, color="Species", shape="Sea", axes =1:2)
p = p + geom_point(size=5)
p + ggtitle("NMDS on Bray-Curtis distance")

#Permanova to assess differences of abundance between species and between RED and MED
library(tidyverse)
otu_table_MD <- data.frame(otu_table_MD[,-1], row.names=otu_table_MD[,1])
Permanova <-adonis2(otu_table_decontam~as.factor(Sea)+as.factor(Species), data=otu_table_MD,
permutations = 9999, method="bray")

dispersion <- betadisper(otu_table_Dist, group=otu_table_MD$Species)
perm <- permutest(dispersion)
summary(perm)
anova(dispersion)
windows()
plot(dispersion, hull=T, ellipse=F, PlotInd =F, LabelInd =TRUE)
library(phyloseq)


#paire-wise permanova
library(devtools)
# devtools::install_github("vmikk/metagMisc", force = TRUE)
library(metagMisc)

MetaData <- read.table("MetaData.csv", sep=";", header=T)
otu_table_DistMD <- as.matrix(otu_table_Dist)
remaining <- as.list(rownames(otu_table_DistMD))
MDpairwise <- droplevels(subset(MetaData, subset=MetaData$Sample %in% remaining))
MDpairwise$Species <- as.factor(MDpairwise$Species)  # Change to Factor, as it is required for
adonis_pairwise

Pairwise <- adonis_pairwise(x = MDpairwise, dd = vegdist(otu_table_decontam, method = "bray"), group.var =
"Species")

Pairwise_tab <- Pairwise$Adonis.tab
Betadisper.tab <- Pairwise$Betadisper.tab
library("writexl")
write_xlsx(Pairwise_tab,"Pairwise_tab.xlsx")
write_xlsx(Betadisper.tab,"Betadisper.tab.xlsx")


                                        #####Dendrogram construction#####
library(stats)
##On the entire sample dataset
#Bootstraps p-value calculations
library(pvclust)
library(vegan)
library(downloader)
library(tidyverse)

#Bray-curtis was not available for pvclust but I found a function that does :
source_url('http://raw.github.com/nielshanson/mp_tutorial/master/taxonomic_analysis/code/pvclust_bcdist.R')
```

```
otu_table_decontamMerge <- otu_table_decontamMD %>% remove_rownames %>%
column_to_rownames(var="Names")
otu_table_decontamMerge <- otu_table_decontamMerge[,c(2:8572)]

Dendrogram_UPGMA_BrayCurtisBT <- pvclust(t(otu_table_decontamMerge), method.hclust="average",
method.dist="bray", n=1000)
plot.pvclust(Dendrogram_UPGMA_BrayCurtisBT, print.pv=F, print.num=FALSE, cex=1.3)


#By merging species
merge_samples_mean <- function(physeq, group){
  group_sums <- as.matrix(table(sample_data(physeq)[ ,group]))[,1]
  merged <- merge_samples(physeq, group)
  x <- as.matrix(otu_table(merged))
  if(taxa_are_rows(merged)){ x<-t(x) }
  out <- t(x/group_sums)
  out <- otu_table(out, taxa_are_rows = TRUE)
  otu_table(merged) <- out
  return(merged)
}

myDataMerge = merge_samples_mean(myDataD, "Species")

#Bootstraps calculations
Dendrogram_merge_UPGMA_BrayCurtisBT <- pvclust(otu_table(myDataMerge), method.hclust="average",
method.dist="bray", n=1000)
plot(Dendrogram_merge_UPGMA_BrayCurtisBT, print.pv="bp", print.num=FALSE, col.pv=c(bp=1))

#Write phylo tree in Newick format
library(ape)
otu_tab_merge <- t(otu_table(myDataMerge))
otu_merge_dist <- vegdist(otu_tab_merge, method = "bray")
tree_merge_BC <- hclust(otu_merge_dist, "average")
plot(tree_merge_BC)

tree_merge_BC <- as.phylo(tree_merge_BC)
write.tree(tree_merge_BC, file = "mt.newick", append = FALSE,
        digits = 10, tree.names = FALSE)
```

Script 3: Pipeline for the phylosymbiosis analysis

- **tree_random.py** : Generate random phylogenetic trees to compare to the bacterial composition dendrogram

```
#!/bin/python2.7
### IMPORT UTILITIES ###
################################################
################## TREES #######################
# Randomize Input List Function
import random
def randomize(a):
   b = []
   for i in range(len(a)):
      element = random.choice(a)
      a.remove(element)
      b.append(element)
```

```
    return b

### RANDOM TREE TOPOLOGY GENERATOR ###
from ete3 import Tree
import numpy
def tree_random_generator(numTrees, numLeafs, leafIds, outDir):
    for i in numpy.arange(numTrees):
        t = Tree()
        leafIds = randomize(leafIds)
        t.populate(numLeafs, names_library=leafIds)
        print(outDir+'tree_'+str(numLeafs)+'_'+str(i)+'.newick')
        #print(t)
        t.write(outfile=outDir+'tree_'+str(numLeafs)+'_'+str(i)+'.newick')


tree_random_generator(numTrees=1, numLeafs=15,
leafIds=['Ec','Ev','Pc','Pcb','Cr','Ac','Cv','Ku','Ov','Pt','Sg','Se','Sl','Sp','Sv'], outDir='corals')
```

- **command.sh** : Calculate scores by comparing random trees to the dendrogram

```
#!/bin/bash
################################################################################
##### PREPARATION #####
conda activate EnvironmentCamille

#to download the whole gitHub
#wget https://github.com/awbrooks19/phylosymbiosis/archive/refs/heads/master.zip
#pour autoriser l'excecution du fichier java
chmod u=rwx TreeCmp/bin/TreeCmp.jar

##### GENERATE RANDOM TREES #####
#generated on python with the script tree_random.py (see precedent step 1)

folderIn=corals
cd ./media/ecolo/home/camille/Phylosymbiosis/corals
unzip random_trees.zip
cd /..
cd ./media/ecolo/home/camille/Phylosymbiosis
for i in $folderIn"/random_trees/"*
do
    echo $i
    cat $i >> $folderIn"/random_trees.newick"
done
#rm -rf $folderIn"/random_trees/" #delete the file with all the trees

#####CALCULATE SCORES#####Cmp.jar file was imported from the GitHub link
# Input the host and microbiome trees and calculate scores
methodIn="rf" #Robinson-Foulds metric #or methodIn="mc" #matching cluster metric

folderIn=corals;refIn="$folderIn"/ht.newick;compareIn="$folderIn"/mt.newick;
outIn="$folderIn"/treecmp_"$methodIn".txt;
java -jar TreeCmp/bin/TreeCmp.jar -r $refIn -d $methodIn -i $compareIn -o $outIn -N #&
compareIn="$folderIn"/random_trees.newick; outIn="$folderIn"/treecmp_"$methodIn"_stochastic.txt;
java -jar TreeCmp/bin/TreeCmp.jar -r $refIn -d $methodIn -i $compareIn -o $outIn -N #&
```

L'INSTITUT agro Rennes Angers	Diplôme : Ingénieur Spécialité : Ingénieur agronome Spécialisation / option : Sciences halieutiques et aquacoles (Ressources des écosystèmes aquatiques) Enseignant référent : Pablo Brosset

Auteur(s) : Camille Prioux Date de naissance* : 27/07/1998	Organisme d'accueil : Centre Scientifique de Monaco Adresse : 8 Quai Antoine 1er, 98000 Monaco Maître de stage : Christine Ferrier-Pagès
Nb pages : Annexe(s) :	
Année de soutenance : 2022	

Titre français : Existe-t-il un signal phylosymbiotique entre les octocoraux et leurs microbiote bactérien dans la zone mésophotique de la mer Méditerranée et de la mer Rouge ?

Titre anglais : Is there phylosymbiosis between octocorals and their associated bacterial microbiota in the mesophotic zone of the Mediterranean and Red Seas?

Résumé (1600 caractères maximum) :

Les coraux forment la structure tridimensionnelle des écosystèmes coralligènes, considérés comme des hotspots de biodiversité. Ce sont des holobiontes, qui forment des interactions avec toutes sortes de micro-organismes, dont des bactéries, jouant un rôle dans leur nutrition et leur santé. Les communautés bactériennes des Scléractiniaires (coraux durs) sont plus étudiées que celles des Octocoralliaires (coraux mous), notamment dans les zones mésophotiques (30-150m de profondeur). Le metabarcoding du gène 16S rRNA a permis d'explorer la composition des communautés bactériennes de 192 échantillons d'octocoralliaires de la zone mésophotique de Méditerranée (expéditions Gombessa V & VI) et de mer Rouge (campagne ENCOR). Un potentiel lien évolutif entre coraux et bactéries (phylosymbiose) a également été exploré. En Méditerranée, les communautés bacteriennes sont dominées par les Endozoicomonadaceae chez les gorgones et les Spirochaetaceae chez Corallium rubrum. Ceci suggère que ces coraux sont des "régulateurs du microbiote" et un signal phylosymbiotique a pu être mis en évidence. Une plus grande diversité taxonomique a été observée en Mer Rouge, suggérant que les coraux tropicaux sont plutôt des "conformateurs", avec un microbiote flexible. Une phylosymbiose n'y a pas été détectée mais d'autres études avec un jeu de données plus large sont nécessaires. Les études futures devraient viser à étudier le rôle fonctionnel des symbiontes microbiens, notamment chez les octocoraux méditerranéens.

Abstract (1600 caractères maximum) :

Corals form the three-dimensional structure of coral reefs and coralligenous ecosystems, which are hotspots of biodiversity. They are holobionts, in symbiosis with a large range of microorganisms such as bacteria. These microbial symbionts play an important role in the nutrition and health of their host. Bacterial communities associated to Scleractinian (hard) corals are however more studied than those associated to octocorals (soft corals), especially in mesophotic zones (30-150m depth). Using amplicon sequencing of the 16S rRNA gene, this study explored the composition of the bacterial communities associated with 192 Alcyonacean octocorals collected in the mesophotic zones of the Mediterranean Sea (Gombessa V & VI expeditions) and Red Sea (ENCOR campaign). Potential phylosymbiosis patterns (evolutionary links between corals and their microbiota) were also investigated. The bacterial communities of Mediterranean octocorals were dominated by Oceanospirillales, such as Endozoicomonadaceae in the gorgonians and Spirochaetaceae in Corallium rubrum. Such stable microbiome suggests that Mediterranean octocorals are "microbiome regulators", and a phylosymbiotic signal was detected. Higher bacterial taxonomic diversity was observed in Red Sea species. Such flexibility in the microbiome composition suggests that these corals behave as "conformers". We did not observe phylosymbiosis but further studies are needed to expand the data set. Future studies should aim to investigate the functional role of the microbial symbionts, especially in Mediterranean octocorals.

Mots-clés : Octocoraux, mésophotique, bioinformatique, microbiote, bactérie, phylosymbiose, Méditerranée, mer Rouge

Key Words: Octocorals, mesophotic zone, bioinformatics, microbiome, bacteria, phylosymbiosis, Mediterranean Sea, Red Sea